

N 70 33961

NASA CR 109865

**COMPUTER MODELING OF ROCKET
ENGINE IGNITION TRANSIENTS**

**FINAL REPORT
CONTRACT NAS7-467
MAY 1970**

**BY
T. R. MILLS AND B. P. BREEN
DYNAMIC SCIENCE A DIVISION
OF MARSHALL INDUSTRIES
2400 MICHELSON DRIVE
IRVINE, CALIFORNIA**

**FOR
NATIONAL AERONAUTICS AND SPACE ADMINISTRATION
JET PROPULSION LABORATORY
PASADENA, CALIFORNIA**

**CASE FILE
COPY**

COMPUTER MODELING OF ROCKET
ENGINE IGNITION TRANSIENTS

Final Report

Contract NAS7-467

May 1970

By

T. R. Mills and B. P. Breen
DYNAMIC SCIENCE, A Division
of Marshall Industries
2400 Michelson Drive
Irvine, California

For

NATIONAL AERONAUTICS AND SPACE ADMINISTRATION
Jet Propulsion Laboratory
Pasadena, California

FOREWORD

This report was prepared for the National Aeronautics and Space Administration, Jet Propulsion Laboratory, Pasadena, California. Project Monitor on this contract was Richard M. Clayton, Liquid Propulsion Section.

This is the final report of a research program conducted to develop a mathematical model of how design and operating parameters influence combustion chamber pressures during the starting transient of a rocket engine. As such, it is based upon work completed and reported in two previous interim reports published under this contract (NAS7-467); "Study of Random Wave Phenomena in Hypergolic Propellant Combustion," June 1967 (Ref. 16), and "Transients Influencing Rocket Engine Ignition and Popping," April 1969 (Ref. 17).

SUMMARY

The objective of this program was to predict the dominant engineering parameters influencing the occurrence of start spiking in rocket engines. A computer program was written to describe transient propellant flow and the pressure/temperature and O/F histories with the chamber prior to ignition. Experimental tests were performed which confirmed the analytical findings. Ignition spiking occurred with fuel leads at low fuel temperature, and even at high fuel temperatures with long vacuum leads; while spiking was reduced by controlled valve opening sequences at nominal temperatures.

The analytical study resulted in a propellant transient flow digital computer program and a chamber pressurization transient digital computer program which was used to obtain the engine starting characteristics. The data from the pressurization program is used in the NASA/Lewis chemical equilibrium/detonation program to predict maximum pressures possible from the transient chamber fuel/oxidizer mixture environment.

TABLE OF CONTENTS

	<u>Page No.</u>
NOMENCLATURE	v
1. INTRODUCTION	1
2. PROPELLANT TRANSIENT FLOW PROGRAM	6
3. CHAMBER PRESSURIZATION TRANSIENT PROGRAM	31
4. EXPERIMENTAL PROGRAM	43
5. CONCLUSIONS	56
6. REFERENCES	57
 APPENDIX A - USER'S MANUAL FOR PROPELLANT TRANSIENT FLOW PROGRAM	 59
 APPENDIX B - USER'S MANUAL FOR CHAMBER PRESSURIZATION TRANSIENT PROGRAM	 65
 APPENDIX C - PROPELLANT TRANSIENT FLOW PROGRAM	 80
 APPENDIX D - CHAMBER PRESSURIZATION TRANSIENT PROGRAM	 87
 DISTRIBUTION	 110

NOMENCLATURE

A_ℓ	Cross-sectional area of propellant line, in^2
A_o	Total cross sectional area of orifices, in^2
A_v	Open area of valve (which varies as the valve opens) in^2
A_{vo}	Area of valve when full open, in^2
B	Compressive bulk modulus, lb/in^2
C_D	Discharge coefficient
C_o	Loss coefficient of orifices
C_m	Capacitance of the propellant manifold (which is variable as the manifold fills), $\text{ft}^3 - \text{in}^2/\text{lb}$
C_v	Loss coefficient of valve
D	Diffusion coefficient of oxidizer vapors to droplet ft^2/sec
d	Diameter of line, in
f	Friction factor
g	Gravitational constant, $32.2 \text{ ft}/\text{sec}^2$
K	Concentration of oxidizer vapor surrounding a droplet, mass fraction
\bar{K}	Local concentration of oxidizer in vapor surrounding a droplet, mass fraction
K_ℓ	Loss coefficient for bends and abrupt line size changes
L_ℓ	Inductance of the propellant line between the tank and the valve, $\text{lb-sec}^2/\text{ft}^3 - \text{in}^2$
L_m	Inductance of the propellant manifold (which is variable as the manifold fills), $\text{lb-sec}^2/\text{ft}^3 - \text{in}^2$
ℓ	Length of propellant line, ft
ℓ_f	Length of line over which friction acts, ft
ℓ_m	Length of propellant manifold, in
M	Mach number
N_l	Number density of droplets with radius σ_l

P_a	Ambient pressure, lb/in ²
P_c	Chamber pressure, lb/in ²
P_f	Final manifold pressure after filling, lb/in ²
P_i	Initial manifold pressure before flow starts, lb/in ²
P_{line}	Pressure in the line upstream of the valve, lb/in ²
P_m	Pressure in propellant manifold, lb/in ²
P_v	Vapor pressure of the propellant, lb/in ²
q	Volumetric flow rate, ft ³ /sec
q_1	Volumetric flow rate of propellants through the valve, ft ³ /sec
q_2	Volumetric flow rate of propellants through the orifices, ft ³ /sec
R_ℓ	Resistance of the propellant line between the tank and the valve, lb-sec/ft ³ -in ²
R_o	Resistance of the orifices, lb-sec/ft ³ -in ²
R_v	Resistance of the valve (which is variable as the valve opens), lb-sec/ft ³ -in ²
r	Radial distance from the surface of the droplet
T	Temperature of gases in the propellant manifold °R
t	Time, seconds
t_f	Time of final manifold pressure after filling, sec
t_i	Time of initial flow into manifold, sec
V_m	Volume of propellant manifold, ft ³
V_{me}	Empty volume of manifold (which varies as the manifold fills), in ³
V_{mo}	Original empty volume of the manifold, in ³
\dot{W}_g	Flow rate of gases initially in the propellant manifold, lb/sec
\dot{W}_o	Flow rate through the orifices, lb/sec
W_{og}	Weight of gases initially in the propellant manifold, lb

1. INTRODUCTION

High pressures usually referred to as pressure spikes or detonation waves can occur during the starting transient of a rocket engine. These high starting pressures can damage the combustion chamber. High pressure spiking has been encountered in both large (Ref. 1) and small scale (Ref. 2) space engines. Engine fixes were made to eliminate the spikes in specific engines while little effort was made to understand the mechanisms involved. At first it was generally accepted that the cause of the pressure waves was the explosion of accumulated propellants in the combustion chamber. However, as a result of recent experimental investigations, it was found that detonatable chemical reaction intermediates can form under start transient conditions (Refs. 3, 4, 5, and 6) and Perlee (Ref. 4) showed that observed hardware deformations could only be explained on the basis of the presence of highly detonatable material. This information provided evidence for a mechanism to explain start transient spiking; conditions within a rocket engine combustion chamber, during the start transient, that are conducive to the formation of these detonatable mixtures would lead to the magnitude of spikes observed. Thus, what was needed was an analytical model describing the occurrence of these unfavorable conditions and also describing how these unfavorable conditions could be avoided by proper engineering design and/or controlled. The details of this model are aimed at establishing temperature, pressure, and O/F conditions which control preignition and intermediate chemistry, while the overall purpose is to show how smooth starts can be engineered into a rocket engine.

The model developed is spatially one-dimensional and is based on time dependent differential equations which describe the physical and chemical processes governing the transient chamber conditions. The overall logic of the model is based on the four processes shown in Figure 1. The equations must account for the four processes shown by Roman numerals I through IV: (I) the liquid propellant transient flow, (II) vaporization, condensation, and freezing of propellants and their effect on the chamber transient pressure and temperature, (III) chemical reaction leading to the formation of detonatable mixtures with the effects of species concentration and temperature considered, and finally (IV) the strength of detonation of the accumulated mixture. The vaporization model incorporates the modeling work of Agosta (Ref. 7) and of Seamans and Dawson (Ref. 8). The present model is unique in that it incorporates the results of previous chemical

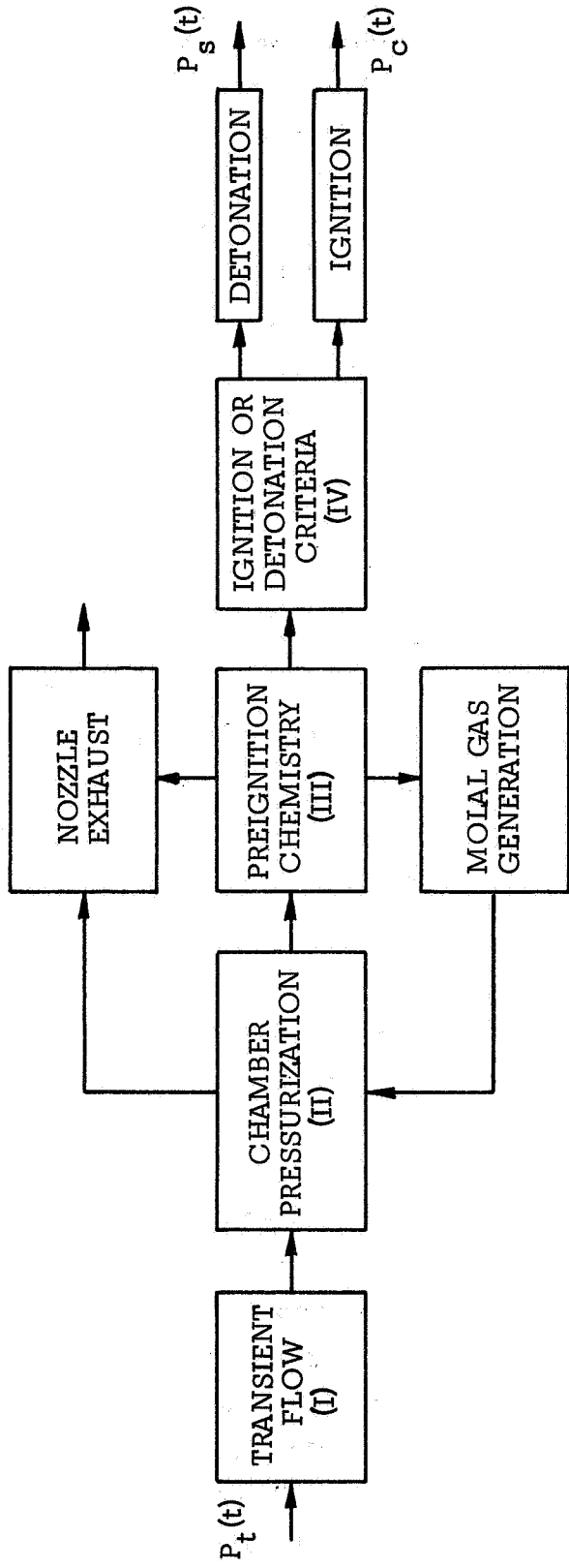
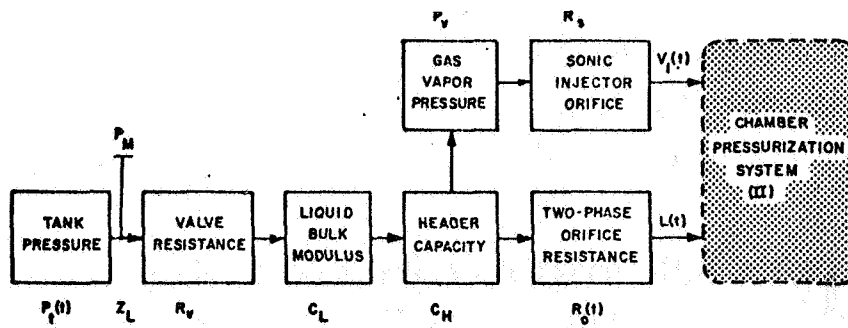
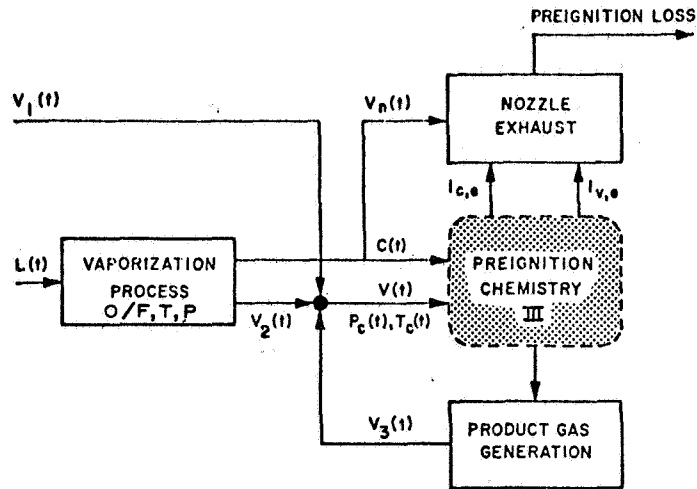


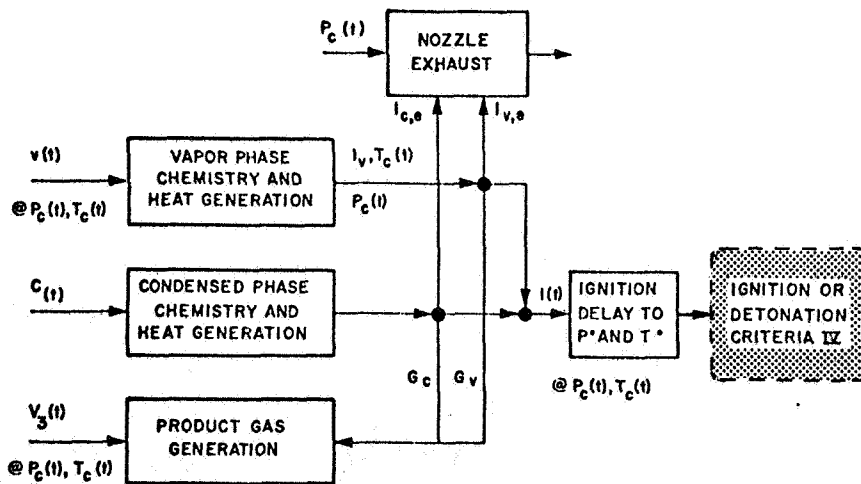
Figure 1. Rocket Chamber Ignition Model



a. Transient Flow Systems (I)



b. Chamber Pressurization System (II)



c. Preignition Chemistry System (III)

Figure 2. Individual Components of Ignition Model

intermediate research on hypergolic ignition mechanisms (Refs. 3 and 9) and on ignition chemistry (Refs. 4, 5, and 10). The model contains several constants which have been evaluated from experimental data published in these references.

The solution of the equations describing the model were performed numerically on the digital computer by a finite difference method. The main objectives of this project were to perform analytical and experimental investigations to:

- (1) Analytically determine the dominant parameters that influence the production of starting transient chamber pressure spikes.
- (2) Determine design criteria for the minimizing of spiking based on study developments.
- (3) Experimentally verify the analytical results and determine the limitations of the analysis and of the computer programs.

In any practical rocket engine system, which relies upon hypergolic ignition, the engine will start once the liquid entering the chamber meets previously determined ignition criteria conditions of temperature and vapor pressure. From this point of view, the starting of an engine involves two characteristic flow delays:

- (1) line and manifold filling, and
- (2) the flow of enough liquid sensible heat to overcome hardware and vaporization heat losses.

Essentially, once enough liquid has entered the chamber so that both the fuel and the oxidizer droplet enter a chamber pressure either equal to or greater than their vapor pressure, then they do not flash vaporize and the engine starts within $\pm 5\%$ of the added two flow delays above.

The individual components of the flow and heat balances are shown in Figure 2. During the first phase of this work (Ref. 16), these components were identified by calculating controlling time constants and from published experimental observations; thus, the controlling model is formulated in the first interim report of this work (Ref. 16). In the second phase of this contract (Ref. 17), the individual components of Figure 2 were described by an analytical model, and the model was programmed for solution so that the characteristics of each component of Figure 2 could be demonstrated. Generally, the importance of the transient flow characteristics was pointed out and it was shown that once enough liquid sensible heat entered the chamber to overcome the hardware heat capacity, the engine started.

In Section 2 of this report, the line manifold and chamber flow (the first delay) are described, while Section 3 describes the heat balances (the second delay) and resulting chamber conditions which the entering liquid encounters and Section 5 relates these flow and vaporization situations to experimental determinations of the occurrence and severity of spiking.

2. PROPELLANT TRANSIENT FLOW PROGRAM

Chamber pressurization transient predictions require a knowledge of the propellant flow into the combustion chamber as a function of time. Analyses were made of the propellant feed system of a typical bipropellant liquid fueled rocket engine. This system is shown schematically in Figure 3. The feed system and the analysis are general and can be used in any gas-pressurized injection scheme regardless of the size of the engine. Likewise, the analysis can be used to predict the response of a future system design or analyze an existing system.

Analysis of the feed system of Figure 3 is similar to a pipeline flow problem. There are two general methods of approach; the controlling parameters can be assumed to be either (1) distributed along the flow line, or (2) lumped at one point in the circuit. Solution of systems (Ref. 11) by a distributed approach involves partial differential equations in space and time. Discontinuities in the system, such as the valves and propellant tank of Figure 3, are the boundary conditions for the problem. Solutions are obtained by methods of characteristics (such as water hammer analysis, Ref. 1). The difficulties in applying this approach are: (1) the solutions are difficult to generalize or only simple configurations may be generalized, and (2) the flow downstream of the valve requires a separate solution which must be matched at the discontinuity (the valve). This second condition requires detailed knowledge of the pressure wave interactions within the propellant manifolds which are difficult to obtain. The approach may be applied to simple configurations where detailed information about the wave interaction effects are desired but overall the more microscopic nonlinear effects of unfilled vs. filled manifolds and time dependent valve resistance and cavitating flow in the orifice are more important to the starting characteristics of the engine.

Solutions of flow systems by a lumped parameter approach are made by considering solutions of quasi-steady-state flow (Ref. 11) or by use of an electrical analogy model. Quasi-steady-state solutions assume (1) no injector flow until the manifolds are full, (2) all loss terms are linear or constant, (3) no inertia or fluid elasticity effects are considered, and (4) all pressure in and flow out of the manifolds occurs discontinuously. These restrictions are quite severe and the results of such analyses give trends only for design changes and minimal details of the flow transient.

By considering a lumped parameter model wherein each element of the fluid system is considered analogous to those of a passive electrical system, the details of the distributed system are retained with the simplicity of the quasi-steady-state approach (Refs. 13 and 14). Basically, the analog model which was decided upon is described on the following pages.

Electrical/Hydraulic Analog Model: The electrical/hydraulic analogy is developed by considering all pressure loss terms lumped in a hydraulic resistance, R_h , all fluid inertia effects lumped in a hydraulic inductance, L_h , and all fluid elasticity effects lumped in a hydraulic capacitance C_h . The lumped hydraulic capacitance can be taken as the compressibility of the vapor because in the case of vacuum starts there always exists a point of cavitation and, therefore, a compressible vapor point. For one side (fuel or oxidizer) of the system shown in Figure 3a, an analogous system can be constructed, Figure 3b.

Writing the pressure drops around the loops of the circuit shown in Figure 3b, the following differential equations result:

$$L_\ell \frac{dq_1}{dt} + R_\ell q_1 + R_v q_1 + \frac{1}{C_m} \int (q_1 - q_2) dt = \Delta P \quad (1)$$

$$L_m \frac{dq_2}{dt} + R_o q_2 + \frac{1}{C_m} \int (q_2 - q_1) dt = 0 \quad (2)$$

Converting the analogous terms to fluid flow parameters as follows:

$$L_\ell = \frac{\rho \ell}{g A_\ell} \text{ (for the line)}$$

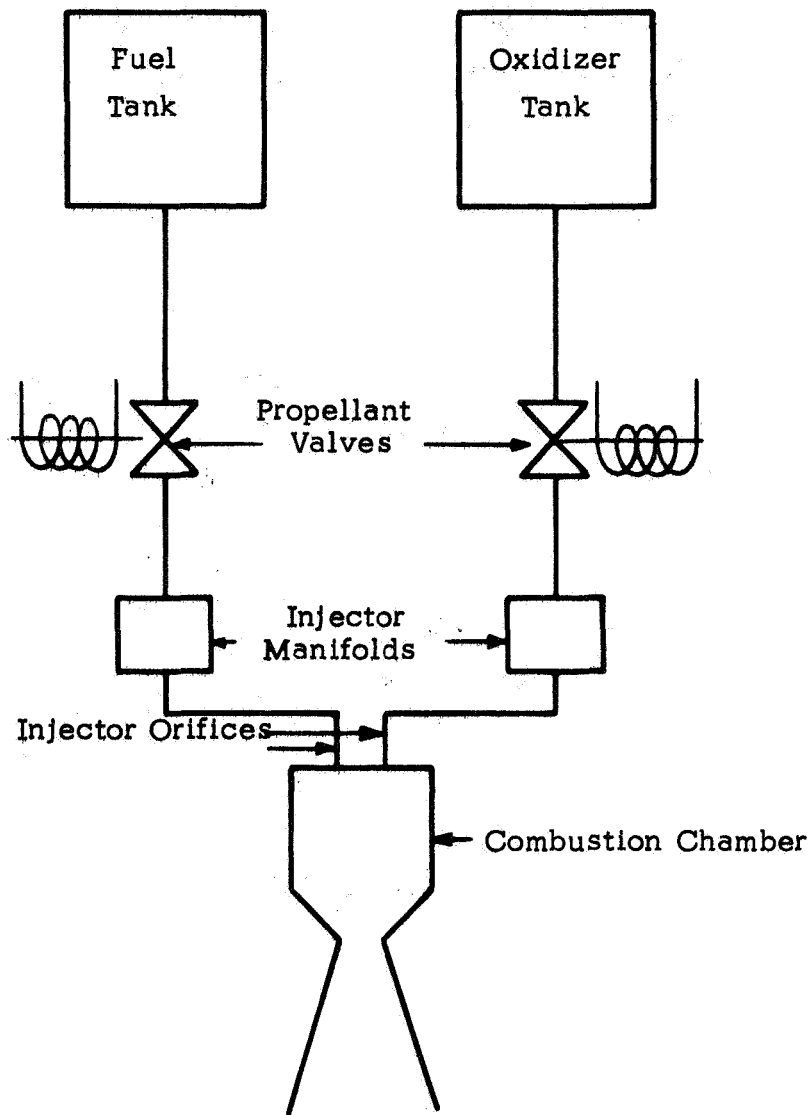
$$L_m = \frac{\rho \ell_m^3}{g V_m} \text{ (for the manifold)}$$

$$C_m = \frac{V}{B} = \frac{V}{P_v}$$

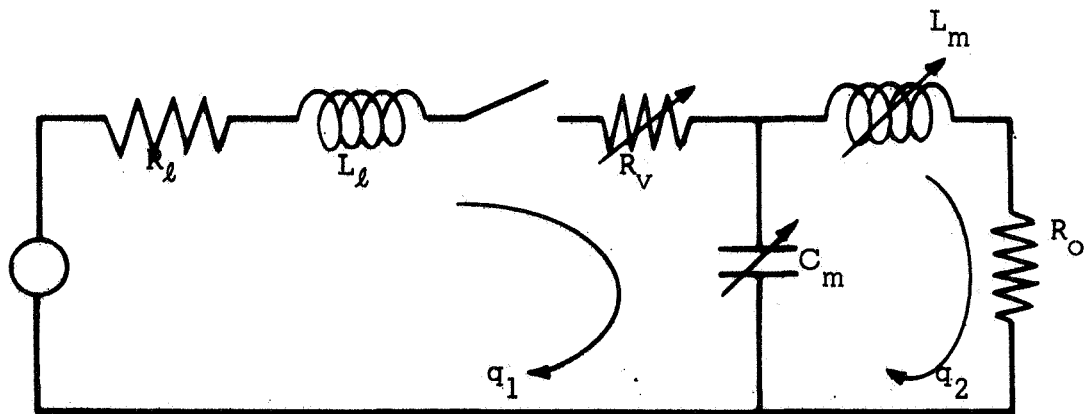
$$R_v = \frac{\rho}{2g (C_v A_v)^2} q \text{ (for the valve)}$$

$$R = K_\ell \rho \frac{q}{2g A_\ell^5} \text{ (for bends and line size changes)}$$

$$R = f \frac{\ell_f}{d} \rho \frac{q}{2g A_\ell^5} \text{ (for friction losses)}$$



a. Schematic Diagram of Propellant Feed System.



b. Analogous Electrical System to Propellant Feed System

Figure 3. Propellant Feed System. Schematic and Analogous Diagrams.

the final differential equations result:

$$\frac{\rho \ell}{gA_\ell} \frac{dq_1}{dt} + (K_\ell + f \frac{\ell_f}{d}) \rho \frac{q_1^2}{2gA_\ell^2} + \frac{\rho}{2g(C_V A_V)^2} q_1^2 + \frac{P_V}{V_m} \int (q_1 - q_2) dt = \Delta P \quad (3)$$

$$\frac{\rho \ell_m^2}{gV_m} \frac{dq_2}{dt} + \frac{\rho}{2g(C_O A_O)^2} q_2^2 + \frac{P_V}{V_m} \int (q_2 - q_1) dt = 0 \quad (4)$$

Solution of the Model: Standard digital computer integration procedures are available for solving nonlinear differential equations shown by Equations (3) and (4). A standard integration subroutine was found to be perfectly satisfactory. The method employed used a 4th order Runge-Kutta start and a 4th order Adams-Moulton fixed step predictor-corrector method used to continue the integration. Comparing predicted and corrected values at each step, the integration step size was halved, doubled, or maintained the same so that the truncation error would remain within prescribed error bounds. The time varying valve area, A_V , is prescribed by either an input table or for valves which open nearly linearly, by the equation:

$$A = A_{VO} \left(\frac{t}{\tau_{VO}} \right)^n. \quad (5)$$

Within the framework of this analysis, the following assumptions are made:

- (1) The liquid propellants are incompressible.
- (2) The compressibility effect in the propellant manifold is due to the vapor in the manifold and is equal to the bulk modulus of vapor. The formation of vapor in the manifold is accomplished adiabatically.
- (3) Wave effects within the system have negligible effects on the transient flow.
- (4) The chamber pressure is constant.

Parametric Effects: Initial cases were calculated to determine the effects of the various system parameters and empirical constants in the analysis. Figures 4 through 10 show the results of these initial cases. Table I shows those parameters which were not varied for these cases. Most of the cases were performed with $n = 1.0$ (linear valve opening); however, a limited number of cases were run for $n = 3$.

TABLE I

TRANSIENT FLOW PARAMETERS HELD CONSTANT DURING
INITIAL PROPELLANT FLOW TEST CASES

line diameter, inches	DI	=	.1875 in.
valve coefficient	CV	=	.7
injector coefficient	CØ	=	.7
orifice diameter, inches	DØI	=	.02 in.
number of orifices	XNØRF	=	4.0
steady-state flow, lb/sec	WSS	=	.08 lb/sec (oxidizer) .067 lb/sec (fuel)

Figure 4 shows the effect on flow rate of varying K_L , the loss coefficient. K_L is approximately 1.0 for one bend or abrupt area change (Ref. 15).

Figure 5 shows the effect on flow rate of varying the valve opening time from 2.5 to 10 ms. There is little effect on the transient shape in each case except to delay the transient as the valve opening time is increased.

The effect of the manifold volume is seen in Figure 6 where manifold volumes of .05, and .025 in³ were considered with a valve having an opening time of 10 ms. For the smaller manifold volume steady-state flow is achieved sooner, however, the overshoot of W_o is greater than for the larger volume (.0901 lb/sec vs .0857 lb/sec).

Figure 7 shows the effect of varying the valve area. The effect of reducing the area is to throttle the flow.

Figure 8 shows the effect of varying the valve transient shape for two valve areas. It is seen that by reducing the initial opening rate the valve can more effectively control the flow through the orifices.

Figure 9 shows the effects of temperature on the start transient. Oxidizer at 540 and 580°R was used for these tests. The differences in transients noted here are due to the difference in vapor pressure (18.5 psia vs 49 psia) of the propellant (N_2O_4) at these two temperatures.

The calculations were made for fuel (hydrazine) at 500°R (Figure 10). Both calculations show flow rate overshoot and extremely rapid flow rise rates. Although both conditions show overshoots, the recovery to steady-state flow is rapid.

Originally the analysis considered the compressibility of the vapors inside the manifold to take place isothermally. Campbell (Ref. 14) showed that rapid compression of gases occur nearly adiabatically. This effect results in the following:

$$C_m = \frac{P_{vm} V_o^{\gamma} \gamma}{V_{me}^{\gamma+1}} \quad (6)$$

where C_m is the capacitance. For nonvacuum starts the propellant manifolds contain air which is expelled as the manifold is filled with propellant. The capacitance pressure term in the differential equation accounts for the change

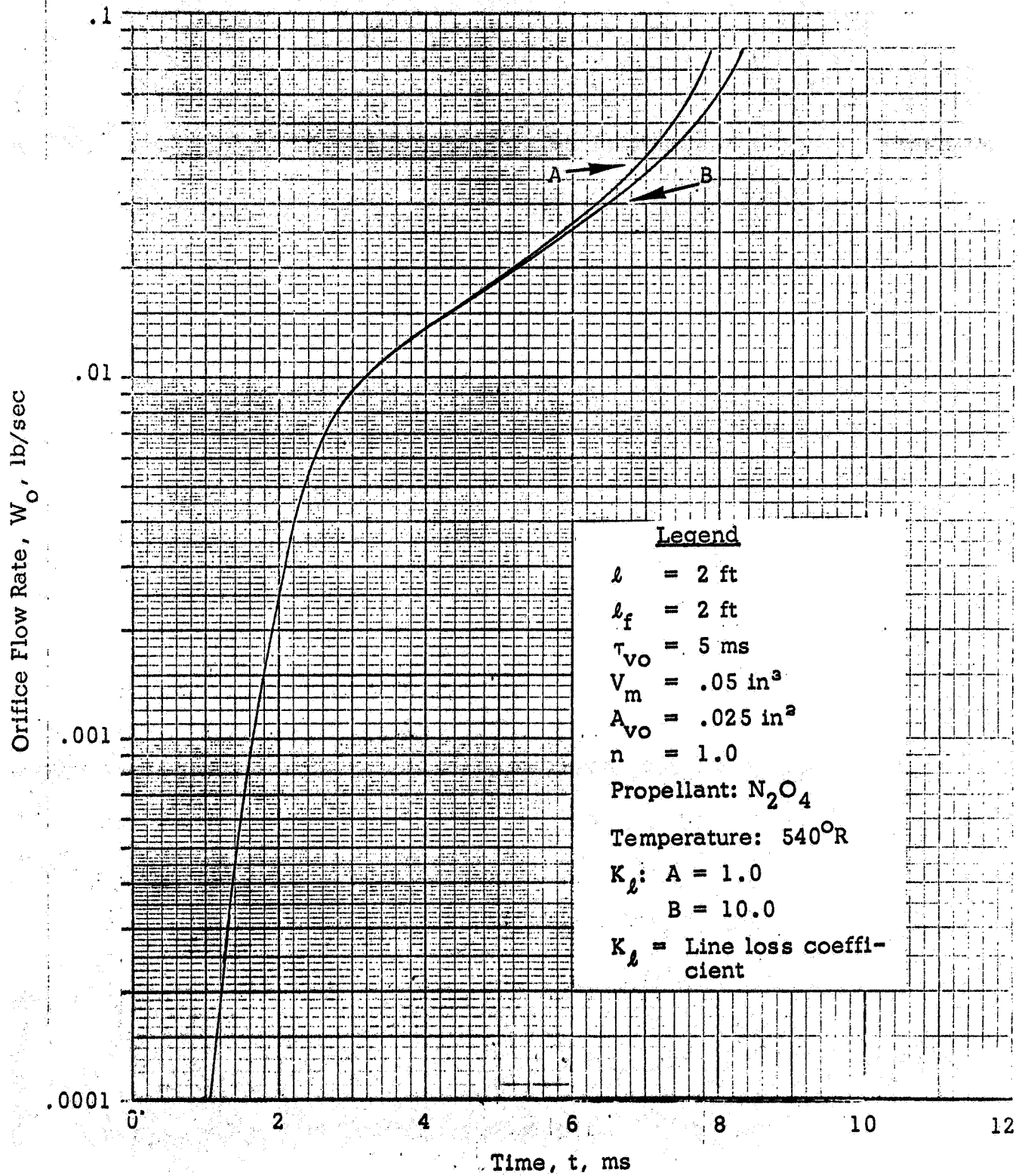


Figure 4. Effect of Loss Coefficient, K_l , on Flow Transient.

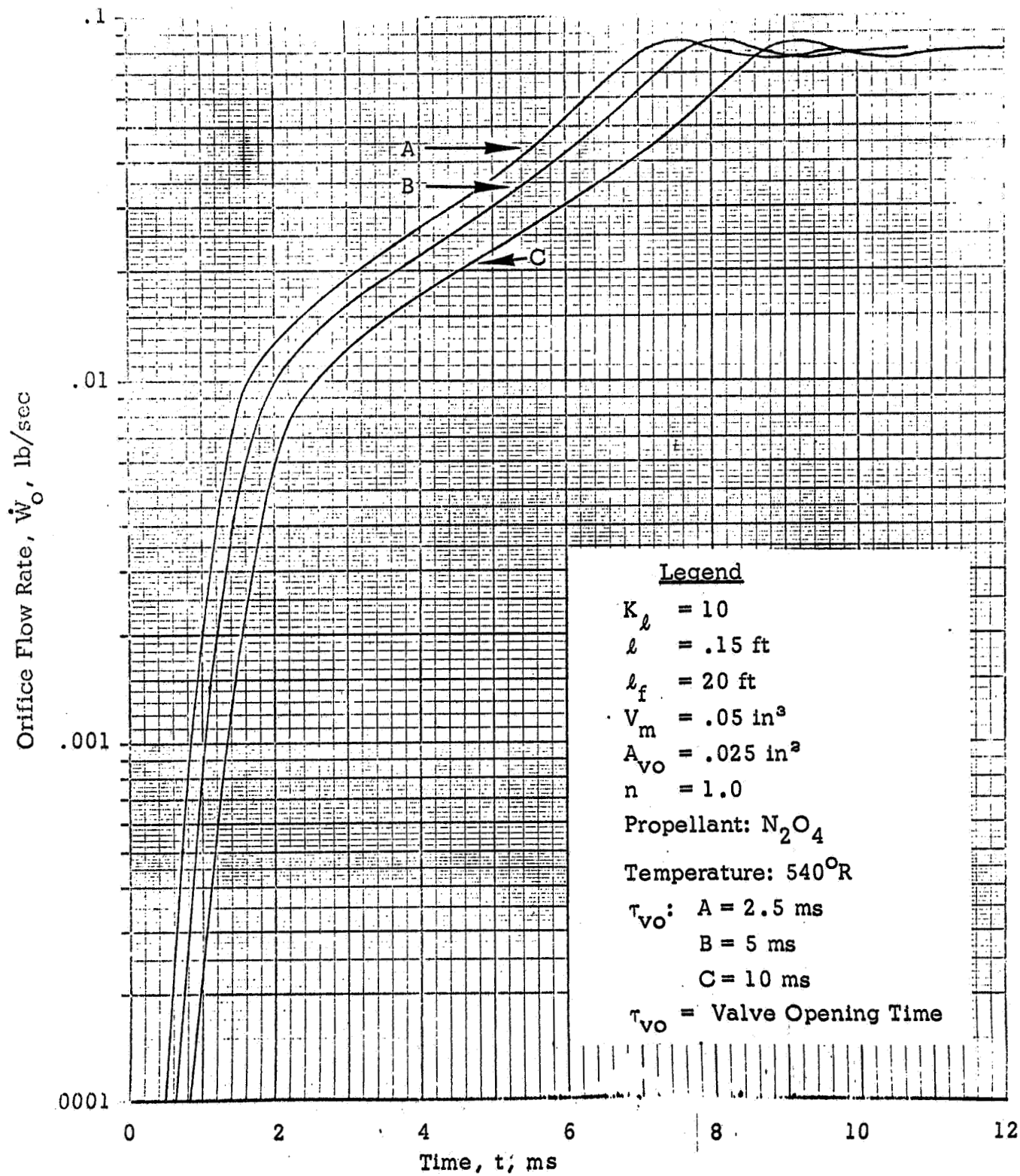


Figure 5. Effect of Valve Opening on Flow Transient.

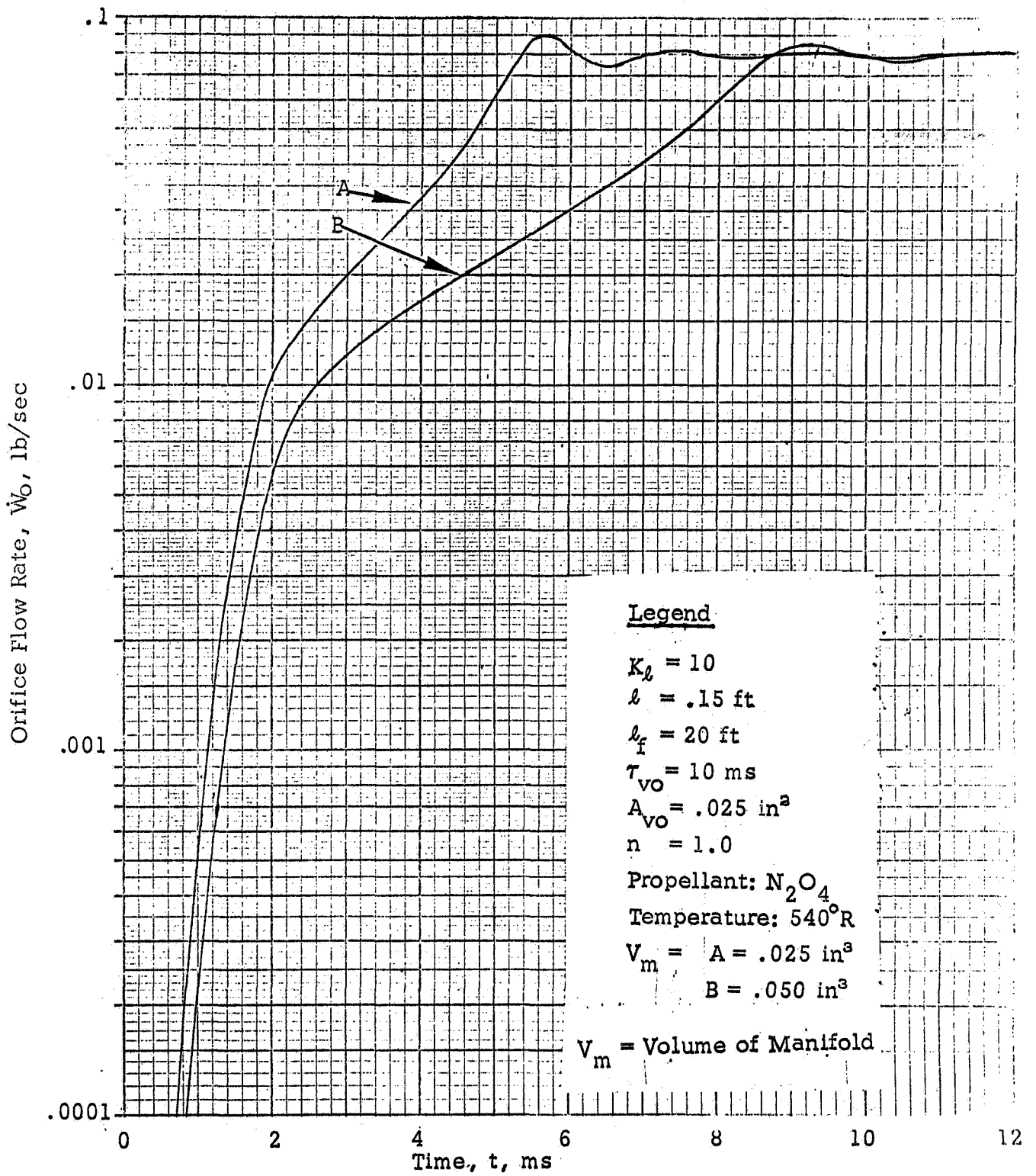


Figure 6. Effect of Manifold Volume on Flow Transient.

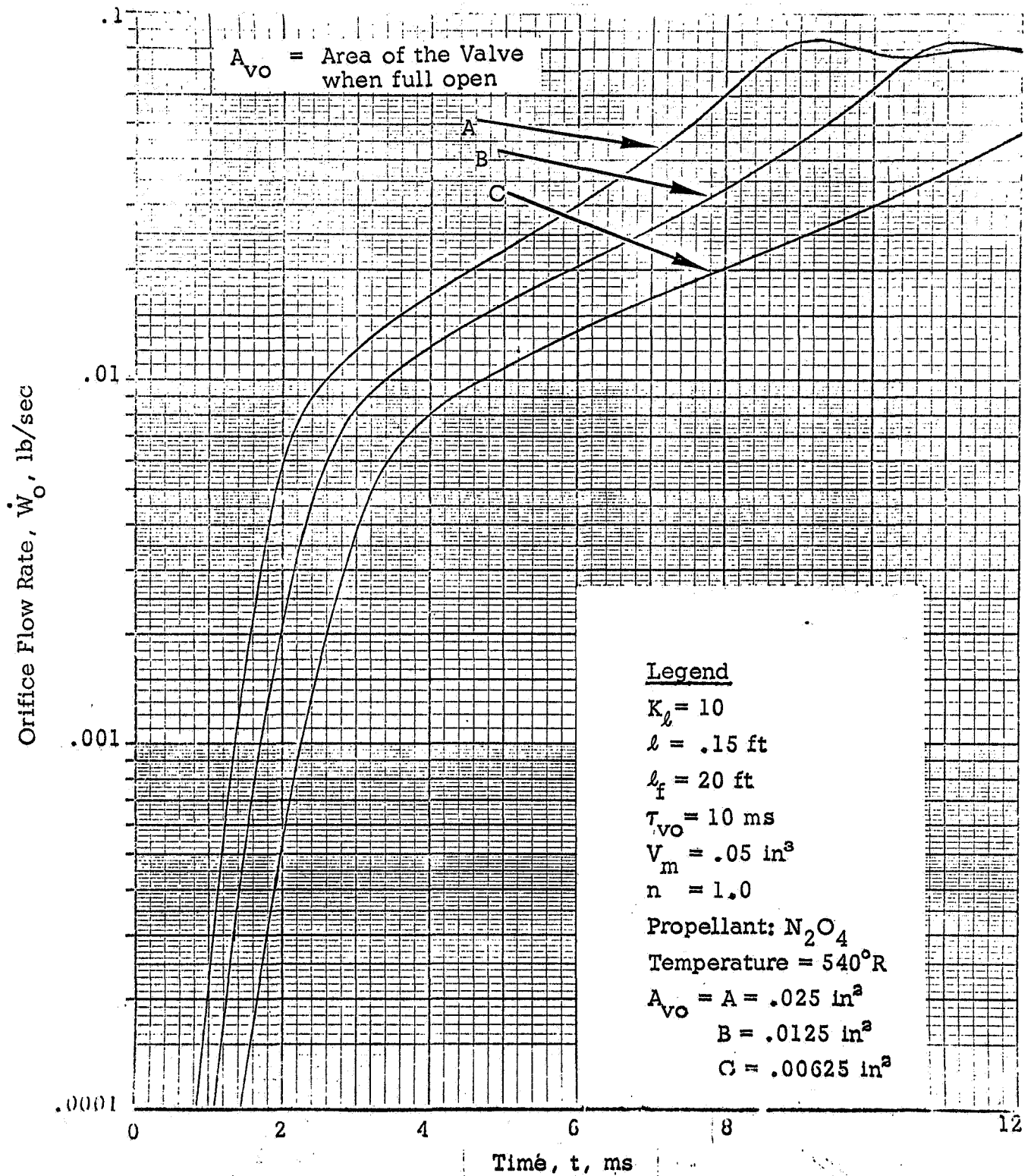


Figure 7. Effect of Valve Open Area on Flow Transient.

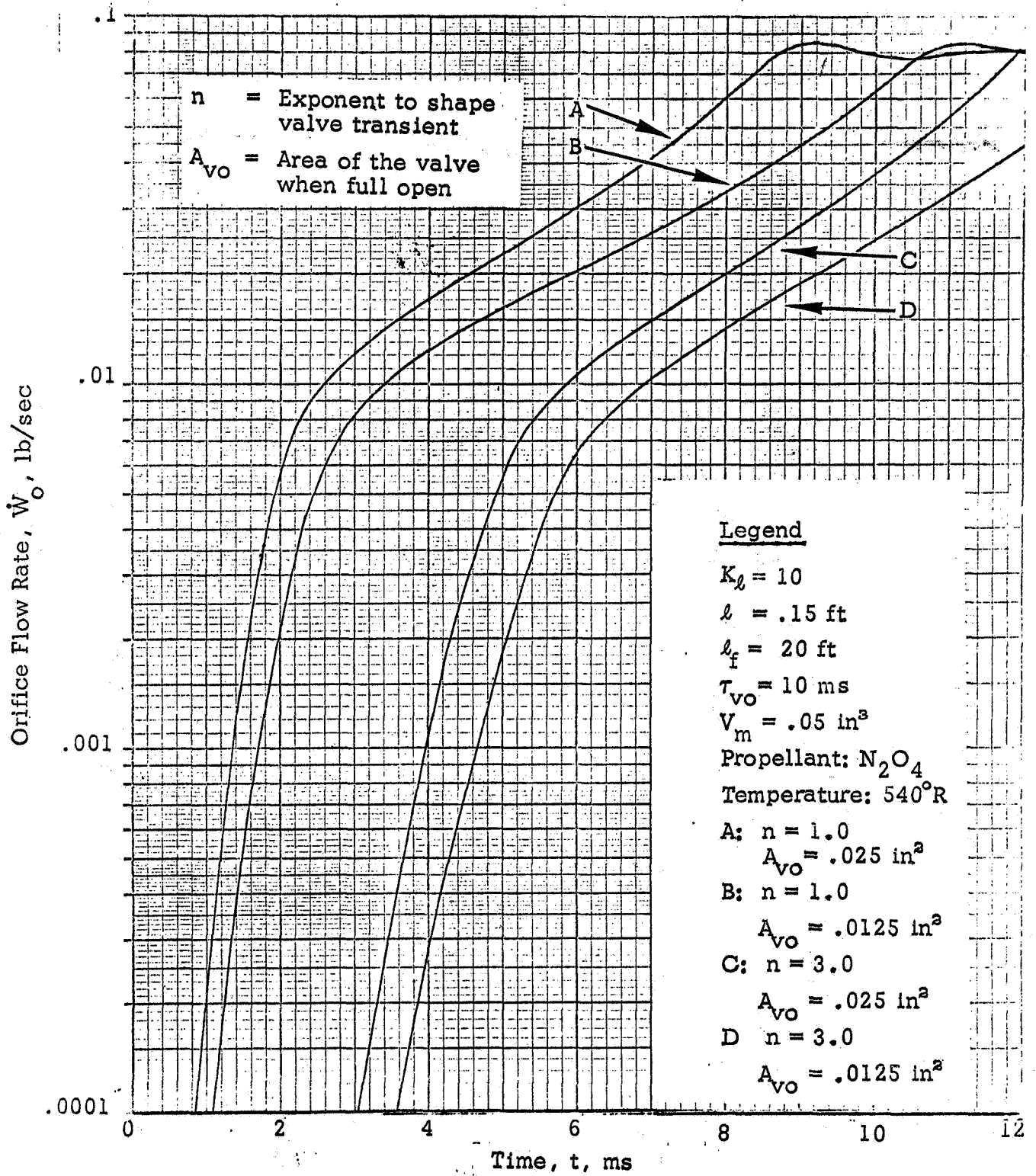


Figure 8. Effect of Valve Transient and Open Area on Flow Transient.

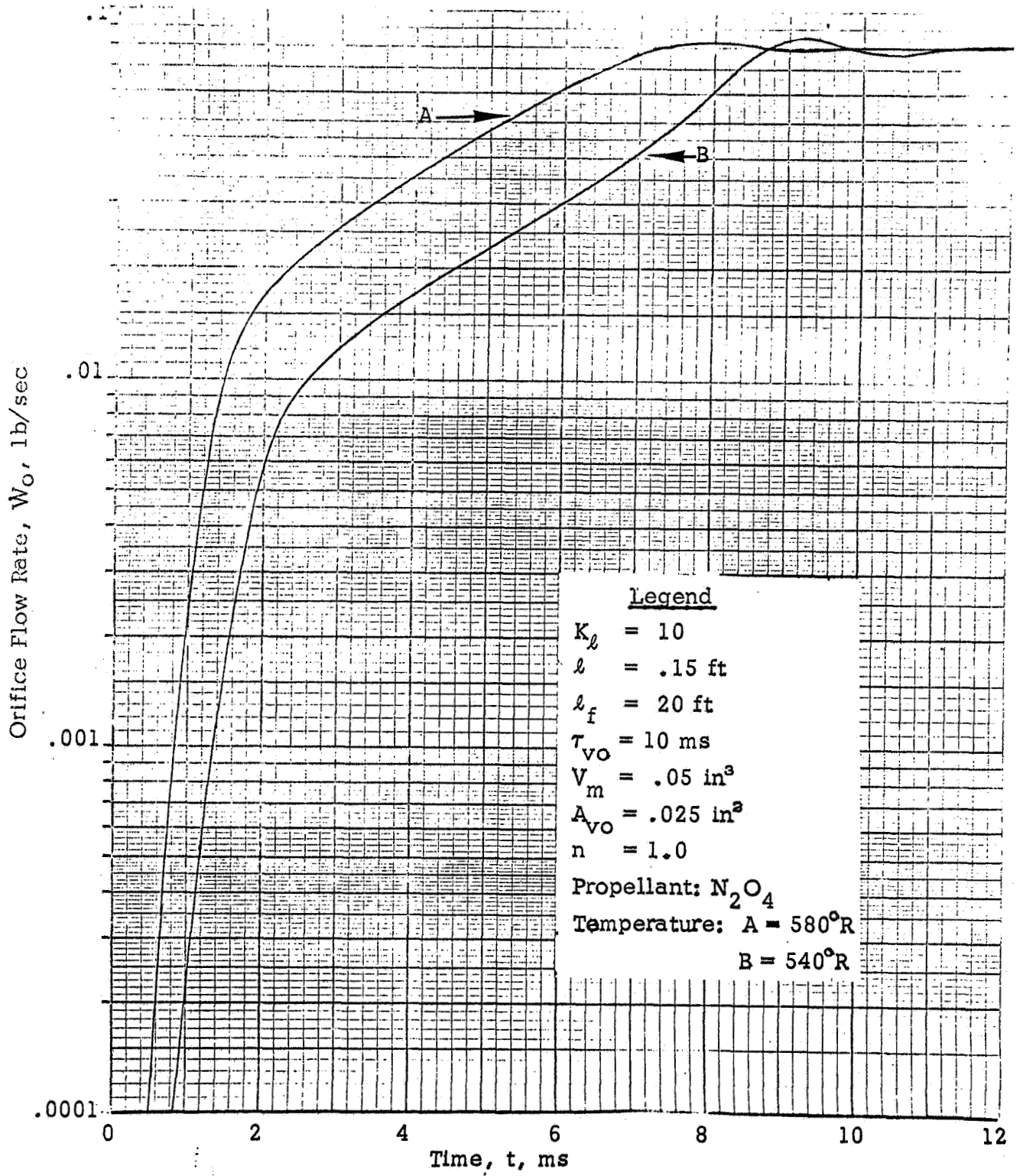


Figure 9. Effect of Oxidizer Temperature on Flow Transient.

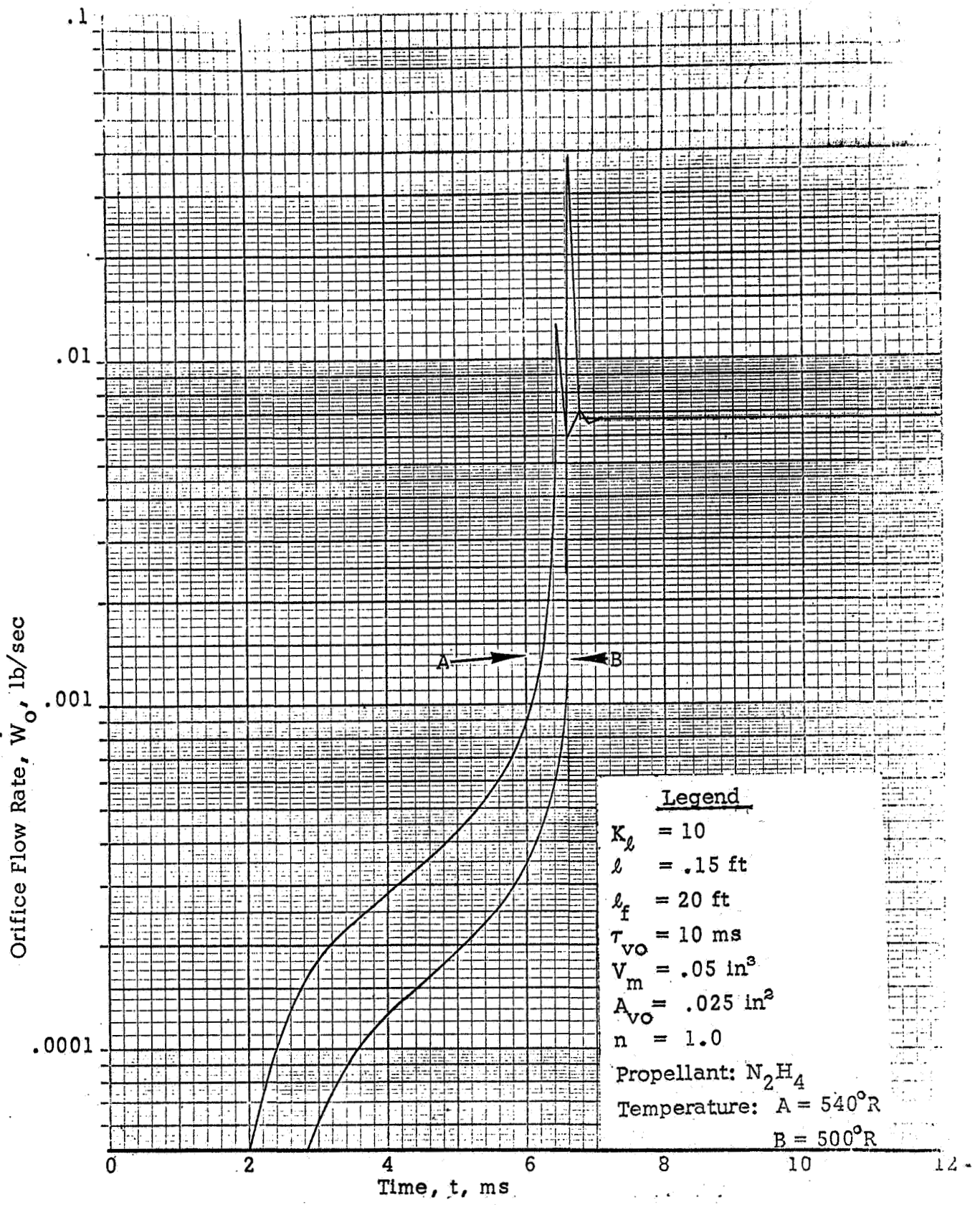


Figure 10. Effect of Fuel Temperature on Flow Transient.

in the manifold volume due to the incoming propellants and the expelled air. This differential equation is:

$$\frac{dP_m}{dt} = P\gamma \frac{\dot{W}_g}{W_{og} - \int \dot{W}_g dt} - P\gamma \frac{q_1 - q_2}{V_{me}} \quad (7)$$

where

$$\dot{W}_g = A_o \sqrt{\frac{\gamma g}{RT}} P_m \frac{M}{(1 + \frac{\gamma-1}{2} M^2)^{\frac{\gamma+1}{2(\gamma-1)}}} \quad (8)$$

and

$$M = \left\{ \frac{2}{\gamma-1} \left[\left(\frac{P_m}{P_a} \right)^{\frac{\gamma-1}{\gamma}} - 1 \right] \right\}^{1/2} \quad (9)$$

For vacuum starts, the manifold pressure was the vapor pressure of the entering propellants until the manifold was full. Thus, the pressure rises from zero to the vapor pressure, remains at vapor pressure until the manifold fills, and then becomes equal to the system fluid pressure.

Valve Opening Effects: Five calculations were made under these conditions (Figures 11 through 15). These cases considered three linear valve openings and two step-wise openings. Table II shows the conditions. The three linear openings are 10, 50, and 100 ms. Figures 11, 12, and 13 show the effect of these opening rates. It is seen that no control of the propellant flow rate is achieved. When the manifold fills a substantial pressure and flow rate overshoot occurs.

To simulate flow control, two step-wise valve openings were considered, Figures 14 and 15. Figure 14 shows the results of a low level step. Under these conditions a substantial reduction in the flow and pressure rise occurs. For the oxidizer flow, no overshoot occurred, and for the fuel flow, the overshoot was reduced. When a medium level step-wise opening was used the results were equivalent to a 50 ms valve opening.

From the propellant transient studies it can be concluded that:

- (1) Propellant flow from the injector prior to the manifold pressure reaching the vapor pressure is controlled by the valve opening transient.
- (2) Propellant flow from the injector prior to the manifold filling after the manifold pressure rises to the vapor pressure, will

be controlled by the injector orifices, the chamber pressure, and finally by the vapor pressure of the propellants in the manifold. The flow control which is possible during this period, therefore, is by controlling the propellant temperature and thus the vapor pressure.

- (3) Propellant flow from the injector can be controlled by valves if the initial valve opening area is small.

TABLE II
 INPUT FOR PROPELLANT TRANSIENT FLOW TEST CASES
 (See Figures 9 - 13)

	<u>Oxidizer System</u>			<u>Fuel System</u>		
density, lb/ft ³	RØ	=	88.9	RØ	=	62.6
line length, ft	XL	=	8.	XL	=	8.
vapor pressure, lb/in ²	PVI	=	18.5	PVI	=	.32
resistance coeff.	XKL	=	16000.	XKL	=	11000.
line dia., in	DI	=	.305	DI	=	.305
discharge coeff.	CV	=	.7	CV	=	.7
resistance length, ft	XLF	=	8.	XLF	=	8.
manifold length, in	XLMI	=	4.	XLMI	=	4.
discharge coeff.	CO	=	.86	CO	=	1.
orifice dia, in	DOI	=	.02	DOI	=	.02
viscosity, lb/ft-sec	XMU	=	.00026	XMU	=	.00058
manifold volume, in ³	VMOI	=	.1037	VMOI	=	.172
number of orifice	XNORF	=	4.	XNORF	=	4.
heat ratio	GAM	=	1.2	GAM	=	1.4
ambient pressure, lb/ft ²	PAMBI	=	0.	PAMBI	=	0.

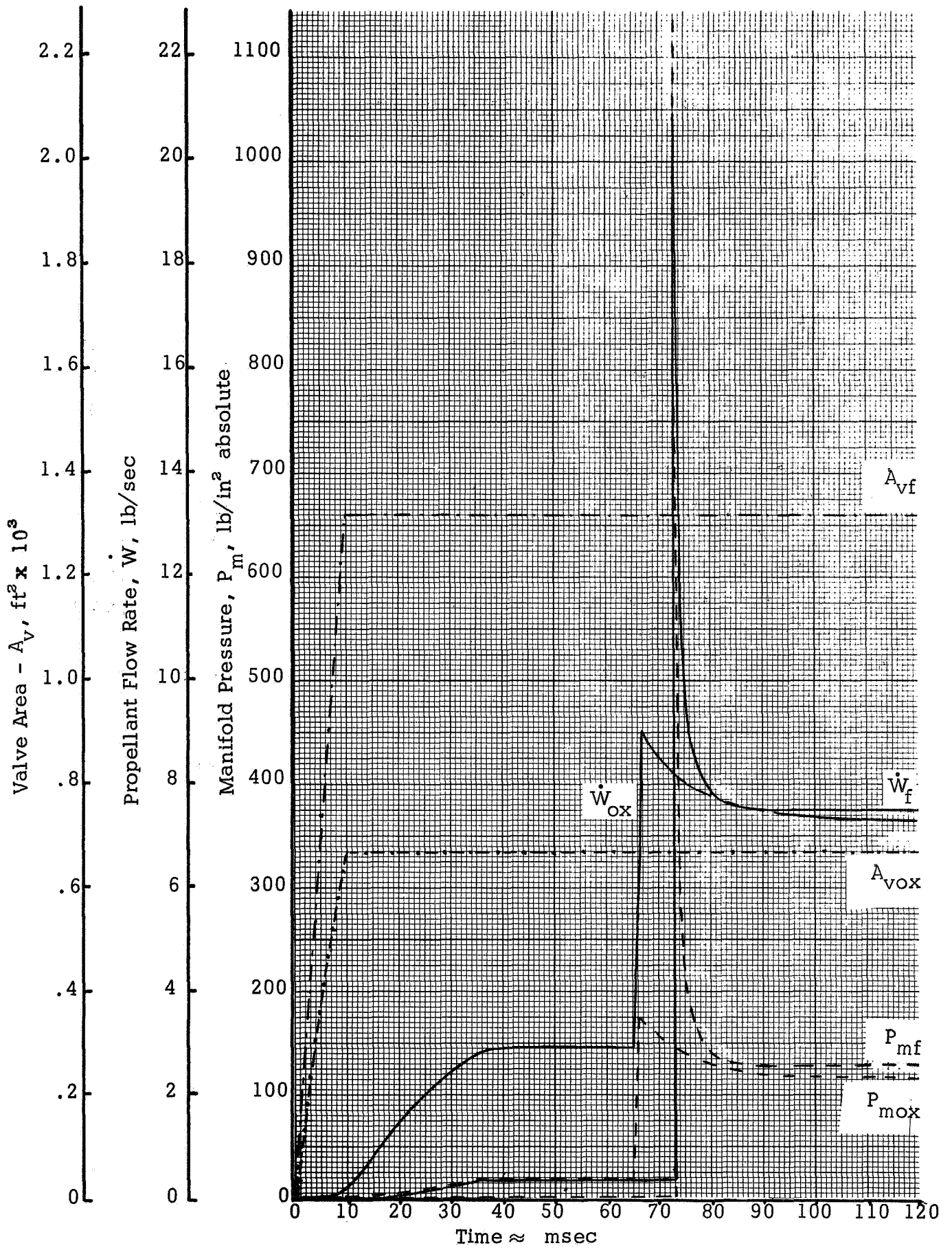


Figure 11. Propellant Flow Transient with Fast Opening Valve.

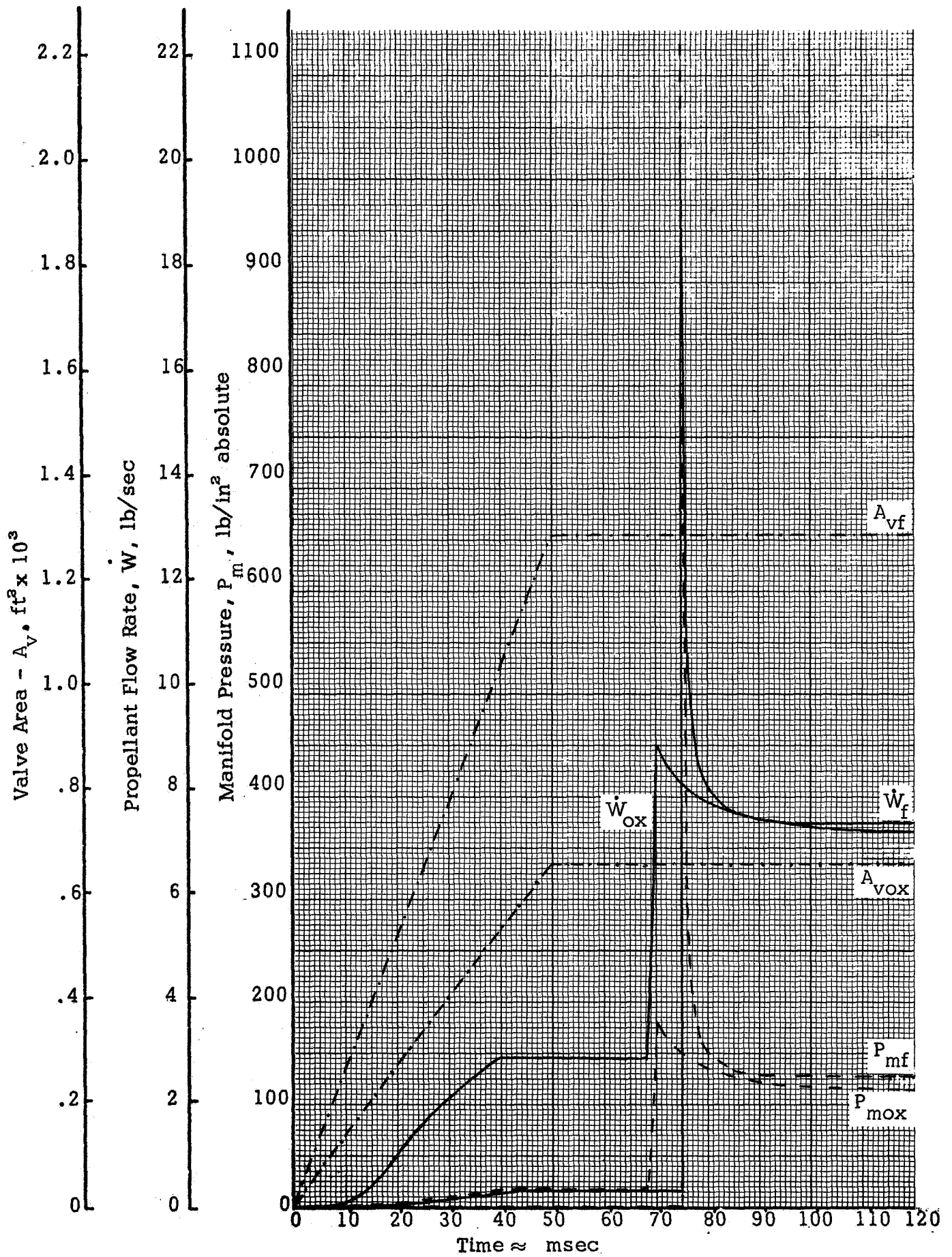


Figure 12. Propellant Flow Transient with Medium Opening Valve.

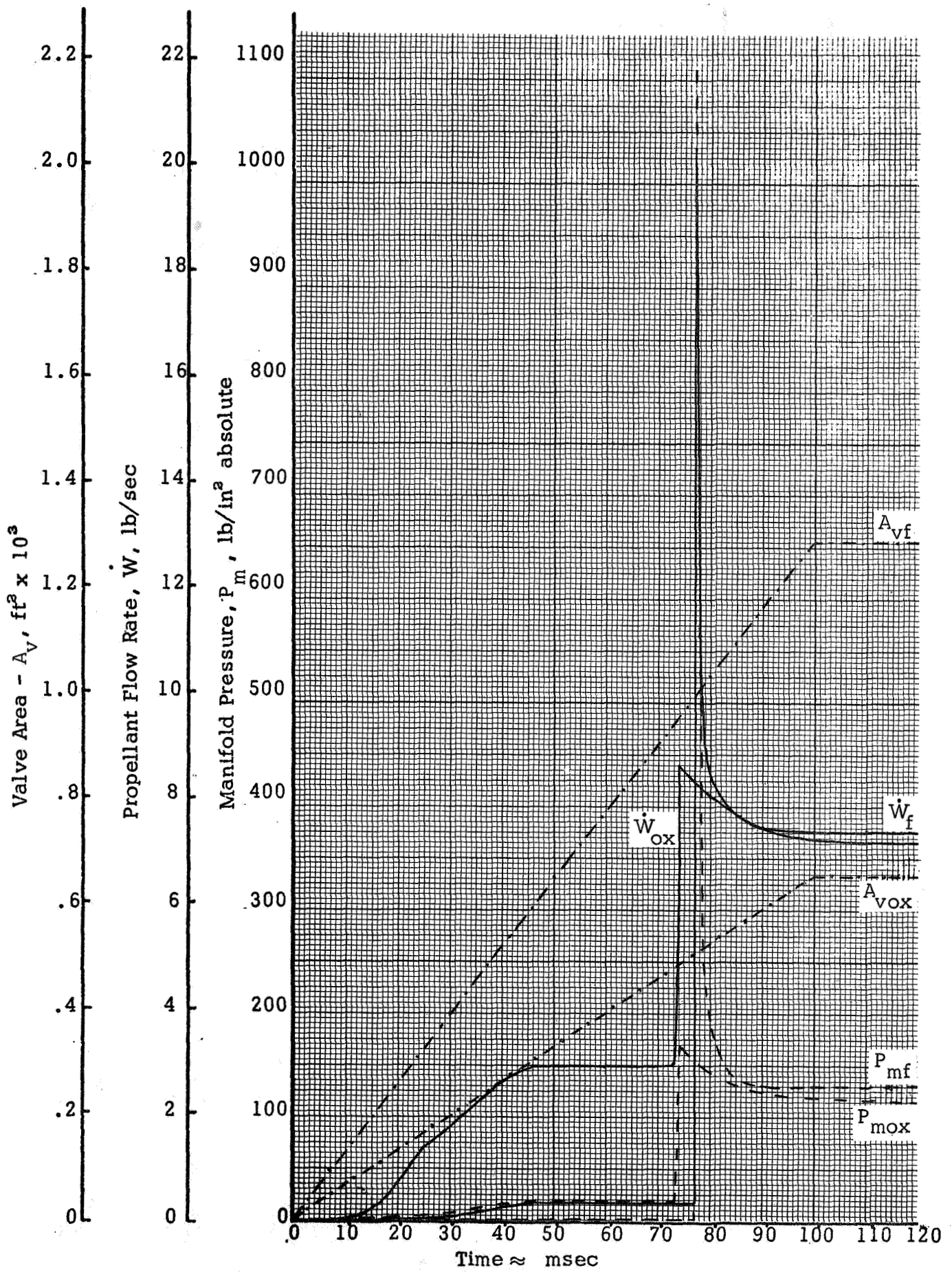


Figure 13. Propellant Flow Transient with Slow Opening Valve.

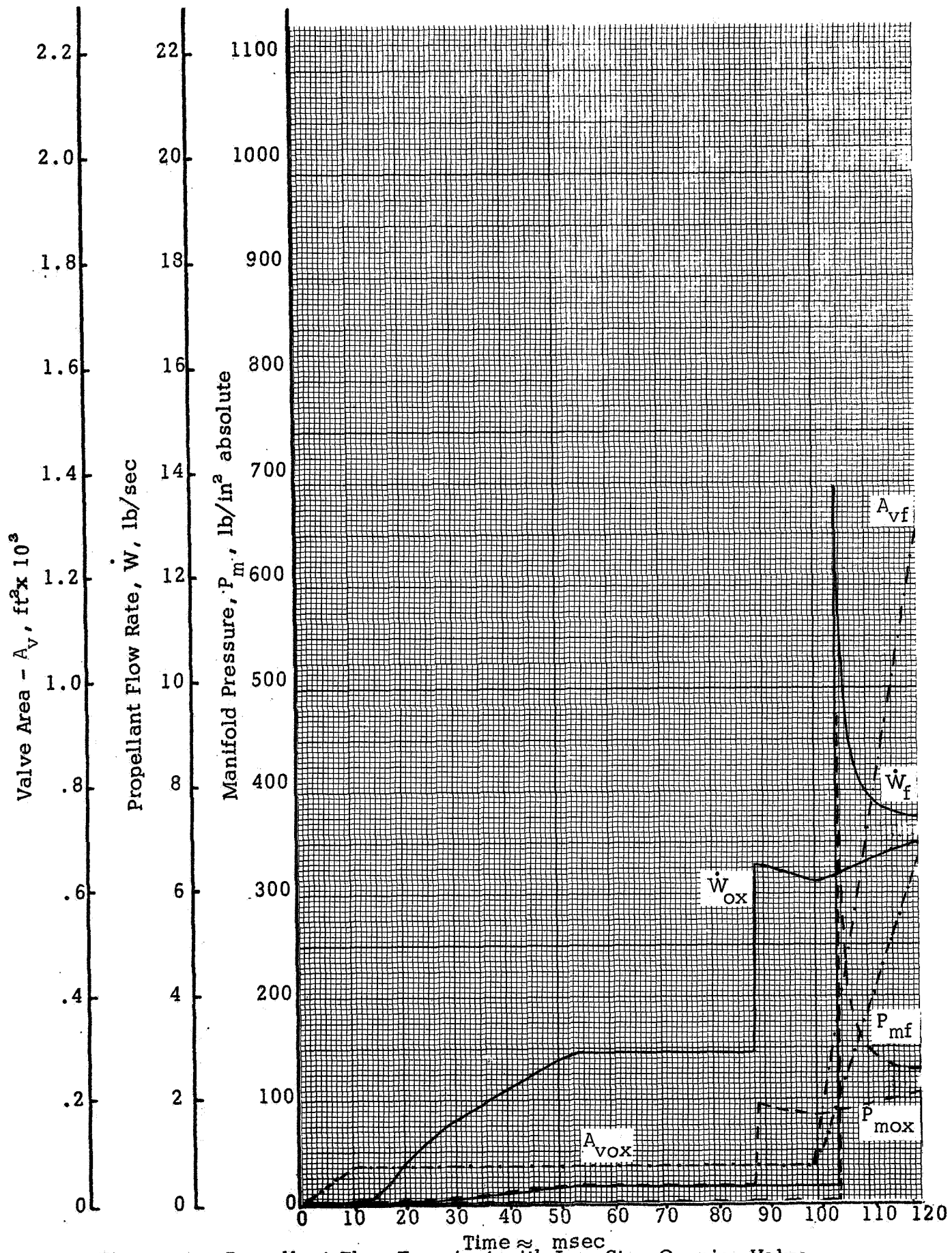


Figure 14. Propellant Flow Transient with Low Step Opening Valve.

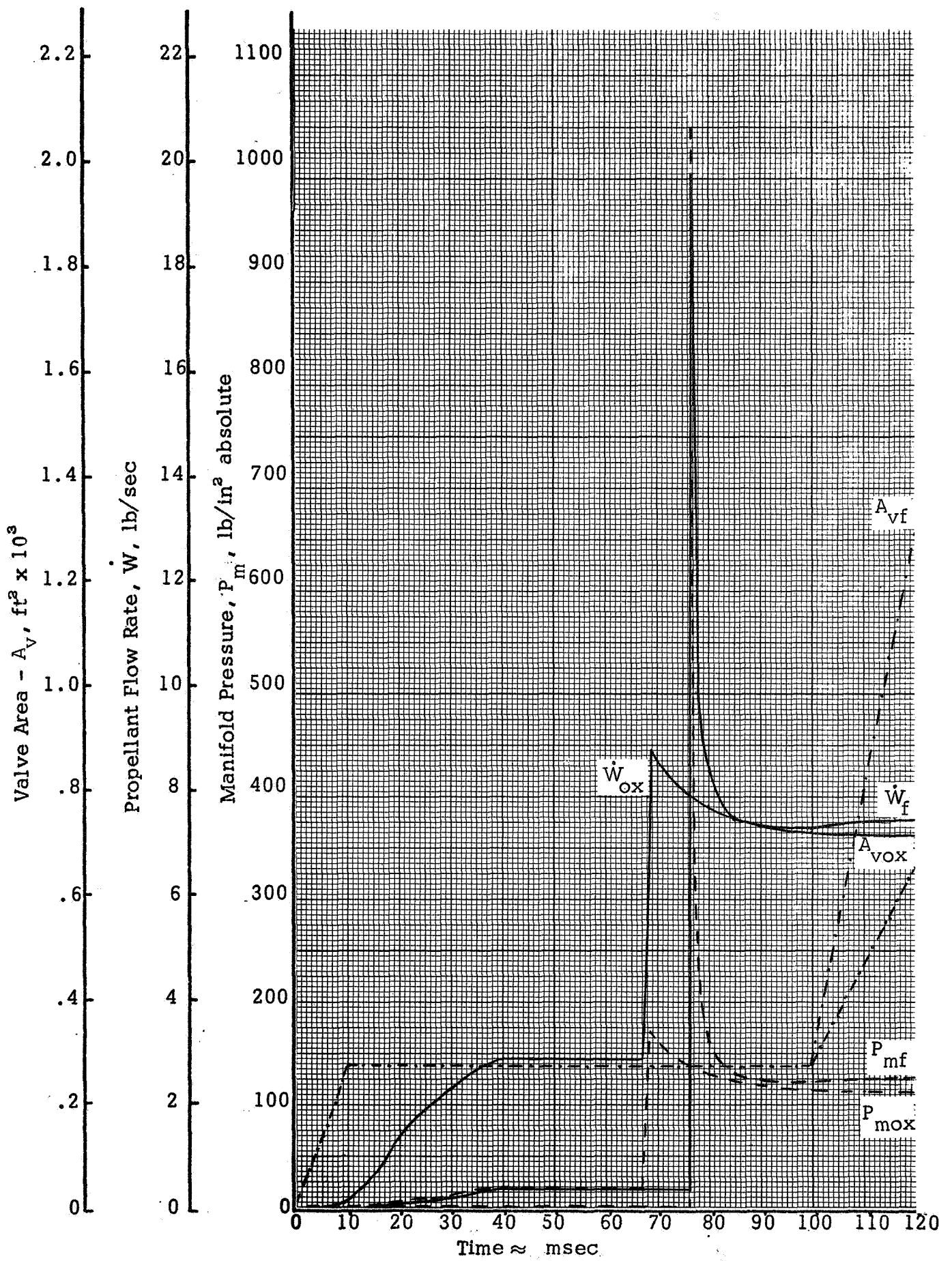


Figure 15. Propellant Flow Transient with Medium Step Opening Valve.

Model Applications

To explore the model's applicability to simulate the start transient of real engines exploratory studies were undertaken to determine if the program was applicable for larger engines, higher density ambient environments, and could predict the preignition pressurization transients.

To accurately predict the initial preignition pressurization transient, it was found from last year's effort that a very small initial step size was needed. The step size was increased as time increased according to the time step-time formula:

$$\Delta t = (t+.1)^{\frac{1}{2}} \times 10^{-5}$$

However, the step size had to remain small to accurately portray the transient. It was found also in the propellant transient model where the step size was controlled by error bounds, that the step size did not increase sufficiently fast, if the valve opened rapidly, in order to calculate long transients. While exploring these conditions, the propellant transient was programmed to simulate a water flow test (Ref. 12) in an attempt to determine the empirical constants within the equation. The test was also performed at atmospheric pressure. Figure 16 shows the experimental and analytical results of this study. The propellant transient model was able to perform the calculation only because the valve opening was very gradual. The calculations were not possible when the valve transient of Figure 17 (Ref. 15) was used, since they program an inordinate amount of time to perform.

From a more basic standpoint, it can be shown that when the propellant flow rate per unit volume of the chamber is low, it is possible for the program to handle the calculations. For instance, if the flow rate per unit volume of the chamber for the experimental engine used in this program is compared to that of the larger engine of Reference 12, it is seen that the flow/volume for the larger engine is twice that of the smaller engine.

<u>Engine</u>	<u>Flow Rate</u>	<u>Volume</u>	<u>Flow/Volume</u>
Large	85 lb/sec	1.169 ft ³	72.7 lb/ft ³ -sec
Small	.147 lb/sec	.00376 ft ³	39.1 lb/ft ³ -sec

Furthermore, the valve opening time and manifold volumes also contribute long transient periods which are difficult to simulate by the techniques developed here. Due to the large amount of computer time needed to perform these

calculations (the propellant transient model and the chamber pressurization transient model), it was decided that the basic program was not applicable to large run times and was applicable only to short transient studies in its present form. From Figure 25, it appears that the propellant transient program will handle transients starting at other than vacuum conditions. The chamber pressurization program has been modified to handle other than vacuum starts and, lacking confirmation from any experimental data, will handle atmospheric starts within the framework of the model.

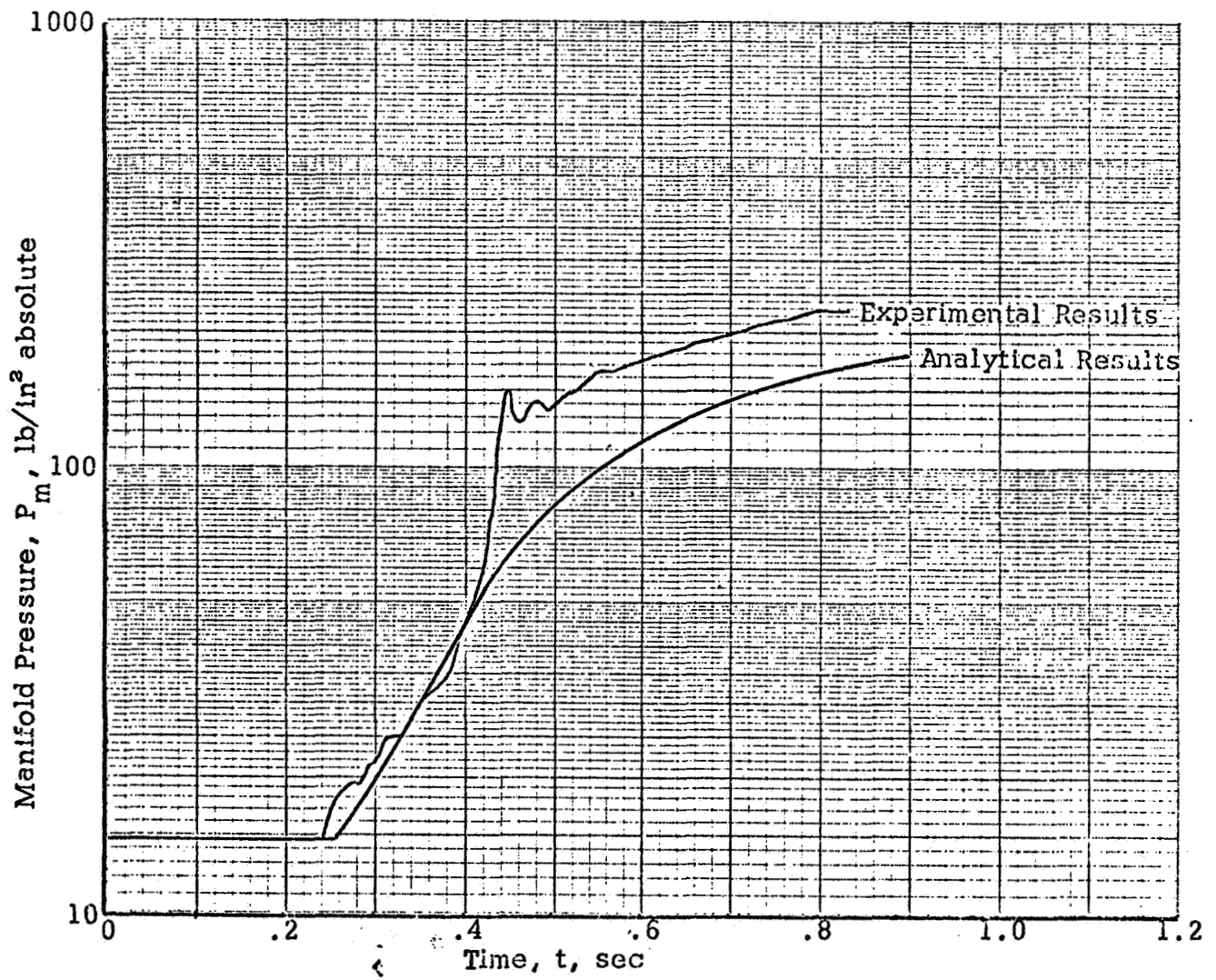


Figure 16. Comparison Between Experimental and Analytical Water Flow Tests on a Large Engine (see Ref. 12).

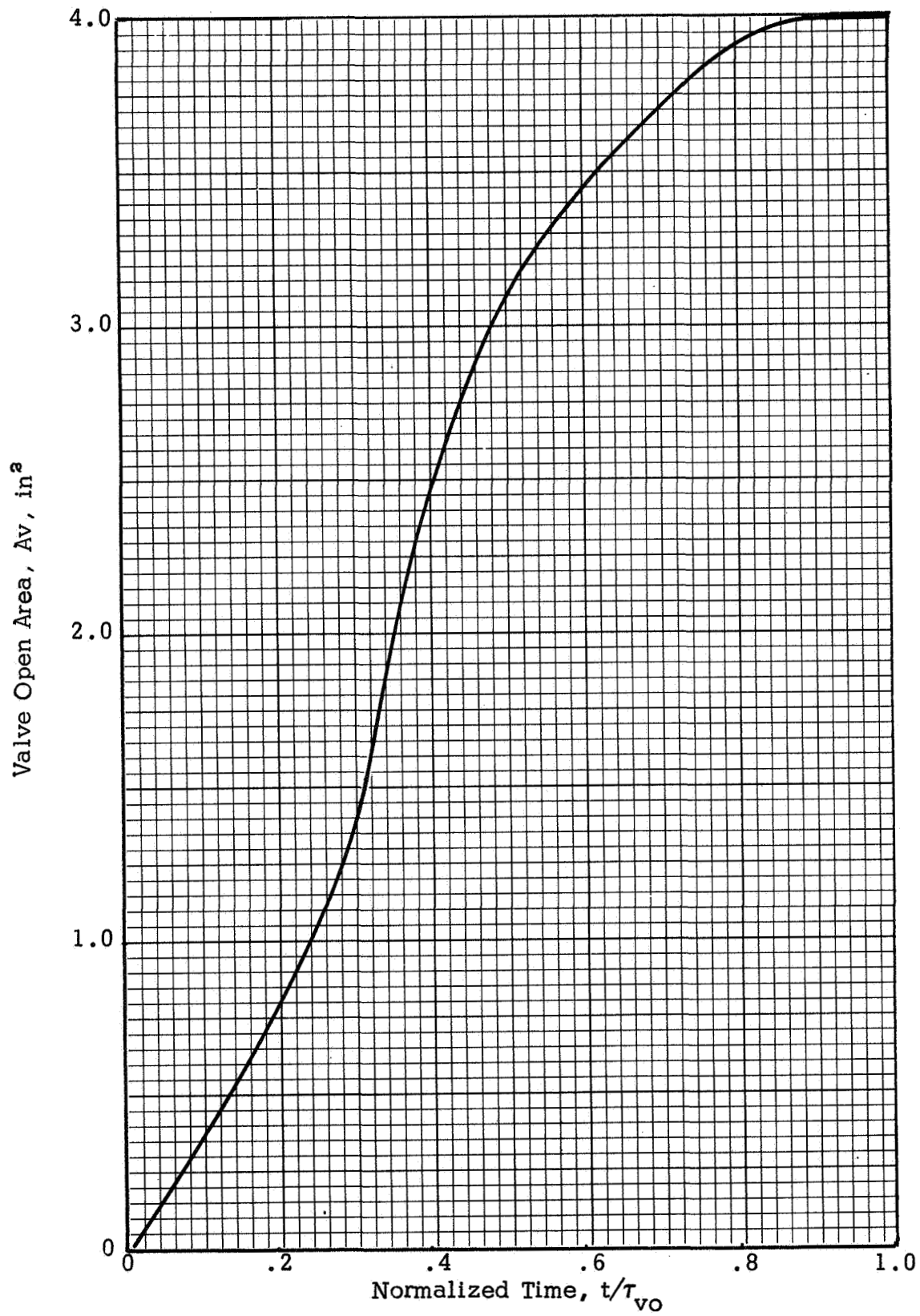


Figure 17. Valve Opening Transient for Larger Engine (see Ref. 12)

3. CHAMBER PRESSURIZATION TRANSIENT PROGRAM

Vaporization Program

The pressurization of a thrust chamber is treated mathematically as a sequence of steady-state processes in very short time intervals. At the start of each new time interval, a new set of drops enter the thrust chamber. These drops undergo vaporization during the time interval as do the drops which entered previously. At any time, each drop has a unique radius, temperature and physical state (solid fraction). The equations used in this part of the program (vaporization) were outlined by Agosta (Ref. 7) and later incorporated into computer programs by Seamans, et al (Ref. 8), and Dynamic Science (Ref. 16).

Basically, the vaporization program accounts for massive operation rates during each time interval to compute the chamber pressure for an arbitrary and transient fuel and oscillator input. Condensation on the chamber wall and mass loss through the nozzle are calculated and used to correct the chamber pressure. The temperature of the gas is based on the mass weighted average of gas, while the different temperatures of each droplet of both the propellant and the fuel for each time interval is accounted for. In accounting for each time interval drop temperature, the radius and also the fraction frozen is accounted for.

Several analytical studies were conducted to improve the operation of the vaporization program and to make it more realistic. These studies investigated the effect of (1) the time step size, (2) the number of initial drop sizes, and (3) the heat transfer between the combustion chamber gases and the chamber wall. Mechanistic additions to the previous year's program of Reference 16 to make it more realistic were (1) preignition reactions, and (2) variable propellant flow rate (by means of tabulated flow rates versus time and/or an orifice flow equation which depends on the chamber pressure).

The ability to use variable time step was particularly important during the initial or zero pressure starting of the calculation. Reduction in time increments from 25×10^{-6} seconds down to the range of 5×10^{-6} seconds showed significant influence on the solution. Reductions from one microsecond to one-half microsecond showed no significant change in pressurization solution. Calculations based on this short time step can be speeded up by drop averaging of drops which have been in the chamber for 5 to 10 time steps because all of these older drops behave in an average way.

The vaporization model was initially set up with a drop size distribution containing three radii of 7.00×10^{-4} , 2.05×10^{-3} , and 4.61×10^{-3} inches, each radius representing respectively 30%, 40%, and 30% of the total propellant injected. This scheme also resulted in high computing costs. In an effort to reduce these costs, a comparison between the three-drop distribution and a one-drop distribution of radius 2.05×10^{-3} inches was made. Nitrogen tetroxide only was injected and from these results there is very little difference in chamber pressure between these two distributions. As a result, the vaporization program now uses a single droplet model having a radius of 2.05×10^{-3} inches.

Preignition Chemistry

Preignition chemical reactions were considered so that ignition could ultimately be achieved. The analytical framework for treating preignition chemistry is as follows: the vapor reaction stoichiometry, heat of reaction and rate of reaction are governed by chamber temperature and reactant vapor partial pressures which are continually computed and followed by the vaporization program. Within this framework shown in Figure 18, the chemical and the controlling physical mechanism limits measured by Zung (Ref. 3) were used.

Preignition reaction intermediates (Refs. 3, 4, and 6) provide both the initiating mechanism for the detonations and the chemical energy to sustain them. Combination of hardware designs (valve configurations, propellant manifolds and manifold volumes, injector configurations, feed system configurations, etc.) combined with the proper operating modes of the system could produce those conditions which are most susceptible to ignition detonations.

To reduce the number of the engineering variables other studies were performed using the Chamber Pressurization Transient Model. Reference 3, a study of N_2O_4/N_2H_4 ignition mechanisms, indicates that hydrazine temperature controls ignition. As the hydrazine temperature is varied, distinct regions (Fig. 19, Ref. 3) are encountered wherein the ignition's mechanisms are different. At the lower temperatures (below approximately $560^\circ R$), reaction between liquid hydrazine and vapor nitrogen tetroxide occurs by reactions on the surface of the hydrazine leading to detonable reaction intermediates.

Detonation Program

Following the running of the vaporization program to ignition or for a specified time, detonation properties were computed for various selected times.

Detonation properties were calculated by the NASA/Lewis detonation program given in Reference 16. This program is well documented in References 16 and 17, so a discussion of the basic principles used is not needed here. To fit the data from the vaporization program to the detonation program, some modifications to the data are necessary. The detonation program is written for gaseous reactants while the reactants calculated by the vaporization program contain liquid droplets in a gaseous atmosphere. Table III is a tabulation of some of the data calculated from the vaporization program; the "f" listed in Table III is the fraction of a liquid propellant species to the total propellant species (liquid and gaseous). This f factor is used to convert the liquid propellant to a pseudo equivalent amount of gaseous reactants. Inherent with this conversion is that all of the liquid will be consumed in the detonation process.

All of each propellant species is converted to vapor reactants having a molecular weight in the ratio: weight of liquid + weight of vapor propellant/weight of vapor propellant ($\mathcal{W}_l + \mathcal{W}_g / \mathcal{W}_g$). The new propellant enthalpy is obtained by adding the gaseous molar enthalpy to the liquid molar enthalpy which has been corrected by the liquid to vapor ratio: $[H = H_l + H_g (\mathcal{W}_l / \mathcal{W}_g)]$. Thus, each liquid propellant species is converted to a pseudo vapor wherein the molecular weight and enthalpy are obtained as outlined above.

Results

Ignition transient studies were conducted using the Chamber Pressurization Transient Program where the propellant temperatures were varied (Ref. 17). In Figure 20, reproduced higher detonation pressures occur as the temperature is decreased. Further, as the time to detonation is increased, and more reaction intermediates are produced, the detonation pressure is increased.

From an empirical standpoint (Refs. 2 and 18), the occurrence and level of spiking is influenced by the sequence in which propellants enter the combustion chamber. Figure 21 from Reference 19 shows the results of these tests. These tests were performed with N_2O_4 /UDMH- N_2H_4 . These results can best be explained by considering the analytical cases shown in Figure 22. When N_2O_4 is injected into a vacuum atmosphere, its high vapor pressure results in a low vapor temperature. The subsequent injection of hydrazine into this low temperature results in the formation of liquid phase reaction intermediates. Figure 23 (Ref. 3) shows the effects of oxidizer vapor temperature on the ignition

of N_2O_4/N_2H_4 . If the N_2O_4 temperature regions in this figure are lowered to a level indicated in the preignition transient of Figure 24, no immediate ignition will occur, but reaction intermediates would form until the heat of reaction raises the temperature to a level high enough for ignition. Furthermore, it appears that for colder propellant temperatures and for longer fuel leads, the time to detonation increases, as well.

In conclusion, from the analytical studies using the Propellant Transient Flow Program and the Chamber Pressurization Transient Program, the following are considered to be the dominant engineering parameters influencing the occurrence of start transient spiking.

- (1) The fuel temperature should be high enough to prevent the formation of detonable reaction intermediates.
- (2) Short oxidizer leads are conducive to spiking if, during the lead condition, the gaseous chamber temperature is reduced to a level where reaction intermediates may form.
- (3) Cold propellant fuel lead conditions become more conducive to spiking than do other lead conditions.
- (4) Controlled propellant transient to achieve rapid ignition will reduce transient spiking.

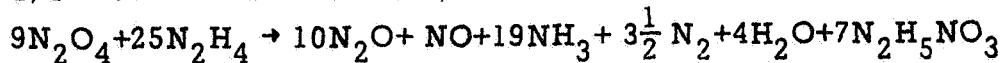
TABLE III

RESULTS OF VAPORIZATION AND DETONATION COMPUTATIONS

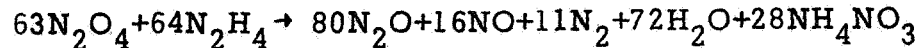
Run No.	t (ms)	T _{ox} (R)	T _{fu} (R)	T _w (R)	Lead	P _c (psia)	T _c (R)	O/F	f (N ₂ O ₄)	f (N ₂ H ₄)	Weight N ₂ O ₄ (lb)	Weight N ₂ H ₄ (lb)	Weight N ₂ H ₅ NO ₃ (lb)	Weight NH ₄ NO ₃ (lb)	P _D (psia)	P _P (psia)	T _D (R)	Ign. (ms)
1	1	540	540	540	o/-	.83	499	1.67	.655	.953	1.38x10 ⁻⁴	8.27x10 ⁻⁴	5.44x10 ⁻⁸	375	201	3285	-	
2	2	540	540	540	o/-	2.12	525	2.15	.710	.945	4.16x10 ⁻⁴	1.94x10 ⁻⁴	6.19x10 ⁻⁷	757	405	3504	-	
3	3	540	540	540	o/-	3.00	551	2.23	.766	.946	6.79x10 ⁻⁴	3.03x10 ⁻⁴	2.20x10 ⁻⁶	1139	610	3520	-	
2	3	540	540	540	2/F	.92	538	.89	.748	.942	1.94x10 ⁻⁴	2.18x10 ⁻⁴	1.91x10 ⁻⁷	498	267	3467	5+	
4	4	540	540	540	2/F	2.17	568	1.44	.770	.945	4.76x10 ⁻⁴	3.29x10 ⁻⁴	1.45x10 ⁻⁶	984	526	3668	-	
5	5	540	540	540	2/Ox	4.27	717	1.67	.799	.954	7.35x10 ⁻⁴	4.34x10 ⁻⁴	3.75x10 ⁻⁶	1367	731	3664	-	
3	3	540	540	540	2/Ox	2.52	526	5.65	.768	.974	6.31x10 ⁻⁴	1.11x10 ⁻⁴	5.44x10 ⁻⁷	695	378	2728	-	
4	4	540	540	540	2/Ox	3.26	545	3.99	.804	.972	8.94x10 ⁻⁴	2.22x10 ⁻⁴	2.21x10 ⁻⁶	1160	626	3067	-	
5	5	540	540	540	2/Ox	3.94	553	3.42	.828	.976	1.15x10 ⁻³	3.30x10 ⁻⁴	4.64x10 ⁻⁶	1596	859	3211	-	
4	1	500	500	540	o/-	.46	478	1.30	.716	.983	9.59x10 ⁻⁵	7.40x10 ⁻⁵	9.64x10 ⁻⁹	237	126	3461	-	
2	2	500	500	540	o/-	1.58	496	2.06	.743	.992	3.82x10 ⁻⁴	1.86x10 ⁻⁴	1.52x10 ⁻⁷	717	383	3514	-	
3	3	500	500	540	o/-	2.42	505	2.23	.776	.994	6.62x10 ⁻⁴	2.97x10 ⁻⁴	5.62x10 ⁻⁷	1317	706	3382	-	
5	4	500	500	540	3/F	.66	487	.70	.761	.994	1.65x10 ⁻⁴	3.48x10 ⁻⁴	3.59x10 ⁻⁸	552	294	3558	-	
5	5	500	500	540	3/F	1.65	505	1.31	.682	.998	4.56x10 ⁻⁴	3.48x10 ⁻⁴	2.47x10 ⁻⁷	1006	538	3675	-	
6	6	500	500	540	3/F	2.40	514	1.60	.805	.996	7.33x10 ⁻⁴	4.58x10 ⁻⁴	7.47x10 ⁻⁷	2004	1072	3750	-	
6	4	500	500	540	3/Ox	2.52	586	7.76	.820	.991	8.85x10 ⁻⁴	1.14x10 ⁻⁴	1.58x10 ⁻⁷	821	451	2389	-	
5	5	500	500	540	3/Ox	2.75	501	5.12	.853	.994	1.16x10 ⁻³	2.26x10 ⁻⁴	6.08x10 ⁻⁶	1385	752	2838	-	
6	6	500	500	540	3/Ox	2.83	500	4.23	.879	.996	1.42x10 ⁻³	3.36x10 ⁻⁴	1.12x10 ⁻⁶	1944	1060	3038	-	
7	1	540	540	580	o/-	.81	498	1.66	.655	.954	1.35x10 ⁻⁴	8.16x10 ⁻⁵	5.23x10 ⁻⁸	375	202	3285	3.6	
2	2	540	540	580	o/-	2.18	543	2.14	.710	.945	4.15x10 ⁻⁴	1.93x10 ⁻⁴	7.78x10 ⁻⁷	756	404	3502	-	
3	3	540	540	580	o/-	3.24	590	2.23	.776	.954	6.76x10 ⁻⁴	3.01x10 ⁻⁴	3.35x10 ⁻⁶	1145	613	3513	-	
8	1	540	540	500	o/-	.81	498	1.66	.655	.954	1.35x10 ⁻⁴	8.16x10 ⁻⁵	5.23x10 ⁻⁸	375	202	3285	-	
2	2	540	540	500	o/-	2.06	511	2.15	.708	.943	4.16x10 ⁻⁴	1.94x10 ⁻⁴	5.22x10 ⁻⁷	759	406	3505	-	
3	3	540	540	500	o/-	2.84	522	2.24	.763	.941	6.81x10 ⁻⁴	3.04x10 ⁻⁴	1.48x10 ⁻⁶	1129	604	3525	-	
9	1	580	540	540	o/-	.95	573	1.65	.665	.956	1.41x10 ⁻⁴	8.54x10 ⁻⁵	2.19x10 ⁻⁷	326	174	3487	2.0	
2	2	580	540	540	o/-	4.63	886	1.95	.688	.975	3.81x10 ⁻⁴	1.88x10 ⁻⁴	1.03x10 ⁻⁶	678	363	3468	-	
3	3	580	540	540	o/-	.59	581	1.51	.716	.955	1.17x10 ⁻⁴	7.78x10 ⁻⁵	2.48x10 ⁻⁸	293	156	3488	-	
10	1	500	540	540	o/-	1.72	502	2.16	.749	.943	4.10x10 ⁻⁴	1.90x10 ⁻⁴	2.95x10 ⁻⁷	726	388	3496	-	
2	2	500	540	540	o/-	2.55	514	2.29	.783	.940	6.88x10 ⁻⁴	3.01x10 ⁻⁴	1.02x10 ⁻⁶	1196	646	3511	-	
3	3	500	540	540	o/-	.95	503	1.82	.658	.874	1.56x10 ⁻⁴	8.54x10 ⁻⁵	9.08x10 ⁻⁸	269	143	3435	3.6	
11	1	540	580	540	o/-	2.28	534	2.21	.709	.860	4.34x10 ⁻⁴	1.96x10 ⁻⁴	9.35x10 ⁻⁷	606	324	3467	-	
2	2	540	580	540	o/-	3.30	581	2.27	.776	.869	6.95x10 ⁻⁴	3.03x10 ⁻⁴	3.62x10 ⁻⁶	890	477	3482	-	
3	3	540	580	540	o/-	.66	495	1.46	.651	.985	1.14x10 ⁻⁴	7.81x10 ⁻⁵	2.07x10 ⁻⁸	322	172	3499	-	
12	1	540	500	540	o/-	1.93	517	2.07	.831	.993	3.96x10 ⁻⁴	1.91x10 ⁻⁴	3.22x10 ⁻⁷	886	474	3538	-	
2	2	540	500	540	o/-	2.73	528	2.19	.762	.998	6.62x10 ⁻⁴	3.02x10 ⁻⁴	1.03x10 ⁻⁶	1431	766	3560	-	

$$400 \leq T \leq 530^{\circ}\text{R}$$

$$\text{O/F} \leq .5 \quad \Delta H = 1123 \text{ Btu/lb}$$

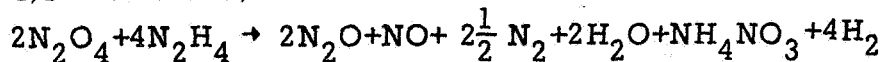


$$\text{O/F} > .5 \quad \Delta H = 2220 \text{ Btu/lb}$$



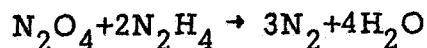
$$530 < T \leq 600^{\circ}\text{R}$$

$$\text{O/F} \leq .5 \text{ and } \text{O/F} > .5 \quad \Delta H = 2605 \text{ Btu/lb}$$

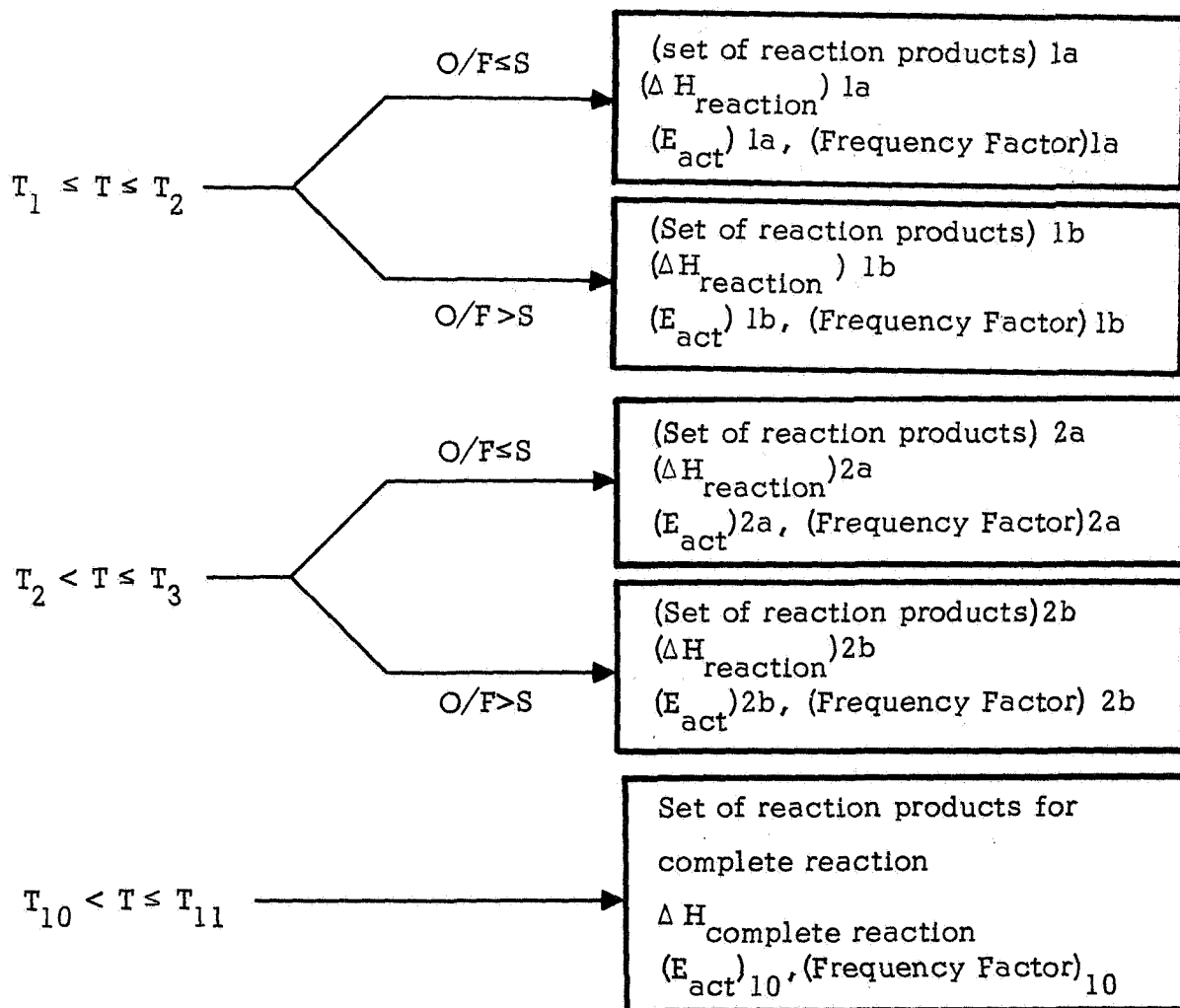


$$600 < T \leq 10,000^{\circ}\text{R}$$

$$\text{O/F} \leq .5 \text{ and } \text{O/F} > .5 \quad \Delta H = 4860 \text{ Btu/lb}$$



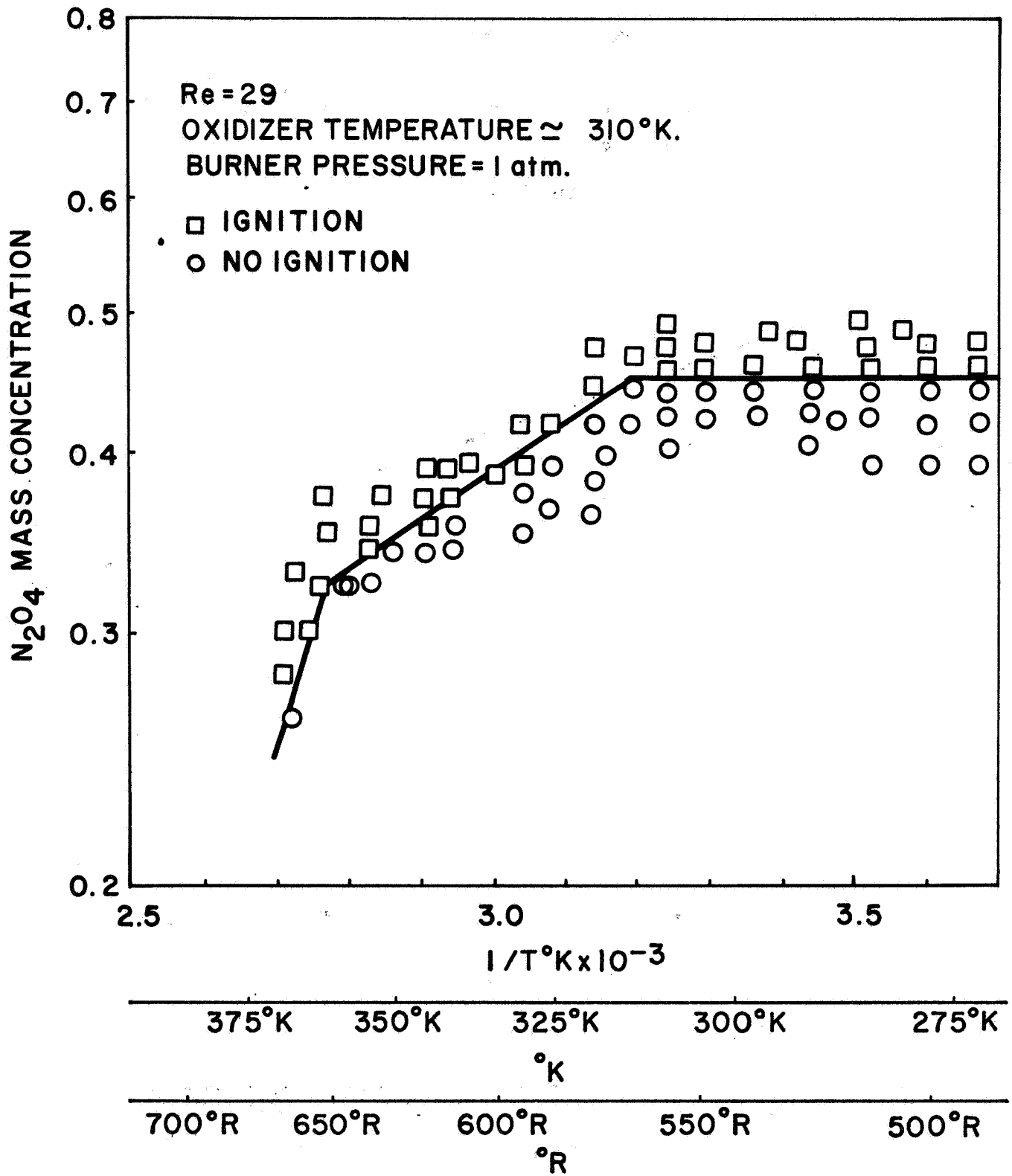
$$E = 7500 \text{ cal/gmole}$$



where, T = gas temperature,

S = stoichiometric oxidizer to fuel ratio

Figure 18. Temperature and O/F Dependent Reaction Paths Measured by Zung (Ref. 3)



HYDRAZINE TEMPERATURE

Figure 19 . Ignition Threshold
 (From Ref. 3)

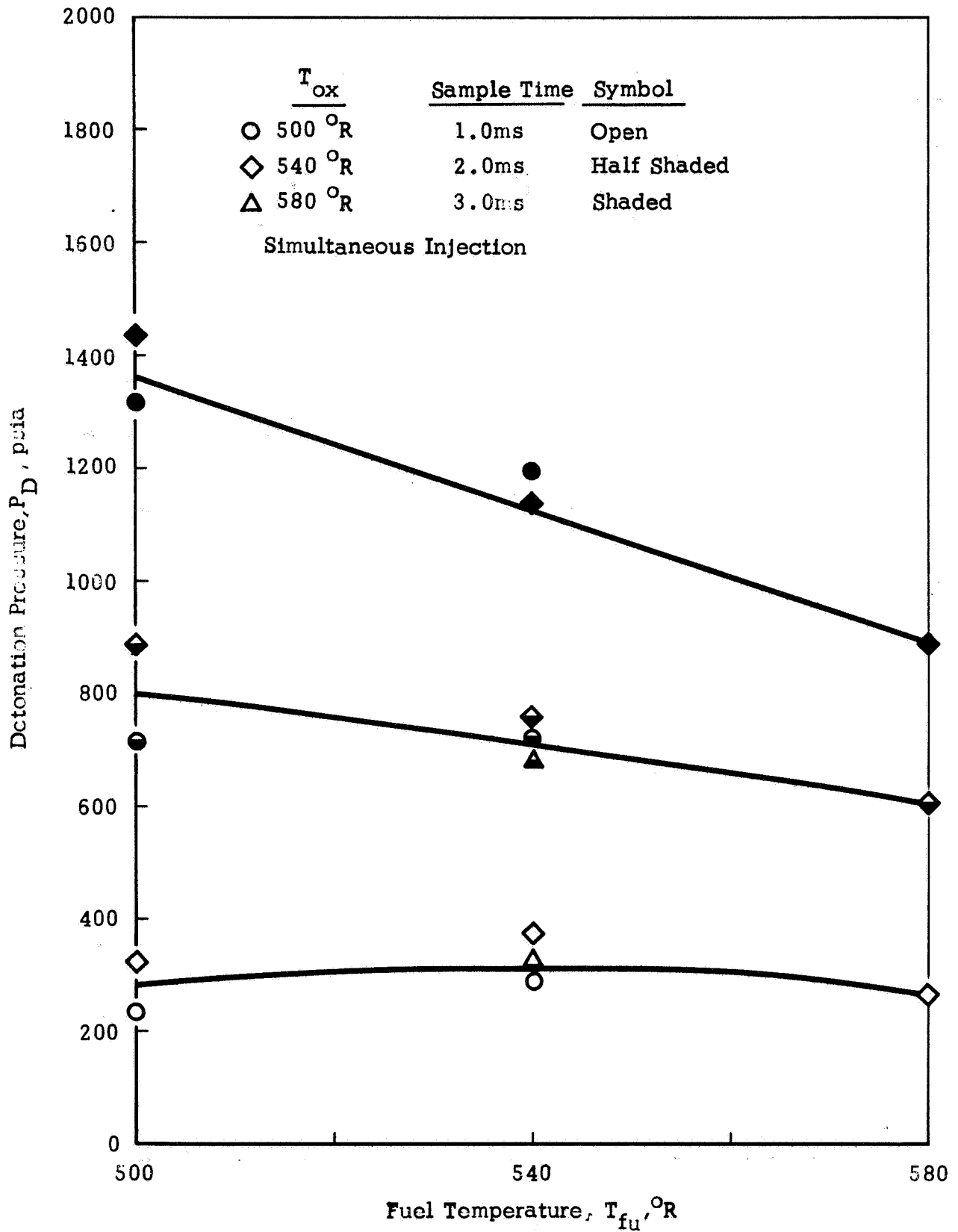


Figure 20. Effect of Fuel Temperature on Detonation Pressure

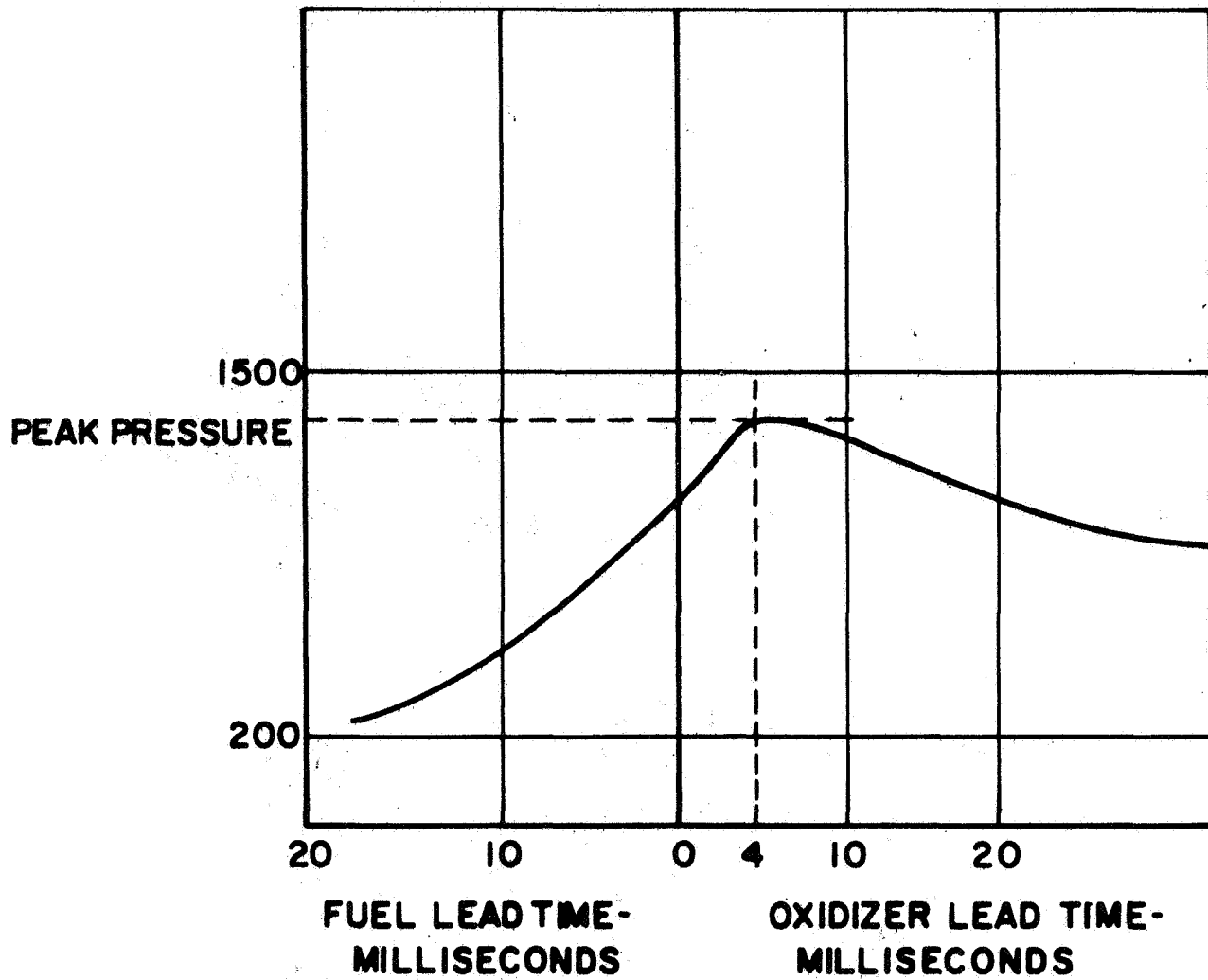


Figure 21. Pressure Peak as a Function of Oxidizer or Fuel Lead.
 (From Ref. 19)

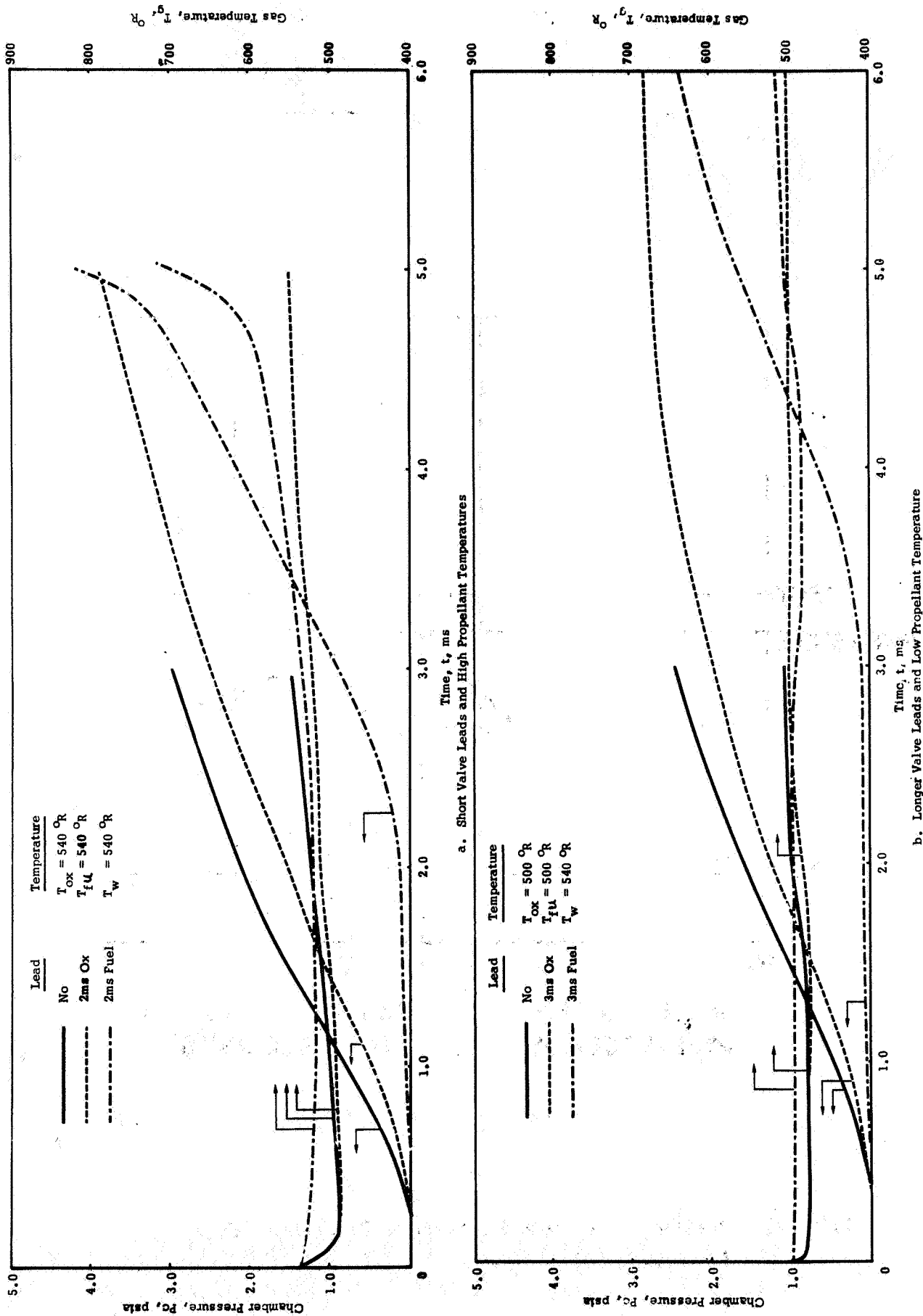


Figure 22 . The Effect of Variable Valve Leads and Initial Temperature on Transient Chamber Pressure and Chamber Gas Temperature .

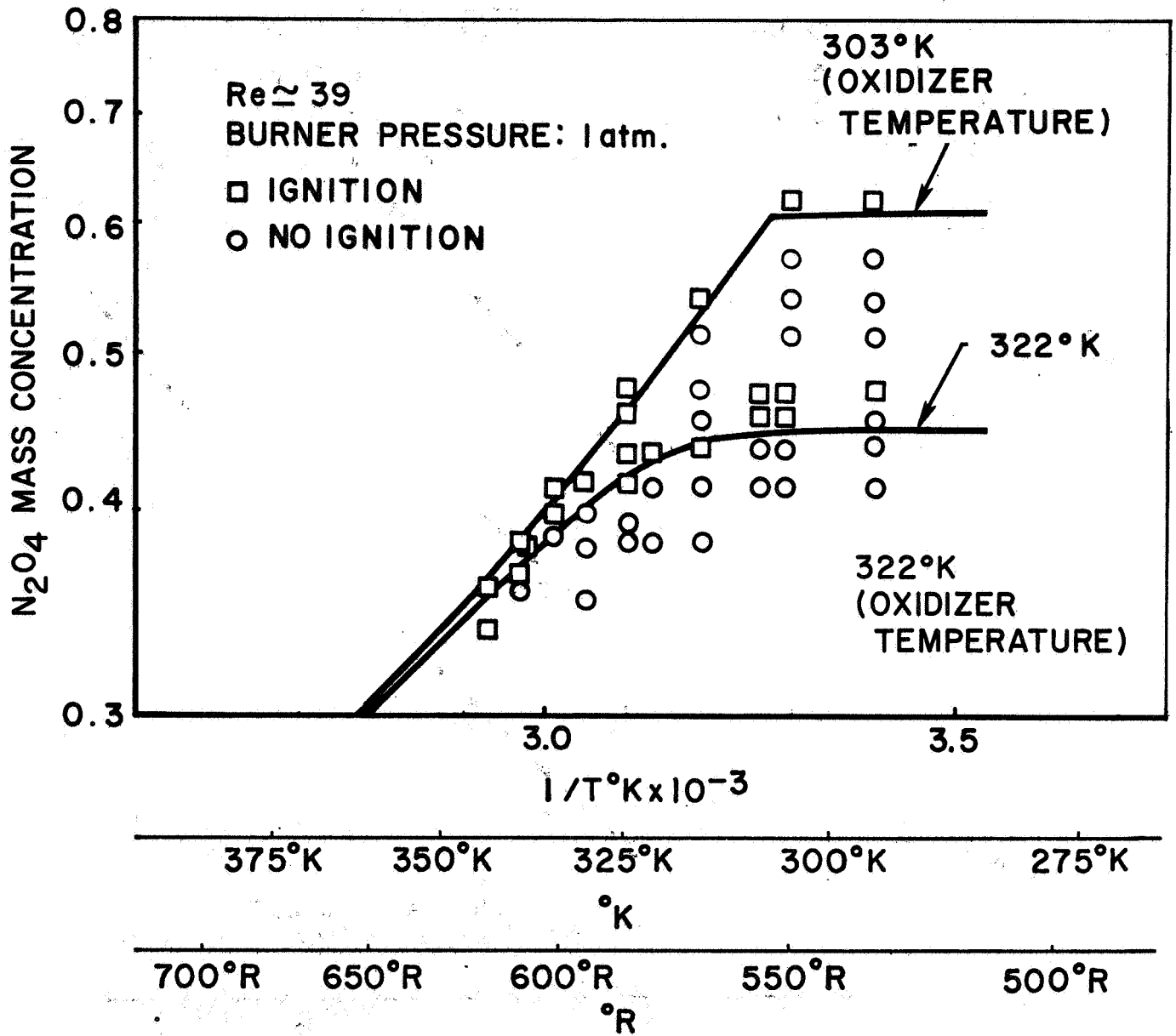


Figure 23 . Ignition Threshold
 (From Ref. 3)

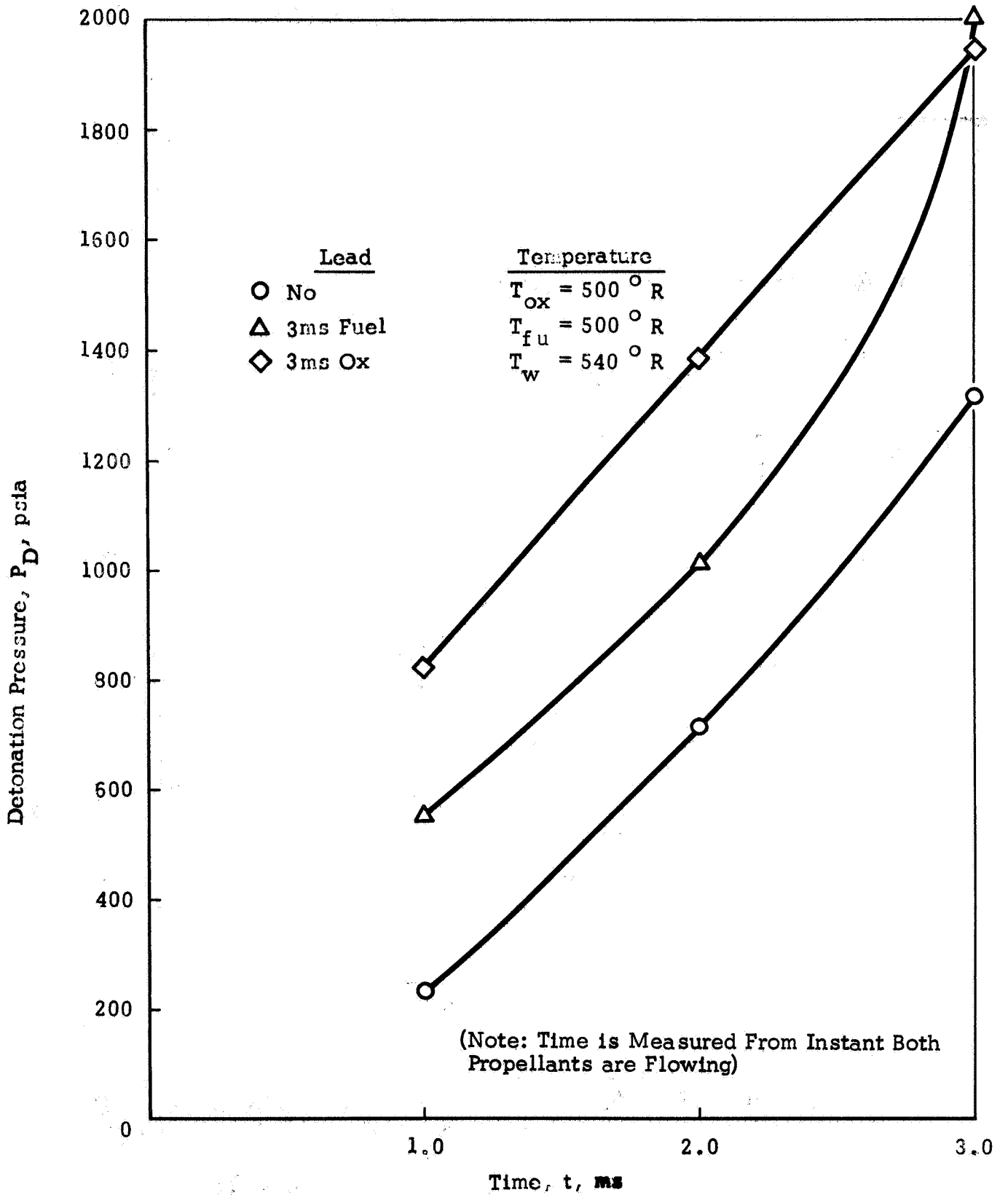


Figure 24. Effect of Propellant Leads and Initial Temperature on Detonation Pressure

4. EXPERIMENTAL PROGRAM

Experiments were performed wherein engineering assumptions and engine parameters influencing spiking could be evaluated in order to determine the applicability of the Start Transient Programs (the Propellant Transient Flow Program and the Chamber Pressurization Transient Program) to predict engine starts.

Hardware and Experimental

From the Start Transient Programs, the following variables were important in influencing the start transient and the start transient spiking behavior: (1) propellant temperature, (2) propellant leads, and (3) the transient behavior of the entering propellants (length and shape of propellant transient). In an attempt to accommodate these assumptions in the experimental hardware, two injectors were fabricated. The first injector (Figure 25), Injector Pattern A (like-on-like) attempts to accommodate the assumption of vapor phase mixing. Pattern A consists of four like-on-like doublet elements which impinge such that the fuel and oxidizer fans do not intersect (Figure 26). This injector keeps the liquid propellants apart while they are being injected and vaporizing, but allow mixing of the propellant vapors. Injector Pattern B (unlike), on the other hand, consists of four mixed twin elements. This injector pattern is used in current high-performance attitude control engines. The effects on the start transient of these two injectors were observed experimentally. These patterns were drilled into a propellant manifold configuration which is the same for both patterns (Fig. 27). Completing the injector-manifold is a cover plate (Fig. 28) which incorporates the instrumentation for the fuel side and which forms the cover for the fuel and temperature conditioning fluid manifolds (Fig. 29). The central oxidizer inlet and manifold is connected to an AN cross into which is plumbed the main propellant valve, the Freon flush valve, the gaseous nitrogen purge valve, and the oxidizer manifold pressure port. The fuel enters the backing plate through two inlets which are similarly connected to an AN cross via two 1/8 inch tubes. The fuel cross is plumbed to the main propellant valve, the gaseous nitrogen purge valve, and the Freon flush valve. During the initial tests, the manifold volumes consisted of the crosses, the connecting tubing, and the injector body. These volumes were .232 in³ and .252 in³ for the oxidizer and the fuel manifolds, respectively.

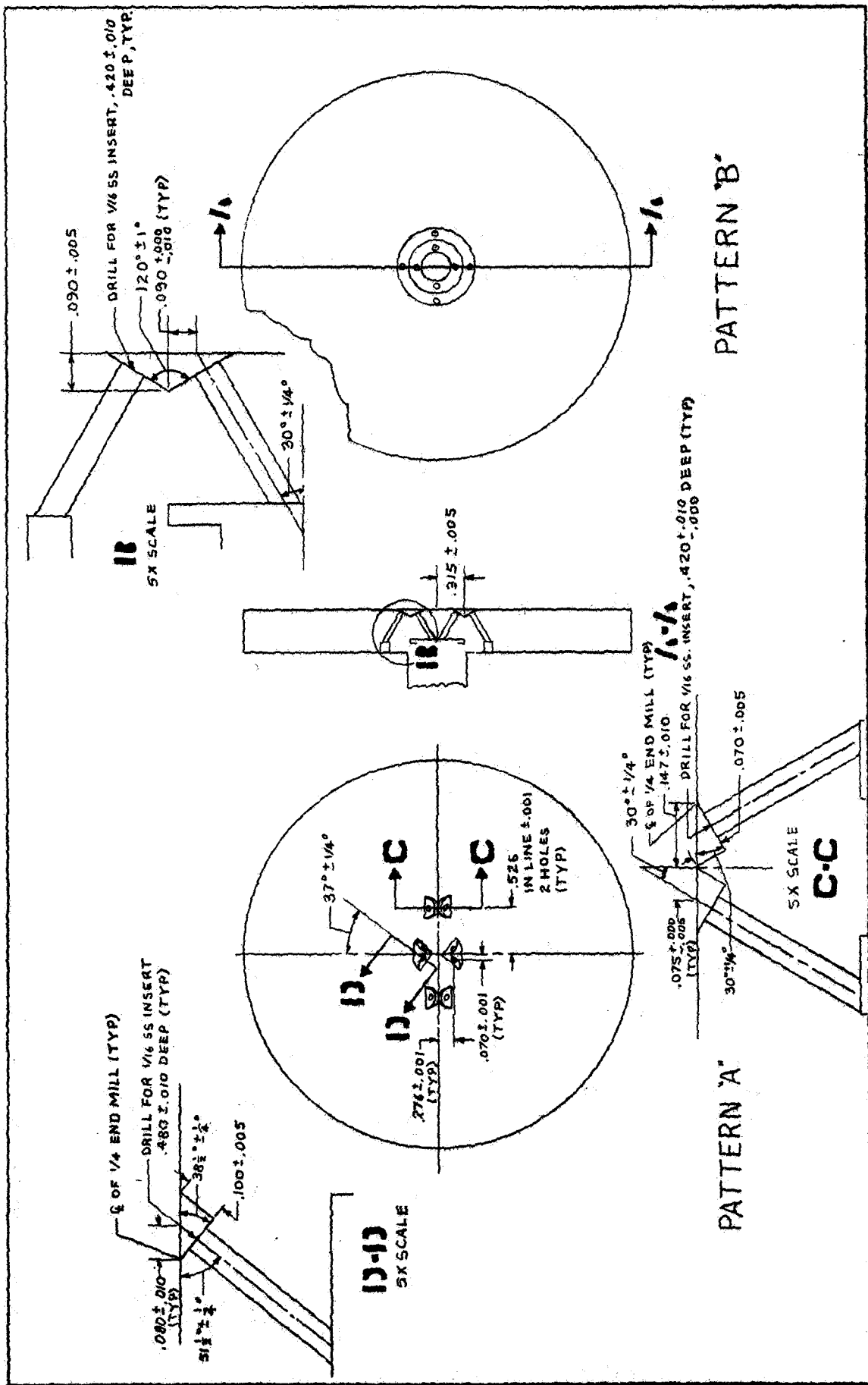
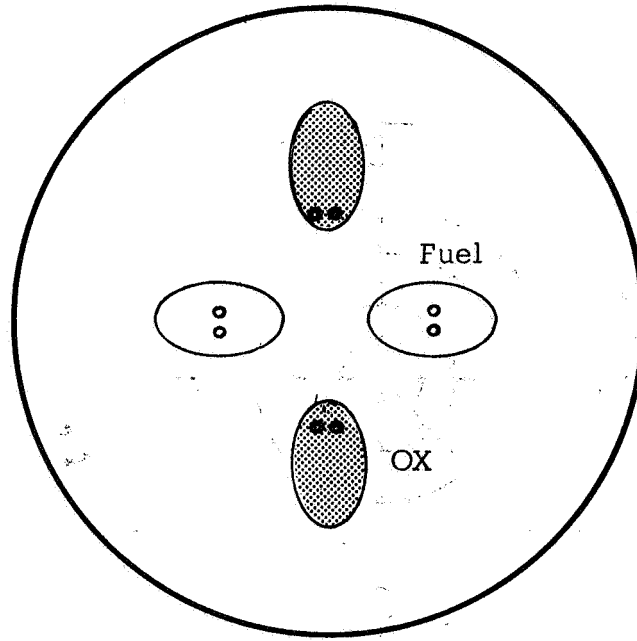
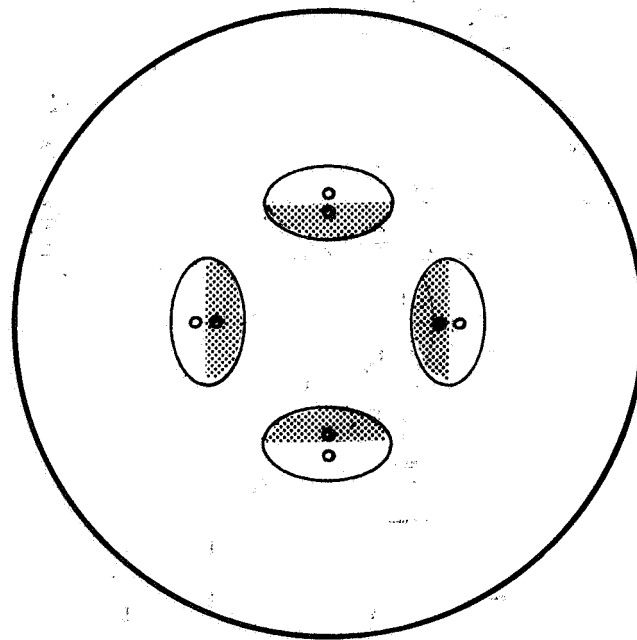


Figure 25. Injector Patterns



Pattern A



Pattern B

Figure 26. Propellant Spray Patterns from Experimental Injectors.

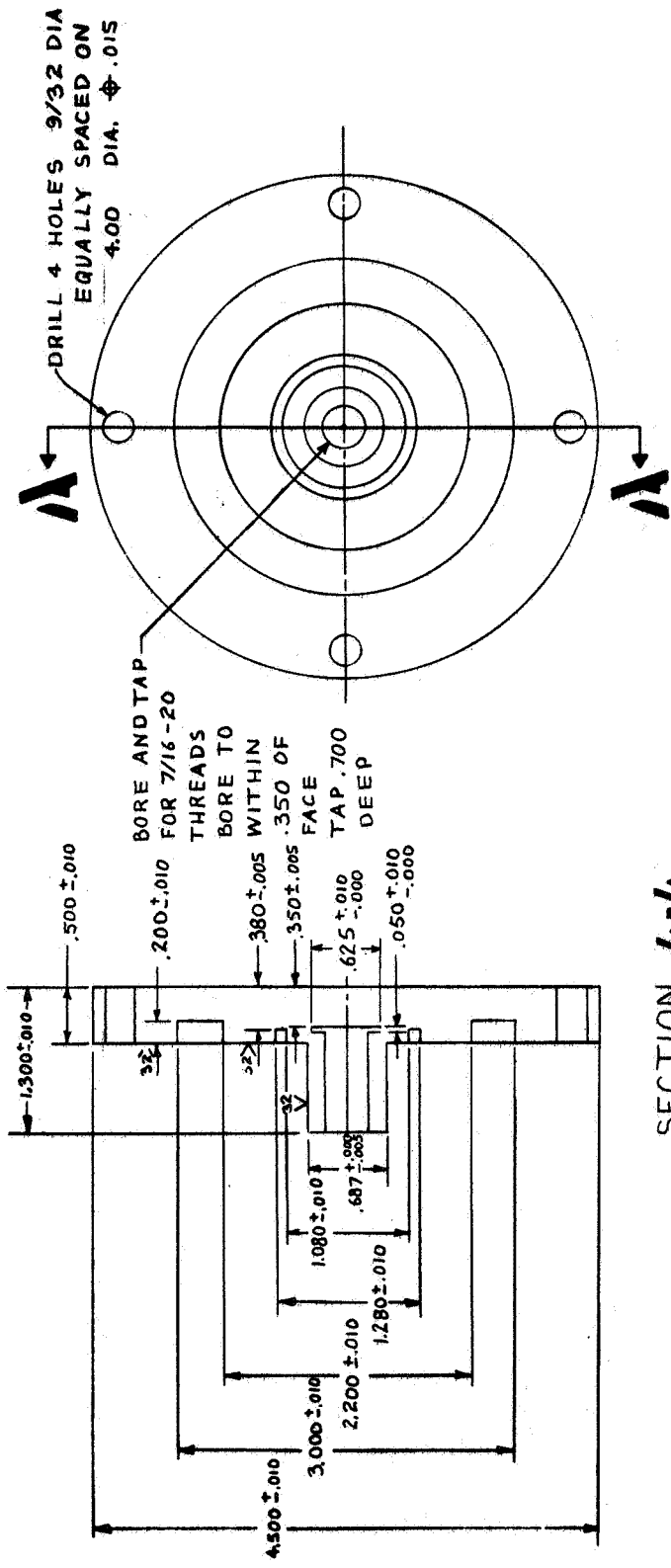


Figure 27. Injector Blank.

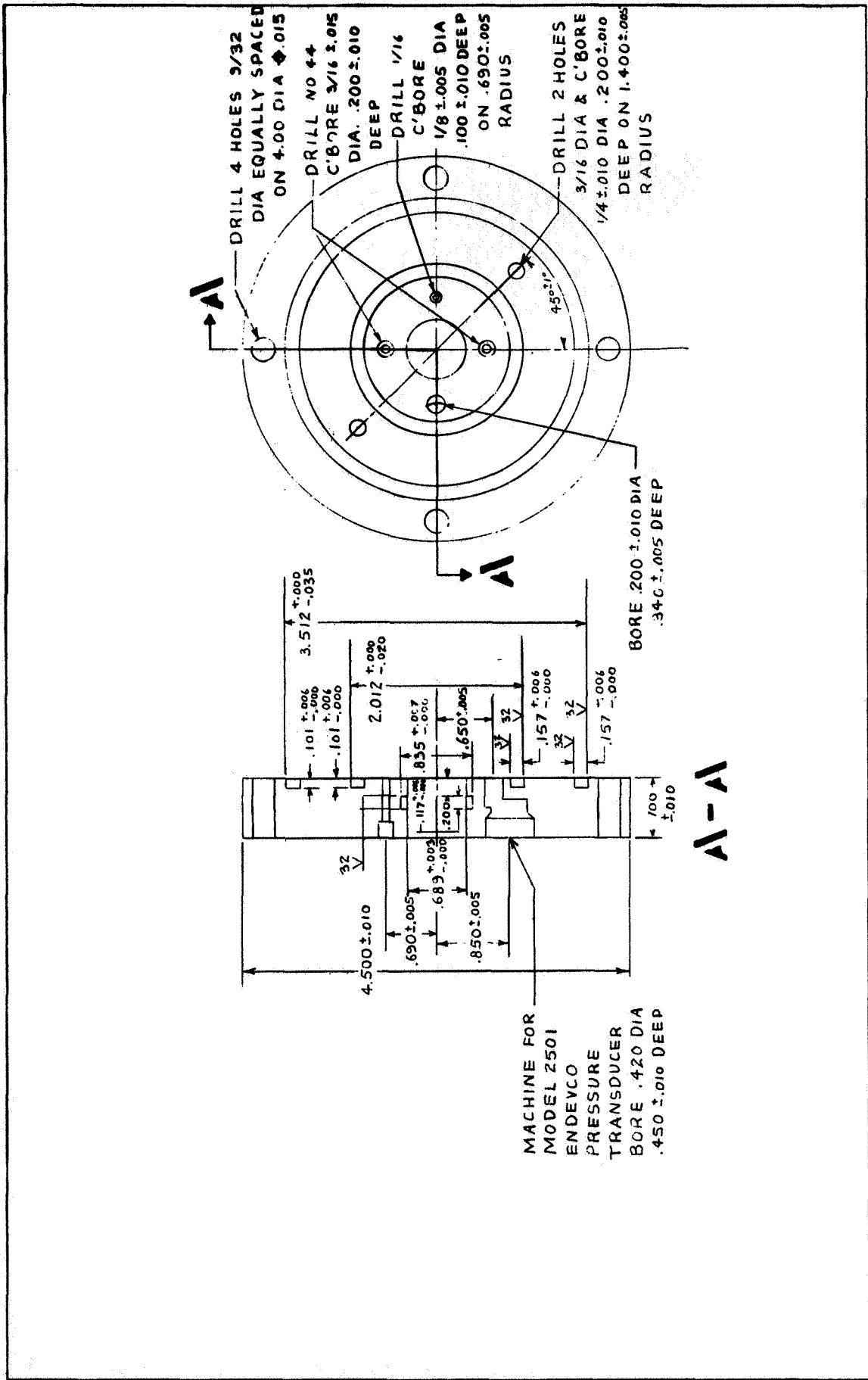


Figure 28. Cover Plate

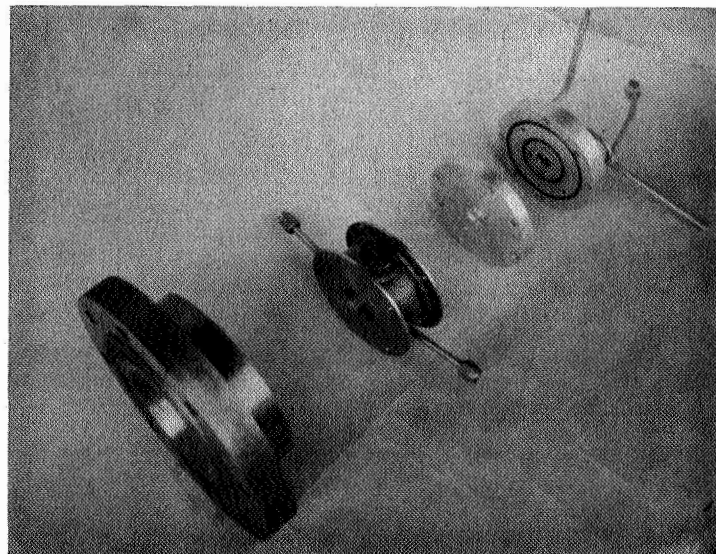
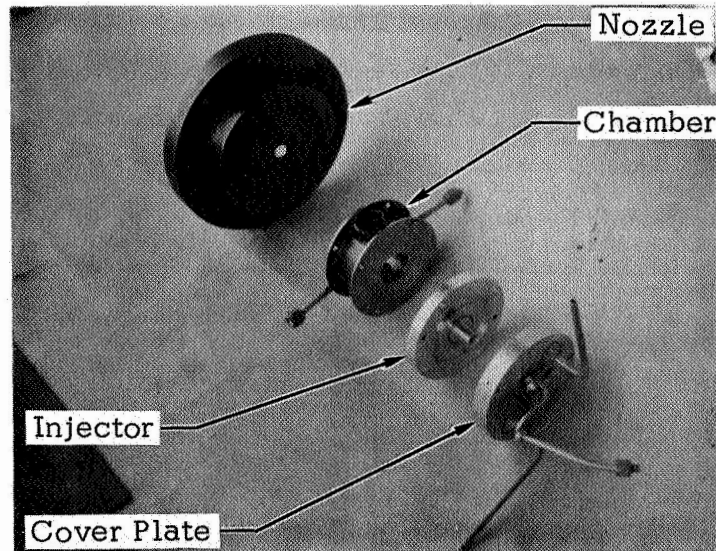


Figure 29. Exploded View of Combustion Chamber and Injector Assembly.

These volumes were subsequently reduced by solder filling some of the manifolds. The final tests were conducted with manifolds having volumes of $.1037 \text{ in}^3$ for the oxidizer and fuel manifolds, respectively.

Completing the experimental hardware are the combustion chamber and the nozzle (Figs. 28 and 29). This hardware was designed to operate under those conditions listed in Table IV. The experimental work was done with a chamber length of 1.75 in. The chamber had two high response pressure transducer ports, a chamber wall thermocouple port and two fluid flow lines leading to the temperature conditioning jacket surrounding the chamber. The assembled components are seen in Figure 30.

During the initial tests, the main propellant valves used were solenoid valves (Echel Valve AF 56C-35). Subsequent tests utilized a pneumatically controlled pintle valve. This valve consists of a pneumatic cylinder with the plunger attached to a yoke which, in turn, lifts the tapered pintles. The valve opening time can be controlled by varying the orifice opening and supply pressure to the pneumatic cylinder. Propellant leads can be varied by adjusting each pintle at the yoke.

The experimental engine was fired downward into an eight cubic foot vacuum tank (Figs. 31 and 32). Between each test, the injector manifolds combustion chamber and vacuum tank were purged with Freon and gaseous nitrogen.

The combustion chamber and the propellants were temperature conditioned by circulating heated or cooled water through jackets surrounding the combustion chamber, the propellant lines, and the injector. High response, flush mounted piezoelectric pressure transducers (Endevco Model 2501 Pressure Transducers) provided the high response pressure data for the tests. Endevco Model 2501-500 (0-500 psia pressure range) pressure transducers were used to measure propellant manifold pressures. These transducers were connected to Endevco Model 2808 charge amplifiers with the amplified signal being recorded on a CEC oscillograph using a 7-361 model galvanometer. Chamber pressure was measured by an Endevco Model 2501-200 (0-2000 psia pressure range) pressure transducer with an Endevco Model 2811 charge amplifier and was recorded on a CEC oscilloscope using a sweep rate of $.5\mu \text{ sec/cm}$ and a 7-361 model galvanometer, and paralleled onto a Tektronix type 535A oscilloscope.

TABLE IV
EXPERIMENTAL OPERATING CONDITIONS

Oxidizer: Nitrogen Tetroxide, N_2O_4

Steady State Flow Rate: $\dot{W}_{ox} = .080 \text{ lb/sec}$

Fuel: Hydrazine, N_2H_4

Steady State Flow Rate: $\dot{W}_f = .067 \text{ lb/sec}$

Mixture Ratio: 1.2

(equal stream momentum for equal fuel and oxidizer orifices)

Steady State Chamber Pressure: 100 psia

Nozzle Throat Diameter: .503 in.

(Nozzle Throat Area: .266 in²)

Nozzle Area Ratio: 40

Thrust: 50 lbf

Manifold Volumes

Oxidizer: 172 in³

Fuel: .1037 in³

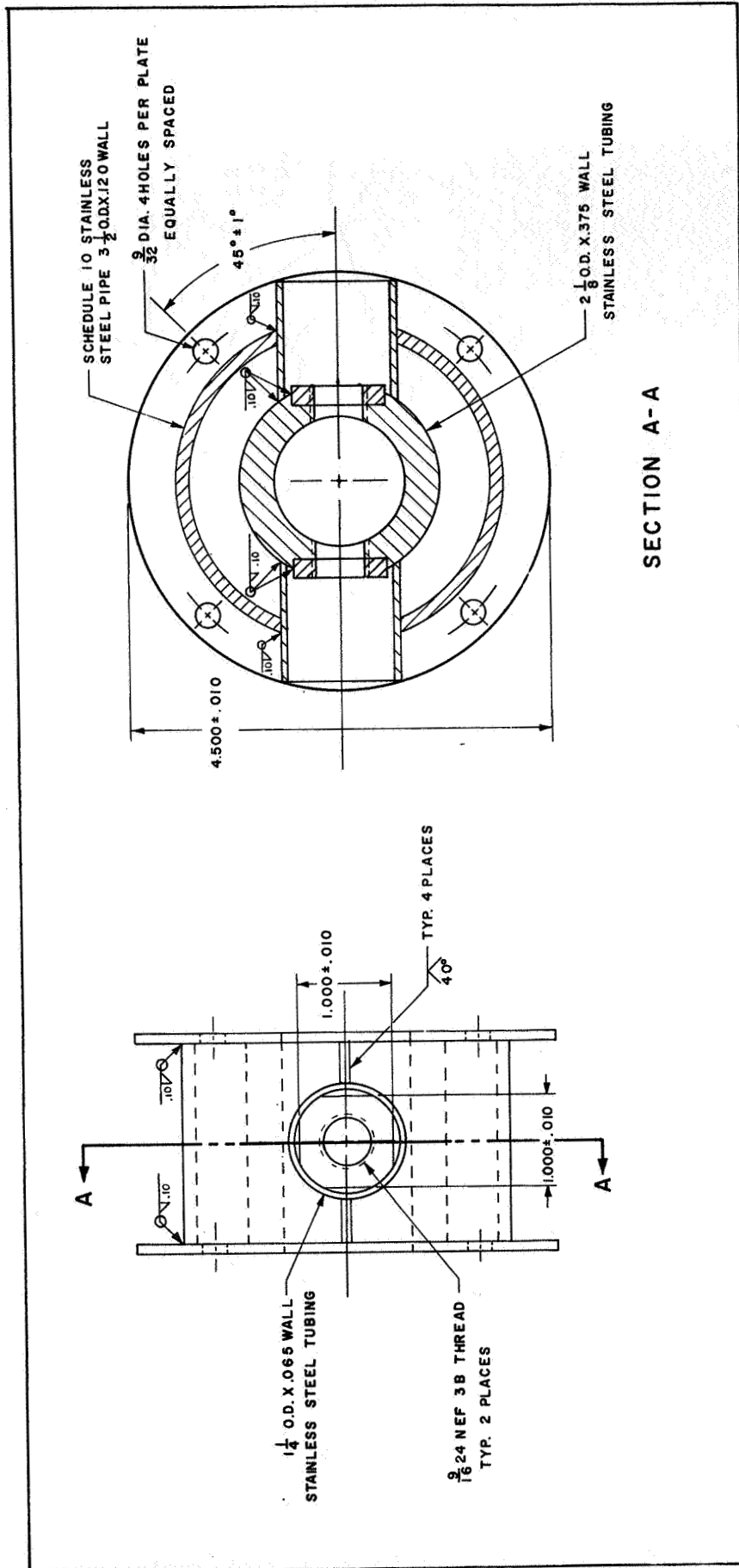
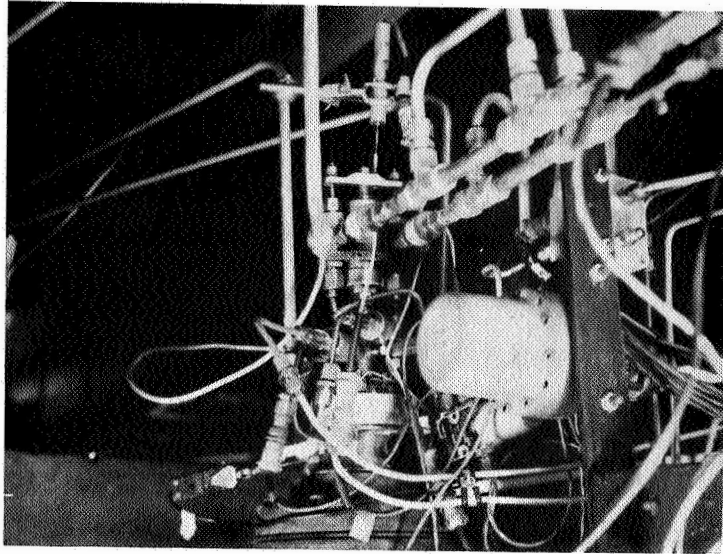
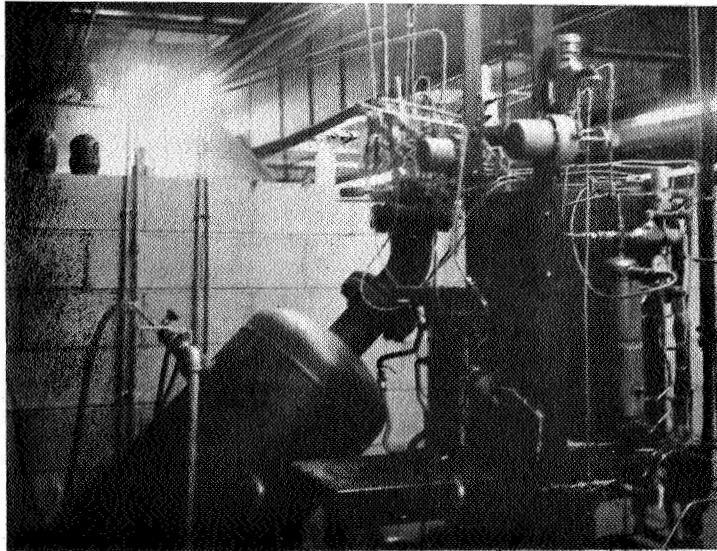


Figure 30 . Experimental Combustion Chamber



A. Assembled Experimental Hardware



B. Experimental Test Stand

Figure 31. Experimental Setup

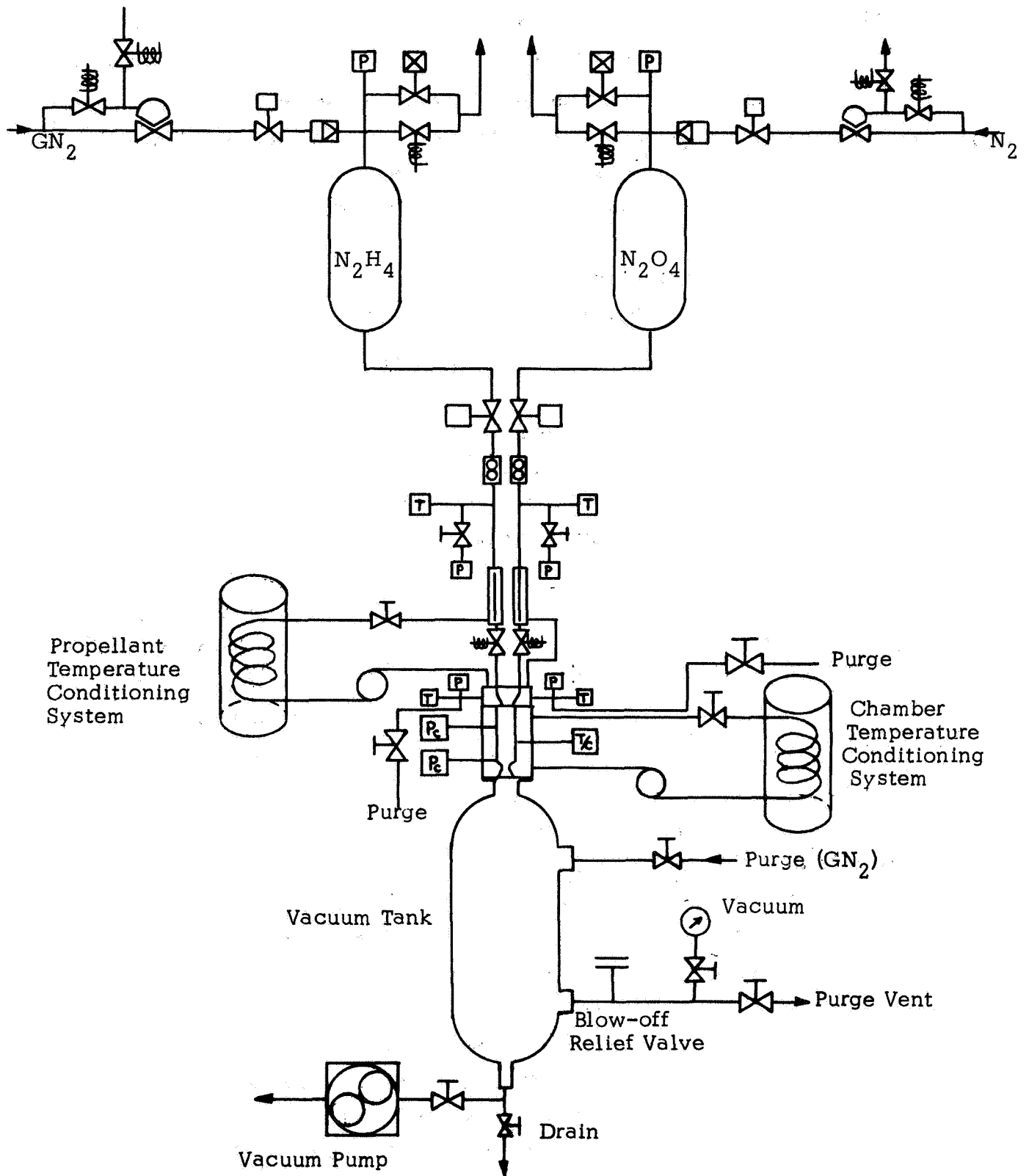


Figure 32. Experimental Test Stand.

Several lower range Taber pressure transducers were used to measure the lower preignition chamber pressure. The signal from the transducer was fed to a Dana amplifier and then recorded on a CEC oscillograph using a 7-346 model galvanometer.

The pressure in the vacuum tank was measured by a General Electric Thermistor Vacuum Gage (Recorder Model 22GC310, Vacuum Gage Tube 22GT). Propellant injection temperatures and chamber wall temperatures are measured with Iron-Constantin thermocouples which are recorded on a CEC oscillograph using a 7-349 model galvanometer. The fuel injection thermocouple was located in the injector fuel manifold opposite the injection pressure transducer port. The oxidizer injection thermocouple was located in the AN cross opposite the injection pressure transducer port.

Results

Table V shows test conditions and pressures resulting from the experimental program. The injector used to obtain the data was a like-on-like doublet which most closely simulated the conditions portrayed in the chamber pressurization model. The propellant temperatures were: 540°R (nominal), 580°R, and 500°R; the propellant valve openings were varied from 5 ms to 40 ms and the propellant leads were varied. The propellant lead conditions were determined from the time difference between the first noticeable increase in chamber pressure and ignition and, therefore, includes any ignition delay. The valve opening was measured by a linear potentiometer which coupled to the valve stem opening. Propellant temperatures were measured by thermocouples located in the injector manifold.

It was found that fuel lead conditions produced highest pressures with cold propellant temperatures (500 to 530°R). The results of this test program demonstrate the influence of fuel leads in the production of detonatable intermediates. Low fuel temperature gave consistent spiking, and long fuel leads at even relatively higher fuel temperatures (175°F) also lead to spiking. Although relatively little time and funding was available for these experiments, the results demonstrate the importance of preignition chemistry and condensed phase reactions of the hydrazine droplet surface. These reactions can be followed with vaporizing fuel droplets (long fuel leads even at higher temperatures) to analytically determine worst or unacceptable start sequences. The effect of propellant leads are seen where the fuel leads produced ignition spikes while the oxidizer lead conditions at low temperature produced none. Lengthening the valve opening time of the fuel system did not significantly reduce or eliminate the spiking tendency which exists at this condition.

TABLE V
EXPERIMENTAL RESULTS

Date Test	Propellant Leads		Valve Opening Time		Temperature (°R)			Spike (psi)
	ox (ms)	Fuel (ms)	Ox (ms)	Fuel (ms)	Ox	Fuel	Wall	
(6/27)								
8	25		4.8	4.8	540	540	540	No
9	10		6.0	6.0	540	540	540	2900
(7/1)								
3	21.9		17.0	17.0	540	540	540	No
4	26.6		21.0	21.0	540	540	540	No
(7/2)								
6	3.8		12.9	12.9	540	540	540	No
7		7.6	18.3	28.3	540	540	540	No
8		12.1	9.0	9.0	540	540	540	No
11	13.1		43.9	43.9	540	540	540	No
(7/3)								
1	7.6		15.7	15.7	540	540	540	No
3	6.2		13.2	13.2	540	540	540	No
4	22.5		43.9	16.0	540	540	540	No
5	10.0		38.2	13.7	530	500	540	No
6	8.3		31.2	9.2	520	500	540	No
7		8.8	21.2	12.2	520	500	540	Yes
8	34.2		37.4	10.2	560	590	540	No
12	15.5		44.0	19.5	570	630	540	No
13		19.6	12.9	39.7	570	640	540	Yes
14		19.3	12.4	34.6	570	630	540	Yes
15		21.8	13.35	39.9	570	640	540	No
16		17.1	13.3	36.2	570	640	540	No
17		9.1	12.6	12.6	530	510	540	3000
18		3.8	13.75	27.2	530	500	540	3500

5. CONCLUSIONS

A computer program has been written to describe rocket engine ignition transients. This program is useful in order of magnitude studies to determine what is influencing time delays and subsequent ISP pulse shape, and, also, the details of chemistry and O/F ratios which control the smoothness of ignition and spiking; finally, a short experimental firing program also performed to demonstrate the predicted trends.

The influence of design and operating variables upon what is going on as the engine starts can be evaluated by a computer program which essentially consists of an accounting system of enthalpy and mass balances with arbitrary propellant input. The propellant input may be calculated from a compatible flow program which essentially consists of a lump parameter analog model of the input hardware influences which affect the input flow. These programs, listed in the Appendix, thus describe flow, vaporization, chemistry, ignition, and/or detonation strength. Hardware parameter can be evaluated by one run after another with changing such things as chamber volume, heat capacity, injection velocity, etc.

Conclusions

The program is useful in evaluation of such things as an order of magnitude study of what design or physical processes are controlling ignition delay. For example, injected drop size or vaporization surface area are not particularly important, because the start is controlled by an enthalpy balance for which the engine starts when the accumulated enthalpy overcomes the engine's heat capacity. Such simplifications can be graphically demonstrated by various size engines, and often the start problem can be reduced to one of propellant flow and a known time delay for enthalpy accumulation. The program is also useful in evaluating the extremes of O/F ratio which can be encountered with hardware fuel or oxidizer leads. These calculations can often be used to interpret the relevance of purely chemical observations.

Chemical observations have shown that condensed phase fuel often reacts without ignition, but with the formation of detonation-sensitive intermediates. This fact was predicted by the computer program and was observed experimentally. Cold fuel gave rise to severe spiking and, also relatively warm fuel, even above 125°F, showed a tendency to spiking with long fuel leads in vacuum environment.

6. REFERENCES

1. Bell Aerosystems: Agena Vacuum Start Improvement Program, (1965)
2. Knox, R.M.; Minton, S.J.; and Zwick, E.B.: Space Ignition. Paper presented at AIAA 2nd Propulsion Jt. Spec. Conf. (Colorado Springs, Colo.) (1966).
3. Zung, L.B.; Breen, B.P.; and Kushida, R.: A Basic Study of Ignition of Hypergolic Liquid Propellants. Western States Section/The Combustion Institute Paper No. 68-43 (Oct. 1968).
4. Perlee, Henry E. and Christos, Theodore: Summary of Hypergolic Ignition Spike Phenomena. U.S. Dept. of the Interior, Bureau of Mines, Final Report No. 3982, April 8 to December 31, 1965.
5. Dauerman, L.; Ray, A.B.; Koehler, G.; and Salser, G.E.: Evidence for the Formation of Azides in the N_2H_4/N_2O_4 Reaction. AIAA Journal (Nov. 1968), p. 2186.
6. Seamans, T.F. and Waser, P.C.: Effects of Additives on Ignition Delay and Chamber Pressurization of Space-Ambient Engines. Tech.Rept. AFRPL-TR-69-68, July 1969.
7. Agosta, Vito D.; and Graus, Geo.: An Investigation of the Impulse Bit Developed by a Pulsed Liquid Propellant Rocket Engine. Curtiss-Wright Corp. (1964).
8. Seamans, T.F. and Dawson, B.E.: Hypergolic Ignition at Reduced Pressures. Air Force Tech.Rept. AFRPL-TR-67-175, (1967).
9. Stevens, M.R.; Fisher, H.D.; Weiss, H.G.; and Breen, B.P.: Effect of Additives on the Ignition Delay Time of Hypergolic Propellants. Western States/The Combustion Institute Paper No. 67-22, (April 1967).
10. Weiss, H.G.: A Basic Study of the Nitrogen Tetroxide/Hydrazine Reaction. Western States Section/The Combustion Institute Paper No. 65-20, (Oct. 1965.)
11. Streeter V.L. and Wylie, E.B.: Hydraulic Transients, McGraw-Hill, New York, C 1967.
12. Clayton, R.M. and Rupe, J. H.: An Experimental Correlation of the Nonreactive Properties of Injection Schemes and Combustion Effects in a Liquid in a Liquid-Propellant Rocket Engine, Part VI The Relation Between the Starting Transient and Injection Hydraulics. Jet Propulsion Laboratory, Tech. Rept. No. 32-255, 29 October 1965.
13. Aerospace Fluid Component Designer's Handbook, Glen W. Howell, ed. Tech.Documentary Rept. No. RPL-TDR-64-25, May 1964, prepared by TRW Space Technology Laboratories under contract AF04(611)-8385 for the Air Force Rocket Propulsion Laboratory, Research and Technology Division, Edwards, California AD 447995, pgs 3.16-1 to 3.16-3.

14. Campbell, Donald P. Sc. D. Process Dynamics, John Wiley & Sons, Inc. London, C 1968, pgs 75-82.
15. Vennard, John K.: Elementary Fluid Mechanics, John Wiley & Sons, Inc. New York, C 1965.
16. Nadig, E. W.; Tkachenko, E.A.; Breen, B.P.: Study of Random Wave Phenomena in Hypergolic Propellant Combustion. Interim Report SN-87, NASA Contract NAS7-467, Dynamic Science, 1967.
17. Mills, T. D.; Breen, B. P., et al; Transients Influencing Rocket Engine Ignition. Interim Rept. Contract NAS7-467, Dynamic Science, April 30, 1969.
18. Propulsion Applications Group, Research Dept. Rocketdyne: Program for the Development of Design Criteria for Eliminating Attitude Control Engine Pressure Spiking Through the Use of Catalysts. No. R-6380P, November 1965.
19. Minton, S. J.; and Swick, E. B.: Hypergolic Combustion Initiated at Low Pressure, Paper presented at the Aviation Space Conference of the American Society of Mechanical Engineers, Los Angeles, Calif. March 1965.

APPENDIX A
 USER'S MANUAL
 For
 PROPELLANT TRANSIENT FLOW PROGRAM

This section is divided into the following subsections:

1. Operating Procedures
2. Description of Program Input
3. Description of Program Output

1. Operating Procedures

This program was developed on the CDC 6400 using FORTRAN IV language. Standard FORTRAN IV CØMMØN is used for all input data.

2. Description of Program Input

This program requires the following groups of data.

- a. Propellant Properties
- b. Hardware Parameters
- c. Flow Properties
- d. Computational Control Information

a. Propellant Properties:

<u>Item Name</u>	<u>Input Quantity</u>	<u>Units</u>
RØ	= density of propellant at the temperature considered	lb/ft ³
PVI	= vapor pressure of propellant at the temperature considered	lb/in ² absolute
XMU	= viscosity of the propellant at the temperature considered	lb/ft-sec
GAM	= specific heat ratio of the vapor propellant	none

b. Hardware Properties:

<u>Item Name</u>	<u>Input Quantity</u>	<u>Units</u>
XL	= length of propellant line which contains accelerating propellant	ft
XLF	= length of propellant line over which friction acts	ft
XLMI	= length of propellant manifold	inches
XKL	= accumulated pressure loss coefficient of system from tank to valve	none

DI	=	diameter of propellant line	inches
DOI	=	diameter of orifices in injector	inches
XNØRF	=	number of orifices in injector	none
VMOI	=	volume of propellant manifold	inches ³
AVOI	=	area of the valve when full open*	inches ²
TVO	=	time for valve to open*	seconds
XN	=	exponent on valve transient to shape its opening*	none
TI(1)	=	points in time table used to specify valve transient ≤ 100 *	seconds
AVTI(1)	=	valve opening areas corresponding to time values $TI \leq 100$ *	inches ²
NT	=	number of tabular values used to describe valve opening*	none

c. Flow Properties:

<u>Item Name</u>		<u>Input Quantity</u>	<u>Units</u>
CV	=	discharge coefficient of valve	none
CO	=	discharge coefficient for injector orifices	none
WSS	=	steady state propellant flow rate*	lb/sec
PCSSI	=	steady state combustion chamber pressure	lb/in ² absolute
PSSI	=	pressure drop across the injector	lb/in ²
DPI	=	overall pressure drop from propellant tank through injector*	lb/in ²
QI(1)	=	initial values of volumetric flow rate*	ft ³ /sec
		QI(1) = propellant flow out of tank	
		QI(2) = propellant flow out of injector	
		QI(3) = $d/dt [\int QI(1)]$	
		QI(4) = $d/dt [\int QI(2)]$	
		QI(5) = gas flow out of manifold	ft ³ /sec
		QI(6) = $d/dt [\int QI(5)]$	
TEMPØ	=	temperature of propellants considered*	°R
XMØWT	=	molecular weight of propellants* (not needed if PAMBI = 0.)	none
PAMBI	=	initial ambient pressure*	lb/in ² -absolute

*See computational control information section.

d. Computational Control Information:

<u>Item Name</u>	<u>Input Quantity</u>	<u>Units</u>
TMAX	= maximum computational time	seconds
TS	= starting time for computations, $\neq 0$	seconds
HO	= initial step size	seconds
HMIN	= minimum step size	seconds
HMAX	= maximum step size	seconds
ELR	= minimum relative error on integrated flow parameters	none
EUR	= maximum relative error on integrated flow parameters (should be a minimum of 32 times longer than ELR)	none
DRP	= print suppression index (printout will occur at every time interval DRP)	seconds
FLAG	= option defining the form of the flow parameters FLAG = 0. requires that WSS, PCSSI, and PSSI be input and DPI be undefined. FLAG = 1.0 requires that DPI be input and WSS, PCSSI, and PSSI be undefined.	none
FLAGT	= option which provides for use of tabular values of valve areas instead of formula. FLAGT = 1. uses table FLAGT = 0. uses formula $AVOI = [time/TVO]^{XN}$ (when FLAGT = 1. option is used, AVOI, TVO, and XN are not needed for input)	none

TABLE A-I shows a typical input listing.

3. Description of Program Output:

<u>Item Name</u>	<u>Input Quantity</u>	<u>Units</u>
T	= time	seconds
H	= time step taken at time I	seconds
WI	= propellant flow rate from propellant tank	lb/sec
W2	= propellant flow rate from injector orifices	lb/sec
Q1	= propellant flow rate from propellant tank	ft ³ /sec

Q2	=	propellant flow rate from injector orifices	ft ³ /sec
DQ1	=	the derivative of Q1	ft ³ /sec ²
DQ2	=	the derivative of Q2	ft ³ /sec ²
IQ1	=	the integral of Q1	ft ³
IQ2	=	the integral of Q2	ft ³
VMF	=	the volume of the propellant manifold which is full	ft ³
VME	=	the volume of the propellant manifold which is empty	ft ³
PVV	=	the pressure inside the propellant manifold	lb/in ² -absolute
AV	=	the open area of the valve	ft ²
WGØUT	=	the amount of gas which has left the propellant manifold if the start occurred in other than vacuum conditions.	lb
WGDØT	=	the flow rate of gas out of the propellant manifold if the start occurred in other than vacuum condition.	lb/sec

TABLE A-II shows a typical output using the input data from TABLE A-I.

TABLE A-I
TYPICAL INPUT DATA FOR OXIDIZER FLOW TRANSIENT

```

$DATA
RO=88.9,
XL=8.,
PVI=18.5,
XKL=16000.,
DI=.305,
CV=.7,
XLF=8.,
XLM=4.,
CU=.86,
DVI=.02,
XMU=.00026,
VMOI=.1037,
TS=.000001,
TMAX=.1,
XNORF=4.,
DRP=.001,
GAM=1.2,
FLAG=1.,
PAMB=0.,
FLAGI=1.,
DPI=490.,
TI(1)=0.,.001,.0015,.002,.0025,.003,.024,
.025,.026,.027,.028,.029,.030,.0306,
.031,.0315,.032,.033,.034,.035,.036,
.037,.038,.0382,.1,
AVTI(1)=0.,.00012,.00045,.0008,.00086,
.00085,.00082,.00067,.0006,.00102,
.0015,.00222,.00265,.00285,
.00275,.0026,.00275,.00305,
.0035,.00425,.00532,.00695,
.00905,.00962,.00962,
NT=25,
$END

```

TABLE A-II - TRANSIENT FLOW ANALYSIS

T H	W1		Q1		DQ1		IQ1		VMF		PVV	
	#2	#1	#2	#1	DQ2	DQ1	IQ2	IQ1	VME	VMF	AV	PVV
0.000001000	0.	0.	0.	0.	1.619567E+00	0.	0.	0.	0.	0.	0.	0.
0.000001000	0.	0.	0.	0.	0.	0.	0.	0.	6.001157E-05	6.001157E-05	8.333333E-10	8.333333E-10
0.00001100	9.872364E-06	1.110502E-07	1.110502E-07	8.842993E-29	6.697786E-01	6.774347E-15	6.774347E-15	6.774347E-15	6.774347E-15	6.774347E-15	1.253013E-09	1.253013E-09
0.00000100	7.861421E-27	8.842993E-29	8.842993E-29	1.662233E-25	3.981357E-21	2.370407E-36	2.370407E-36	2.370407E-36	6.001157E-05	6.001157E-05	9.166667E-10	9.166667E-10
0.00001200	1.266291E-05	1.424399E-07	1.424399E-07	1.662233E-27	3.065376E-01	2.029368E-14	2.029368E-14	2.029368E-14	2.029368E-14	2.029368E-14	3.753606E-09	3.753606E-09
0.00000100	1.477725E-25	1.662233E-27	1.662233E-27	1.662233E-25	3.572874E-20	6.816535E-35	6.816535E-35	6.816535E-35	6.001157E-05	6.001157E-05	1.000000E-09	1.000000E-09
0.00001300	1.437527E-05	1.617015E-07	1.617015E-07	8.520929E-27	1.777336E-01	3.576036E-14	3.576036E-14	3.576036E-14	3.576036E-14	3.576036E-14	6.614391E-09	6.614391E-09
0.00000100	7.575105E-25	8.520929E-27	8.520929E-27	1.617015E-07	1.109431E-19	5.174538E-34	5.174538E-34	5.174538E-34	6.001157E-05	6.001157E-05	1.083333E-09	1.083333E-09
0.00001400	1.614646E-05	1.816250E-07	1.816250E-07	2.638912E-26	5.112456E-02	5.241690E-14	5.241690E-14	5.241690E-14	5.241690E-14	5.241690E-14	9.695256E-09	9.695256E-09
0.00000100	2.345993E-24	2.638912E-26	2.638912E-26	1.816250E-07	2.383630E-19	2.124360E-33	2.124360E-33	2.124360E-33	6.001157E-05	6.001157E-05	1.166667E-09	1.166667E-09
0.01003600	1.120698E-02	1.260628E-04	1.260628E-04	7.039705E-11	1.641536E-01	6.344402E-08	6.344402E-08	6.344402E-08	6.344402E-08	6.344402E-08	1.176222E-02	1.176222E-02
0.00012800	6.258298E-09	6.039705E-11	6.039705E-11	1.260628E-04	3.500162E-07	1.179012E-14	1.179012E-14	1.179012E-14	5.994813E-05	5.994813E-05	8.498333E-07	8.498333E-07
0.02002000	5.027899E-02	5.655679E-04	5.655679E-04	4.723095E-09	3.181782E-01	4.217726E-07	4.217726E-07	4.217726E-07	4.217714E-07	4.217714E-07	7.923258E-02	7.923258E-02
0.00102400	4.198832E-07	4.723095E-09	4.723095E-09	5.027899E-02	1.567434E-05	1.241780E-12	1.241780E-12	1.241780E-12	5.958980E-05	5.958980E-05	5.557222E-06	5.557222E-06
0.03077200	5.781477E-02	6.503349E-04	6.503349E-04	6.333892E-08	-9.694469E-04	1.100825E-06	1.100825E-06	1.100825E-06	1.100796E-06	1.100796E-06	2.120720E-01	2.120720E-01
0.00102400	5.630830E-06	6.333892E-08	6.333892E-08	6.503349E-04	1.094957E-04	2.879081E-11	2.879081E-11	2.879081E-11	5.891078E-05	5.891078E-05	5.902012E-06	5.902012E-06
0.04101200	5.775195E-02	6.496282E-04	6.496282E-04	2.597207E-07	-6.094335E-04	1.766387E-06	1.766387E-06	1.766387E-06	1.766208E-06	1.766208E-06	3.488766E-01	3.488766E-01
0.00204800	2.308917E-05	2.597207E-07	2.597207E-07	6.496282E-04	2.890066E-04	1.785206E-10	1.785206E-10	1.785206E-10	5.824537E-05	5.824537E-05	5.891853E-06	5.891853E-06
0.05125200	5.769356E-02	6.489714E-04	6.489714E-04	6.868825E-05	-5.261726E-04	2.431285E-06	2.431285E-06	2.431285E-06	2.430646E-06	2.430646E-06	4.923950E-01	4.923950E-01
0.00409600	6.106386E-05	6.868825E-05	6.868825E-05	5.769356E-02	5.612711E-04	6.394035E-10	6.394035E-10	6.394035E-10	5.758093E-05	5.758093E-05	5.881694E-06	5.881694E-06
0.06354000	5.763066E-02	6.482639E-04	6.482639E-04	1.642725E-06	-8.680425E-04	3.228278E-06	3.228278E-06	3.228278E-06	3.226264E-06	3.226264E-06	6.738850E-01	6.738850E-01
0.00409600	1.460383E-04	1.642725E-06	1.642725E-06	6.482639E-04	1.019055E-03	2.013137E-09	2.013137E-09	2.013137E-09	5.678531E-05	5.678531E-05	5.869504E-06	5.869504E-06
0.07173200	5.758039E-02	6.476984E-04	6.476984E-04	2.632263E-04	-6.524592E-04	3.759093E-06	3.759093E-06	3.759093E-06	3.755350E-06	3.755350E-06	8.007191E-01	8.007191E-01
0.00409600	2.340082E-04	2.632263E-04	2.632263E-04	5.758039E-02	1.406310E-03	3.742410E-09	3.742410E-09	3.742410E-09	5.625622E-05	5.625622E-05	5.861377E-06	5.861377E-06
0.08402000	5.751628E-02	6.469773E-04	6.469773E-04	4.786154E-06	-1.001369E-03	4.554483E-06	4.554483E-06	4.554483E-06	4.546273E-06	4.546273E-06	1.000031E+00	1.000031E+00
0.00409600	4.254891E-04	4.786154E-06	4.786154E-06	6.469773E-04	2.124122E-03	8.210227E-09	8.210227E-09	8.210227E-09	5.546530E-05	5.546530E-05	5.849187E-06	5.849187E-06

APPENDIX B
 USER'S MANUAL
 For
 CHAMBER PRESSURIZATION TRANSIENT
 PROGRAM

This section deals with the use of the program and is divided into the following subsections:

1. Operating Procedures
2. Description of Program Input
3. Description of Program Output

1. Operating Procedures

This program was developed on the CDC 6400 using FORTRAN IV language. Standard FORTRAN IV COMMON is used for all input data.

2. Description of Program Input

- a. Propellant Properties
- b. Chemical Reaction Parameters
- c. Transport Properties
- d. Hardware Properties
- e. Computational Control Information

a. Propellant Properties:

<u>Item Name</u>	<u>Input Quantity</u>	<u>Units</u>
RØN(1,1)	= table of oxidizer density (up to 10 values may be used)	lb/ft ³
TRØN(1,1)	= table of temperatures corresponding to oxidizer density RØN(1,1) (up to 10 values may be used)	°R
RØN(1,2)	= table of fuel density (up to 10 values may be used)	lb/ft ³
TRØN(1,2)	= table of temperatures corresponding to fuel density RØN(1,2) (up to 10 values may be used)	°R
NØØØ	= number of values used to define density table used	none
CPN(1,1)	= table of specific heat at constant pressure of liquid oxidizer (up to 10 values may be used)	Btu/lb°R

TCPN(1,1)	=	table of temperatures, corresponding to liquid oxidizer specific heat (up to 10 values may be used)	$^{\circ}\text{R}$
CPN(1,2)	=	table of specific heat at constant pressure of liquid fuel (up to 10 values may be used)	$\text{Btu}/\text{lb}^{\circ}\text{R}$
TCPN(1,2)	=	table of temperatures corresponding to liquid fuel specific heat (up to 10 values may be used)	$^{\circ}\text{R}$
NØCP	=	number of values used to define liquid propellant specific heat table	none
CPGN(1,1)	=	table of specific heat at constant pressure of vapor oxidizer (up to 10 values may be used)	$\text{Btu}/\text{lb}^{\circ}\text{R}$
TCPGN(1,1)	=	table of temperatures corresponding to oxidizer vapor specific heat at constant pressure (up to 10 values may be used)	$^{\circ}\text{R}$
CPGN(1,2)	=	table of specific heat at constant pressure of vapor fuel (up to 10 values may be used)	$\text{Btu}/\text{lb}^{\circ}\text{R}$
TCPG(1,2)	=	table of temperatures corresponding to fuel vapor specific heat at constant pressure (up to 10 values may be used)	$^{\circ}\text{R}$
NØCPG	=	number of values used to define vapor propellant specific heat table	none
CPGP	=	specific heat of vapor product	$\text{Btu}/\text{lb}^{\circ}\text{R}$
PVN(1,1)	=	table of vapor pressure for oxidizer (up to 10 values may be used)	lb/ft^2
TPVN(1,1)	=	table of temperatures corresponding to oxidizer vapor pressure (up to 10 values may be used)	$^{\circ}\text{R}$
PVN(1,2)	=	table of vapor pressure for fuel (up to 10 values may be used)	lb/ft^2
TPVN(1,2)	=	table of temperatures corresponding to fuel vapor pressure (up to 10 values may be used)	$^{\circ}\text{R}$
NØPV	=	number of values used to describe vapor pressure tables	none
GAM(1)	=	specific heat ratio of vapor oxidizer and vapor fuel	none
GAMP	=	specific heat ratio of vapor products	none

XMU(1)	=	viscosity of oxidizer vapor and fuel vapor	lb/ft-sec
XK(1)	=	thermal conductivity of oxidizer vapor and fuel vapor	Btu/ft-sec ^{°R}
XM(1)	=	molecular weight of oxidizer and fuel	none
XMP	=	molecular weight of vapor products	none
TAU(1)	=	heat of vaporization for oxidizer and fuel	Btu/lb
TAUF(1)	=	heat of fusion for oxidizer and fuel	Btu/lb
TAUS(1)	=	heat of sublimation for oxidizer and fuel	Btu/lb
TFP(1)	=	freezing temperature of oxidizer and fuel	°R
PVW(1)	=	vapor pressure of oxidizer and fuel evaluated at the chamber wall temperature	lb/in ²
TGI(1)	=	initial vapor temperatures of the oxidizer and the fuel	°R
PG(1)	=	initial partial pressure in the chamber due to oxidizer vapor, and fuel vapor	lb/in ²

b. Chemical Reaction Parameters:

<u>Item Name</u>		<u>Input Quantity</u>	<u>Units</u>
CFØRPR	=	stoichiometric oxidizer to fuel ratio	none
RM	=	experimentally determined exponent for fuel concentration in reaction rate equation	none
RN	=	experimentally determined exponent for oxidizer concentration in reaction rate equation	none
EACTT(1)	=	activation energy for each preignition reaction path	ft/lb/mole
AAT(1)	=	Arrhenius reaction rate constant for each preignition reaction path	cc/mole-sec
A(J,I,1)	=	relative formula weights of species in balanced preignition reactions for oxidizer rich reactions	
A(J,I,2)	=	relative formula weights of species in balanced preignition reactions for fuel rich reactions	

I corresponds to reaction paths within the temperature range TTABLE (I) and TTABLE (I+1). Maximum I is NN

J corresponds to specified species in balanced reaction. Maximum J is 12, where J=1 is reactant species on which the enthalpy of reaction is based. J=2 species is second reactant species. All other species are unspecified.

TTABLE(1)	=	table of temperatures which define reaction paths (must be NN+1 values)	$^{\circ}\text{R}$
YREACT(1,1)	=	enthalpy of reaction for fuel rich reactions	Btu/lb
YREACT(1,2)	=	enthalpy of reaction for oxidizer rich reactions	Btu/lb
CØNCR	=	critical oxidizer vapor concentration below which liquid fuel and oxidizer vapor reaction takes place (concentration of oxidizer vapor/concentration of all vapors)	none
TCR	=	critical temperature below which liquid fuel and oxidizer vapor reaction takes place	$^{\circ}\text{R}$
HEATX	=	heat of reaction for liquid fuel - oxidizer vapor reaction	Btu/lb
HFLIQ(1)	=	heat of formation of liquid oxidizer and fuel	calories/mole

c. Transport Properties:

<u>Item Name</u>		<u>Input Quantity</u>	<u>Units</u>
HC(1,1)	=	heat transfer coefficient between oxidizer vapors and wall when $T_w > T_g$, between oxidizer vapors and wall when $T_w < T_g$, and between gaseous products and wall when $T_w > T_g$	$\text{Btu}/\text{ft}^2 \text{-sec}^{\circ}\text{R}$
HC(1,2)	=	heat transfer coefficient between fuel vapors and wall when $T_w > T_g$, between fuel vapors and wall when $T_w < T_g$, and between gaseous products and wall when $T_w < T_g$	$\text{Btu}/\text{ft}^2 \text{-sec}^{\circ}\text{R}$
VDRØP(1)	=	velocity of oxidizer and fuel drops	ft/sec
ALPHA	=	accommodation coefficient (fraction of vapor that impinges on chamber wall and remains as condensate)	none
RGI(1)	=	initial radius of oxidizer and fuel droplet	ft

WLIQ(1,1)	=	table of transient propellant flow rates of first entering species (up to 25 values may be used)	lb/sec
TLIQ(1,1)	=	time table corresponding to values of WLIQ(1,1) (up to 25 values may be used)	sec
NLIQ(1)	=	number of entries in WLIQ(1,1) table	none
WLIQ(1,2)	=	table of transient propellant flow rates of second entering species (up to 25 values may be used)	lb/sec
TLIQ(1,2)	=	time table corresponding to values of WLIQ(1,2) (up to 25 values may be used)	sec
NLIQ(2)	=	number of entries in WLIQ(1,2) table	none
PGADD(1,1)	=	table of time variable backpressures affecting the oxidizer transient pressure (up to 10 values may be used)	lb/in ² -absolute
PGADDT(1,1)	=	time table corresponding to values of PGADD(1,1) (up to 10 values may be used)	sec
PGADD(1,2)	=	table of time variable backpressures affecting the fuel transient pressure (up to 10 values may be used)	lb/in ² -absolute
PGADDT(1,2)	=	time table corresponding to values of PGADD(1,2) (up to 10 values may be used)	sec
WGI(1)	=	initialized flow rate of oxidizer and fuel (small number needed to start program)	lb/sec

d. Hardware Properties:

<u>Item Name</u>		<u>Input Quantity</u>	<u>Units</u>
AC	=	combustion chamber internal surface area	ft ²
VC	=	combustion chamber volume	ft ³
TW	=	combustion chamber wall temperature	°R
ASTAR	=	chamber nozzle throat area	ft ²

e. Computational Control Information:

<u>Item Name</u>	<u>Input Quantity</u>	<u>Units</u>
NN	= number of preignition paths used (up to 10 paths may be specified)	none
M(1)	= starting time in terms of number of calculations for oxidizer and fuel	none
TMAX	= maximum running time	sec
DELTN	= initial step size	sec
ND1	= first integration step to be selected for print	none
ND2	= last integration step to be selected for print	none
ND3	= print every ND3rd step between ND1 and ND2	none
IUNIT	= unit on which punched output will be written	
MSPEC	= number of chemical species (must be 10)	
IFPLOTT	= option for plot routine IFPLOTT=1 will plot	
PLTIME	= real time for plot generation such that job does not run to maximum time plots are generated	real sec
IDEBUG	= provides intermediate output when IDEBUG=T or .TRUE.	none
TDETØN(1)	= specifies time at which detonation calculations are to be performed (up to 40 values may be specified)	sec
TCRIT(1)	= normalized averaging criteria based on stored droplet temperature for oxidizer and fuel	none
RCRIT(1)	= normalized averaging criteria based on stored droplet radius for oxidizer and fuel	none
XCRIT(1)	= normalized averaging criteria based on stored droplets' percent frozen for oxidizer and fuel	none

A typical input listing is shown in Table B-I

3. Description of Program Output

<u>Item Name</u>	<u>Output Quantity</u>	<u>Units</u>
TIME	= time	milliseconds
F	= ratio of liquid propellant species to total propellant (liquid and gaseous) species	none
GEVAP	= mass of propellant evaporated	lb
GCØND	= mass of propellant condensed	lb
PG(1)	= partial pressure due to oxidizer	lb/in ² -absolute
PG(2)	= partial pressure due to fuel vapors	lb/in ² -absolute
PGP	= partial pressure of gaseous reaction products	lb/in ² =absolute
PGTØTAL	= total pressure due to oxidizer, fuel, and product vapors	lb/in ² -absolute
TFINAL	= temperature of gaseous chemical species in chamber after reaction	°R
TAVERG	= temperature of gaseous chemical species in chamber before reaction	°R
TG	= temperature of vapors in chamber (when only one propellant is flowed)	°R
TQP	= temperature of gaseous products	°R
REACT	= amount of material which has reacted	lb
WTØTAL	= total accumulated propellant flow	lb

Table B-II shows typical output from this program.

TABLE B-I

TYPICAL OUTPUT FROM CHAMBER PRESSURIZATION TRANSIENT PROGRAM

DATA

0.828E+03,	0.8E+03,	0.0,	0.0,	0.44E+03,	0.3E+02,	0.323E+03,	0.98E+02,	0.72E+02,
0.665E+03,	0.0,	0.184E+03,	0.128E+03,	0.0,	0.0,	0.88E+02,	0.3E+02,	0.0,
0.36E+02,	0.0,	0.8E+02,	0.92E+02,	0.64E+02,	0.0,	0.0,	0.0,	0.84E+02,
0.72E+02,	0.0,	0.0,	-0.13582279375555-271,	0.25135643210431-275,	-0.39700464175606+147,			
-0.17273786375623-269,	0.0,	0.0,	0.21617297246502-234,	0.21614890238669-234,	-0.65534496091041E+05,			
0.11858914554931-275,	0.0,	0.15298744170073-275,	0.85050255900059-276,	0.85050255900059-276,	0.21294757227603-275,			
-0.39715158738624+147,	0.0,	0.19482294932728+287,	0.75729000761011-276,	0.75729000761011-276,	0.21272721163444-275,			
-0.2559925353527E+03,	0.0,	0.21745243943817-234,	0.11532780805385-275,	-0.15806768428534E+48,				
0.20016840476187-215,	0.0,	0.20016840476194-215,	0.87313303684335-135,	0.14250811913572-229,				
0.5566370259428-232,	-0.0,	0.17188269222276-163,	-0.18244976066085E+85,	-0.2901670524926E+67,				
-0.43367745686545E-18,	-0.0,	0.43367664695243E-18,	-0.36122077587999+135,	0.69510155693575-233,				
0.40458470762016E+21,	-0.0,	0.33776806730399E+17,	-0.17120435812387-163,	0.41269788332367+302,				
0.37081433997814-196,	-0.0,	0.16148792519923-163,	-0.15499222954431E+73,	0.78520130321385-218,				
0.13835549509949-275,	-0.0,	0.26496672796006-168,	0.37079804194034-196,	0.3438392644259E+17,				
0.2179518380989-234,	-0.0,	0.55696707465143+257,	-0.89298649031397-188,	-0.14627079234395+258,				
0.9017895290987E+19,	0.0,	0.17024994049059-236,	-0.53405579132036-188,	-0.26496716631387-168,				
-0.17244699917004+258,	-0.0,	0.73708312970777+166,	0.25014013182887-234,	-0.26507694759199-188,				
-0.13524857809596E+26,	0.0,	0.87420566905358-234,	0.58571722199409-125,	0.27287358476128-235,				
-0.39711591501974+147,	-0.0,	0.17385318083065-269,	-0.33819589202512E+74,	0.21336625749504-275,				
0.69253647379666-233,	-0.0,	0.39708542323283+147,	-0.39686440695086+147,	-0.53175839015117-255,				
0.14653336088908-217,	-0.0,	0.68468170399224-191,	-0.1735380313286-190,	-0.3469390758793-190,				
0.17502901446447-233,	-0.0,	0.70607336520797E+82,	-0.48636605007671E+52,	-0.51015653789851-196,				
-0.1515313840057-175,	0.0,	0.78976594956068-218,	-0.34707606213463-190,	0.1752440109971-233,				
-0.70607336520797E+82,	-0.0,	0.48636605007671E+52,	-0.51108736227436-196,	-0.15211458466793-175,				
-0.17385318087708-269,	0.0,	0.5796E+04,	0.2048E+04,	0.352E+04,	0.48E+03,	0.0,		
0.308E+03,	0.1296E+04,	0.0,	0.224E+04,	0.184E+03,	0.128E+03,	0.0,	0.88E+02,	0.0
0.3E+02,	0.0,	0.7E+02,	0.36E+02,	0.8E+02,	0.92E+02,	0.64E+02,	0.0,	0.0,
0.0,	0.0,	0.84E+02,	0.72E+02,	0.0,	0.46269146330188E+33,	-0.6487850186703-272,		
0.79031924002696-218,	0.0,	0.41310995316056-184,	0.21930331691454E+33,	0.46269242560684E+33,				
0.79031924002696-218,	-0.0,	0.2445712346419-137,	-0.3970490572155+147,	0.22098265131588-234,				
0.46269146330188E+33,	-0.0,	0.85733688869182-197,	-0.15211458466793-175,	0.22113562008227-234,				
0.46269146330188E+33,	-0.0,	0.1505680185945-175,	-0.15153138406057-175,	-0.6487850186703-272,				
0.79031924002696-218,	-0.0,	0.23408345934477-137,	0.34659246864352-236,	-0.86507489716579E+52,				
0.30329584251388E+29,	-0.0,	0.24457123263982-137,	0.88623173567032-234,	0.46269014795905E+33,				
0.13354590447402-122,	-0.0,	0.2445712296367-137,	0.86684601178035-234,	0.46269014795905E+33,				
-0.1503991749263-182,	-0.0,	0.13149105550894-196,	0.1288184591094-122,	0.34680511081317-236,				
-0.89495827701724-186,	-0.0,	0.27344789860833-185,	0.80000182318689-218,	-0.36171062866348E+28,				
0.11804053703866-234,	-0.0,	0.73500696324619-272,	-0.13149105550894-196,	-0.7336305025346-272,	0.0,			
-0.9153239052129-270,	0.0,	0.10922959988258+296,	0.23974342629277-275,	0.69859767480929-177,				

TABLE B-I (Cont.)

0.732389255111-276, -0.39719535049498+147, -0.39723841204938+147, 0.732389255111-276,
 0.1692385150475E+25, -0.0487888823821-276, -0.26431679984573E-47, -0.14672607925017-271,
 0.16788215973156-217, -0.512795136597974E+49, 0.488194222307768-125, 0.12329876117195-105,
 -0.18335588767831-115, 0.46782093357675-228, 0.46810401973417-228, 0.18271707886418-230,
 0.21688979109624-275, -0.73363049513185-272, -0.385099810458-199, 0.11645892716435-275,
 0.22107887995052-275, -0.73363049513185-272, 0.23006959412719-275, -0.73363049513185-272,
 0.74417567714993-218, -0.39719535049498+147, -0.36111518427087+135, -0.39705052868656+147,
 0.22351871345038-234, 0.80581157308285-218, -0.43123213095907-217, 0.80581157308285-218,
 -0.39719842324784+147, -0.36125093969162+135, -0.3969040355539+147, -0.28206025569569-202,
 0.84653006743200-276,

AAT = 0.16E+12, 0.16E+12, 0.3512716046+166-130, -0.39692199010401+147,
 0.14430402203370+157, 0.89609817666403+299, 0.83541241302893-218, -0.72672044054601-272,
 -0.39691684652827+147,

AC = 0.131E+30,

ALPHA = 0.1E+01,

ASTAK = 0.411E-52,

CFORPF = 0.5E+00,

CP6N = 0.5E+00, 0.217E+01, 0.225E+01, 0.215E+01, 0.45E+00, -0.105387361+3429E+38,
 -0.5221248110547E+49, 0.76425449454233, -0.58507572521864E+28, 0.24108190683431-234,
 0.57E+00, 0.53E+00, 0.5E+00, 0.455E+00, 0.393E+00, -0.15885561076711E-25,
 -0.1036104677475E+50, 0.7853628469866-234, -0.96741857422103E+37, 0.12051503018877-234,

CP6P = 0.1E+01,

CPN = 0.14E+00, 0.17E+00, 0.288E+00, 0.354E+00, 0.366E+00, 0.379E+00, 0.395E+00, 0.421E+00
 0.4768879541186-234, -0.25091389874178-167, 0.229E+00, 0.314E+00, 0.477E+00, 0.728E+00
 0.614E+00, 0.858E+00, 0.858E+00, 0.925E+00, 0.18643962778021-230, 0.31279380290997-229

CV6 = 0.97E+00, 0.36E+00,

DELIN = 0.1E-03,

DI MAX = 0.262944221171-259,

DI MIN = 0.2528020745832-115,

TABLE B-I (Continued)

PVN	=	0.388E+03,	0.108E+04,	0.347E+04,	0.965E+04,	0.3355E+05,	0.23548742654185E-28,
		-0.86362310107237E-46,	0.3149142587426-229,	-0.26472647093504-188,	-0.1030992882977-115,	0.75E+01,	0.72E+02,
		0.23999759440685-234,	0.288E+03,	0.864E+03,	0.432E+04,	-0.1036395917286E+50,	
		-0.15768365533513-167,	-0.1639430767248-124,				
PVV	=	0.965E+04,	0.864E+03,				
PVW	=	0.954E+03,	0.111E+02,				
RGI	=	0.171E-03,	0.171E-03,				
RM	=	0.1E+01,					
RN	=	0.1E+01,					
RON	=	0.1182E+03,	0.945E+02,	0.829E+02,	0.775E+02,	0.698E+02,	0.63E+02,
		0.24310650678934-231,	0.64194584375651E+29,	0.44770967259614E+68,	0.715E+02,	0.639E+02,	
		0.576E+02,	0.502E+02,	0.455E+02,	0.416E+02,	-0.36108468761147+135,	-0.91693967686746E+87,
		0.26443248729552-191,	0.88484977820118-218,				
TAU	=	0.178E+03,	0.607E+03,				
TAUF	=	0.654E+02,	0.171E+03,				
TAUS	=	0.237E+03,	0.85E+03,				
TCPGN	=	0.455E+03,	0.54E+03,	0.558E+03,	0.572E+03,	0.65E+03,	0.48424542321814-234,
		0.40868652358879E+18,	0.58849049613707E-26,	-0.56339302605008-198,	-0.39708732972202+147,		
		0.54E+03,	0.68E+03,	0.8E+03,	0.54E+03,	0.108E+04,	-0.36124938348506+135,
		0.87524932660122-218,	-0.40422959548899-173,	0.11532780805385-275,	0.12887998751133-275,		
TCPN	=	0.15E+03,	0.204E+03,	0.4719E+03,	0.472E+03,	0.52E+03,	0.546E+03,
		0.13924832134815+312,	-0.36116851752959+135,	0.161E+03,	0.271E+03,	0.4949E+03,	0.495E+03,
		0.76E+03,	0.81E+03,	0.86E+03,	0.96E+03,	-0.31941333363523-185,	-0.36101595031962+135,
TFP	=	0.47184E+03,	0.4954E+03,				
TGI	=	0.54E+03,	0.54E+03,				
TMAX	=	0.5E-01,					

TABLE B-I (Continued)

TP	=	0.0, 0.1E-03, 0.2E-03, 0.3E-03, 0.4E-03, 0.5E-03, 0.6E-03, 0.7E-03, 0.8E-03, 0.9E-03, 0.1E-02, 0.2E-02, 0.1E-01, -0.6221504724848-186, 0.27843927066593+300, 0.22945112349065-234, -0.36099875312807+135, 0.12229748460903+301, -0.60564471776888+142, 0.3012189453724-229, 0.0, 0.1E-03, 0.2E-03, 0.3E-03, 0.4E-03, 0.5E-03, 0.6E-03, 0.7E-03, 0.8E-03, 0.9E-03, 0.1E-02, 0.2E-02, 0.1E-01, -0.12486896688438+146, -0.84304868051574-187, -0.7711924024834-187, -0.43367753441506E-18, 0.14840204188531-232, 0.96783951745301-237, 0.21245588808235-215,
TPVN	=	0.472E+03, 0.505E+03, 0.55E+03, 0.595E+03, 0.66E+03, 0.72908384548722-270, 0.77730653632408-233, 0.77738356048447-233, -0.25817327871111-213, -0.30122111704602+135, 0.492E+03, 0.552E+03, 0.6E+03, 0.65E+03, 0.74E+03, -0.96488042731694-111, -0.21133930616936E+38, 0.86957809932183-218, -0.39693946305476+147, -0.36119894922707+135,
TRON	=	0.3495E+03, 0.4737E+03, 0.61E+03, 0.66E+03, 0.71E+03, 0.74E+03, -0.53065213082936E+37, 0.59676220492351-207, -0.10363959171499E+50, 0.24063187367222-234, 0.483E+03, 0.485E+03, 0.69E+03, 0.834E+03, 0.778E+03, 0.105E+04, 0.0, -0.36942527263909-114, 0.15788132967560-229, 0.61671866389451-232,
TIABLE	=	0.4E+03, 0.53E+03, 0.6E+03, 0.1E+05, 0.54467632976101E+17, -0.50179273861745-187, 0.11386091566665E+37, -0.44888219770582E+47, 0.9282855997986-237, 0.60830850963552-232,
TW	=	0.54E+03,
VC	=	0.376E-02,
VDROP	=	0.8E+02, 0.8E+02,
WGI	=	0.1E-07, 0.1E-07,
XK	=	0.14E-04, 0.36E-05,
XM	=	0.92E+02, 0.32E+02,
XMP	=	0.4E+02,
XMU	=	0.5E-05, 0.6E-06,
XR	=	0.1E+01, 0.1E+01,
YK	=	0.129E-03, 0.129E-03, 0.344E-03, 0.989E-03, 0.1633E-02, 0.215E-02, 0.243E-02, 0.2663E-02, 0.2808E-02, 0.295E-02, 0.3E-02, 0.305E-02, -0.17510348878417-199, -0.17273822881578-269, -0.36114857035082+135, -0.36119893568853+135, -0.17385317893791-269, -0.15513717557568+145, -0.36120715723279+135, 0.132E-03, 0.132E-03, 0.298E-03, 0.507E-03, 0.1E-02, 0.123E-02, 0.132E-02, 0.143E-02, 0.15E-02, 0.152E-02, 0.153E-02, 0.154E-02, 0.154E-02, 0.19329969043184E+37, 0.27837352882358E+18, -0.12486868173244+146, -0.27707513863968-190, 0.15465256186183E+38, 0.22651353260289-234, -0.14807298884747-189,

TABLE B-I (Continued)

YREACT = 0.1123E+04, 0.2605E+04, 0.486E+04, -0.13573062411117-185, -0.4367505006875-161,
 -0.38818110362597E+70, -0.42381131515697-161, -0.21134411462655E+71, -0.38818110362597E+70,
 -0.3970490572155+147, 0.222E+04, 0.2605E+04, 0.486E+04, -0.21134610588706E+71,
 -0.38756238516339E+70, -0.36122333971234+135, -0.1419344806777-175, -0.73363051931988-272,
 -0.10478531855812-108, 0.10752873506502E+50,

ICASE = 1000,

MSPEC = 10,

HFLIQ = -0.25E+04, 0.12E+05,

IUNIT = 6,

ND1 = 1,

ND2 = 100000,

ND3 = 2,

PGP = 0.0,

TFINAL = 0.1E+01,

IFPLOI = 0,

PLTIME = 0.3E+02,

IDEION = 0.2E+02, 0.4E+02, 0.6E+02, 0.8E+02, 0.9E+02, 0.1E+03, 0.12E+03, 0.1E+11, 0.1E+11,
 0.1E+11, 0.1E+11, 0.1E+11, 0.1E+11, 0.1E+11, 0.1E+11, 0.1E+11, 0.1E+11, 0.1E+11, 0.1E+11,
 0.1E+11, 0.1E+11, 0.1E+11, 0.1E+11, 0.1E+11, 0.1E+11, 0.1E+11, 0.1E+11, 0.1E+11, 0.1E+11,
 0.1E+11, 0.1E+11,

ICRII = 0.1E-02, 0.5E-03,

RCRII = 0.2E-02, 0.1E-02,

XCRII = 0.1E+11, 0.1E-09,

PGAUD = 0.0, 0.0, 0.0, 0.0, 0.0, 0.0, 0.0, 0.0, 0.0, 0.0, 0.0, 0.0, 0.0, 0.0, 0.0, 0.0, 0.0, 0.0,

NPG = 0,

TABLE B-I (Continued)

CONCR = 0.5E+00,
 ICR = 0.53999E+03,
 XKBAR = -0.41508296559865E-52,
 HEATX = 0.1E+04,
 IDEBUG = T,
 WLIQ = 0.0, 0.1E-03, 0.1E-02, 0.37E-02, 0.134E-01, 0.196E-01, 0.293E-01, 0.293E-01, 0.825E-01,
 0.775E-01, 0.752E-01, 0.74E-01, 0.727E-01, 0.72E-01, 0.72E-01, -0.10445673036381E+50,
 0.19154274902884-236, -0.24091362111454-109, -0.39720938686675+147, 0.43536385125157-124,
 0.19178802719029-149, -0.40424548216055-173, 0.14650569636576-217, 0.11845692916435-275,
 -0.22669644116145+140, 0.0, 0.5E-03, 0.11E-02, 0.23E-02, 0.33E-02, 0.375E-02, 0.375E-02,
 0.1283E+00, 0.95E-01, 0.835E-01, 0.812E-01, 0.775E-01, 0.763E-01, 0.753E-01, 0.751E-01,
 0.46559493824895-237, -0.38977326688899+147, -0.35445304385506+135, 0.48819551563344-125,
 -0.3544359383752+135, -0.35443572163346+135, -0.35443433491784+135, -0.35444265254616+135,
 -0.35444126544977+135, -0.35443871070643+135,
 TLIQ = 0.0, 0.5E-02, 0.1E-01, 0.15E-01, 0.25E-01, 0.35E-01, 0.48E-01, 0.765E-01, 0.775E-01,
 0.85E-01, 0.9E-01, 0.95E-01, 0.105E+00, 0.12E+00, 0.128E+00, 0.0, 0.0, 0.0, 0.0, 0.0, 0.0,
 0.0, 0.0, -0.71394244806269-260, -0.1254900519996+246, -0.31361169113931E+2, 0.43E-01,
 0.5E-01, 0.55E-01, 0.6E-01, 0.65E-01, 0.7E-01, 0.105E+00, 0.106E+00, 0.1075E+00,
 0.109E+00, 0.11E+00, 0.113E+00, 0.115E+00, 0.12E+00, 0.128E+00, 0.86352889272752-165,
 -0.48445441158777E-59, 0.31242941009043-235, -0.52212333520125E+49, 0.97001590942197-237,
 0.55947490410617E+17, 0.78258962961875-236, 0.77937455705288-177, 0.94720862006616E+55,
 0.10465980011779+299,
 NLIQ = 15, 15,
 SEND

TABLE B-II
TYPICAL OUTPUT FROM CHAMBER PRESSURIZATION TRANSIENT PROGRAM

TIME (MILLISEC) = 1.1000E-02

PRESSURES (PSIA)	TEMPERATURES (DEGR)	REACTION PARAMETERS	WEIGHTS AND FACTORS
OXID = 2.4512E-05	TFINAL= 5.5069E+02	HEACT(O)= 5.1816E-19	WTOTAL(O)= 9.9981E-09
FUEL = 9.6188E-07	TAVERG= 5.5069E+02	HEACT(F)= 3.6046E-19	WTOTAL(F)= 9.9999E-09
TOTAL = 2.5474E-05	TUP = 5.5223E+02	DELTA = 4.7421E-07	F(O) = 8.5643E-01
PGP = 1.3815E-13			F(F) = 9.9804E-01

PRODUCT CONCENTRATIONS

N2O4 = 9.9981E-09	N2H4 = 9.9999E-09	N2O = 0.	N2O = 1.3816E-18
NO = 4.7099E-19	NH3 = 8.2725E-26	N2 = 1.0990E-18	H2O = 5.6519E-19
N3H5O3 = 4.6229E-25	N2H4O3 = 1.2560E-18		

Output with oxidizer and fuel flowing

TIME	PG	GEVAP	GCOND	TG	WTOTAL	F
1.0000E-03	2.1043E-06	1.2564E-10	0.	5.4000E+02	1.0000E-08	9.8744E-01
2.0000E-03	8.1998E-06	3.6519E-10	0.	5.4000E+02	3.0000E-08	9.8364E-01
3.0000E-03	2.2061E-05	8.3219E-10	0.	5.3868E+02	7.0000E-08	9.8110E-01
4.0000E-03	4.7007E-05	1.5018E-09	0.	5.3770E+02	1.3040E-07	9.7834E-01
5.0000E-03	8.6093E-05	2.3594E-09	0.	5.3666E+02	2.1140E-07	9.7548E-01
6.0000E-03	1.4245E-04	3.4097E-09	0.	5.3562E+02	3.1322E-07	9.7257E-01
7.0000E-03	2.1931E-04	4.6602E-09	0.	5.3465E+02	4.3605E-07	9.6961E-01
8.0000E-03	3.2004E-04	6.1173E-09	0.	5.3378E+02	5.8010E-07	9.6662E-01
9.0000E-03	4.4808E-04	7.7872E-09	0.	5.3302E+02	7.4560E-07	9.6359E-01
1.00451E-02	6.0696E-04	9.6753E-09	0.	5.3234E+02	9.3275E-07	9.6053E-01

Output with oxidizer only flowing

APPENDIX C

PROPELLANT TRANSIENT FLOW PROGRAM

COMMON/NAME1/EU(6),EL(6),TEMPS(9,6),Q(6),DQ(6),H,T
COMMON/NAMES/TV0,XN,AV,AV0,VME,VM0, XKL,F(3),XL,D,PM

1 ,DP,VMF,PSS

2 ,XNRE,DRP

3 ,NN

4 ,W(3),RO,XLF

5 ,COE,PVV,PV,PVI,GAM

COMMON/NAMEC/CRE,C1,C2,C3,C4,C5

COMMON/MARKET/ TEMPO,XMOWT,PAMB,A0

DIMENSION QI(6)

EXTERNAL AUXSUB

NAMelist/DATA/RO,XL,PVI,XKL,DI,CV ,XLF,XLMI,C0,DOI

1 ,XMU,AV0I,TV0,XN,VM0I,WSS ,TMAX,TS,XNORF,XNRE

2 ,H0,ELR,EUR,HMAX,HMIN,DRP

3 ,GAM,PCSSI

4 ,COE

5 ,FLAG,PSSI,DPI

6 ,QI

5 ,TEMPO,XMOWT,PAMBI

G=32.174

PI=3.14159265

PAMB=0.0

GAM=1.

FLAG=0.

PCSSI=0.

COE=.5

XN=1.

TS=0.

XNRE=.25

H0=1.E-7

ELR=.00003

EUR=.002

HMAX=1.E-3

HMIN=1.E-7

DRP=0.

LC=18

CONTINUE

NN=4

DO 100 K=1,NN

QI(K)=0.

READ (5,DATA)

WRITE(6,DATA)

NN=4

PAMB=PAMBI*144.

IF(PAMBI .NE. 0.0) NN=6

D=DI/12.

XLM=XLMI/12.

```

D0=D0I/12.
AV0=AV0I/12.**2
VM0=VM0I/12.**3
PCSS=PCSSI*12.**2
PV=PVI*12.**2
PM=GAM*PV
C
AL=PI*(D/2.)**2
A0=PI*(D0/2.)**2*XNORF
C
CRE=4.*RO/PI/XMU/D
C1=G*AL/RO/XL
C2=RO/(2.*G*AL**2)
C3=RO/(2.*G*CV**2)
C4=G/RO/XLM**2
C5=RO/(2.*G*(C0*A0)**2)
C
QQ=WSS/RO
CALL FSUB(QQ,CRE,XNRE,FQ)
IF(FLAG .EQ. 0.) GO TO 15
PSS=PSSI*144.
DP=DPI*144.
GO TO 16
15 CONTINUE
PSS=C5*QQ**2
DP=PSS+((XKL+FQ*XLF/D)*C2*C3/AV0**2)*QQ**2+PCSS
PSSI=PSS/144.
DPI=DP/144.
16 CONTINUE

WRITE(6,900) AV0,VM0,AL,A0,CRE,C1,C2,C3,C4,C5,PSSI,DPI
900 FORMAT(///,* AV0,VM0,AL,A0,CRE =*,5E15.5
1 ,/,* C1,C2,C3,C4,C5 =*,5E15.5
2 ,/,* PSS,DP =*,2E15.5)
C
C
T=TS
H=H0
DO 21 K=1,NN
21 Q(K)=QI(K)
ICNT=0
DO 2 K=1,NN
DO 2 J=1,9
2 TEMPS(J,K)=0.
C
CALL AUXSUB
L=0
CALL PRINT(L)
C
10 CONTINUE
DO 3 K=1,NN
EU(K)=ABS(Q(K))*EUR+1.E-20
3 EL(K)=ABS(Q(K))*ELR+1.E-20
CALL RKAM(T,H,Q,DQ,AUXSUR,NN,0.,EU,EL,HMAX,HMIN,ICNT,TEMPS,NN)
IF(L .GT. LC) L=0
CALL PRINT(L)
IF(T+H .LT. TMAX) GO TO 10
C

```



```
H=TMAX-T  
ICNT=0  
CALL RKAM(T,H,Q,DQ,AUXSUB,NN,0.,EU,EL,HMAX,HMIN,ICNT,TEMPS,NH)  
CALL PRINT(L)  
GO TO 1
```

C
C

```
END
```

SUBROUTINE AUXSUB

C
 COMMON/NAME1/EU(6),EL(6),TEMPS(9,6),Q(6),DQ(6),H,T
 COMMON/NAMES/TV0,XN,AV,AV0,VME,VM0, XKL,F(3),XL,D,PM
 1 ,DP,VMF,PSS
 2 ,XNRE,DRP
 3 ,NN
 4 ,W(3),RO,XLF
 5, COE,PVV,PV,PVI,GAM
 COMMON/NAMEC/CRE,C1,C2,C3,C4,C5

C
 C
 CT=AMAX1(.005 ,AMIN1(1.,(T/TV0)**XN))
 AV=AV0*CT
 VMF=Q(3)-Q(4)
 VME=VM0-VMF
 PVV=COE * PM * VMF * VM0**GAM / VME**(GAM+1.0)
 PVV=AMAX1(PVV,PV)
 CALL GAS(VM0,GAM,VME,VMF,DQ(5),Q(5) ,PVV,Q(6),DQ(6),Q)
 CALL FSUB(Q(1),CRE,XNRE,F(1))

C
 DQ(1)=C1*(DP-(XKL+F(1)*XLF/D)*C2*Q(1)**2-C3*Q(1)**2/AV**2
 1 -PVV)
 IF (VMF .LE. .7 *VM0) GO TO 10
 DQ(2)=C4*VMF*(-C5*Q(2)**2
 1 +PVV-PVI)
 GO TO 11
 10 DQ(2)=0.
 11 CONTINUE
 DQ(3)=Q(1)
 DQ(4)=Q(2)

C
 RETURN
 END

```

SUBROUTINE GAS (VM0,GAM,VME,VMF,WDOT,WGOUT,PVV,PMAN,DPVV,Q)
COMMON/MARKET/ TEMPO,XMOWT,PAMB,A0
COMMON/CHECK/TM,XM
DIMENSION Q(1)
NAMELIST/BUG/PVV,WLEFT,WO,WGOUT,VSP,TM,PRAT,XM,WDOT,DPVV,Q,VME
DATA IST/0/
IF(PAMB.EQ. 0.0)RETURN
IF(IST .EQ. 1)GO TO 100
IST=1
PMAN=PAMB
R=1545./XMOWT
WO= VM0*PAMB/R/TEMPO
CON1= VM0/WO
CON2= CON1**GAM
CON3= CON2/CON1
CON4= GAM*PAMB*CON2
CON5= A0*SQRT( 32.174*GAM/R )
XPON= (GAM+1.0)/2.0/(GAM-1.0)
GM102= (GAM-1.0)*0.5
100 CONTINUE
PVV=PMAN
WLEFT=WO-WGOUT
VSP=VME/WLEFT
TM=PVV*VSP/R
PRAT=(PVV/PAMB)**( (GAM-1.0)/GAM)
PRAT=AMAX1(PRAT,1.0)
XM= SQRT( 2.0*( PRAT-1.0)/(GAM-1.0) )
IF( XM .GT. 1.0) XM=1.0
WDOT= CON5*PVV*XM/SQRT(TM)/( 1.0+ GM102*XM**2)**XPON
DPVV=PVV*GAM*( Q(1)-Q(2)-WDOT*VME/WLEFT)/VME
WRITE(6,BUG)
RETURN
END

```

SUBROUTINE FSUB(Q,CRE,XNRE,F)

RE=CRE*Q

IF(RE.LT.1187.0) F = 64.0 / RE

IF(RE.GE.1187.0) F = 0.3164 / (RE**XNRE)

IF(RE.LT.1.0) F = 64.0

RETURN

END

SUBROUTINE PRINT(L)

COMMON/NAME1/EU(6),EL(6),TEMPS(9,6),Q(6),DQ(6),H,T
COMMON/NAMES/TV0,XN,AV,AV0,VME,VM0,XKL,F(3),XL,D,PM
1,DP,VMF,PSS
2,XNRE,DRP
3,NN
4,W(3),RO,XLF
5,COE,PVV,PV,PVI,GAM
COMMON/NAMEC/CRE,C1,C2,C3,C4,C5
COMMON/CHECK/TM,XM

IF(L.NE.0) GO TO 1

PNEXT=T-4.*DRP

WRITE(6,900)

900 FORMAT(1H1,40X,23HTRANSIENT FLOW ANALYSIS,//

1	,	*	T		W1		Q1	DQ1
2			IQ1		VMF		PVV	WG OUT*/
3	,	*	H		W2		Q2	DQ2
4			IQ2		VME		AV	WG DOT*/

CONTINUE

IF(T.LT.PNEXT) RETURN

PNEXT=PNEXT+DRP

L=L+1

DO 2 I=1,2

W(I)=Q(I)*RO

PVVI=PVV/144.

WRITE(6,90) T,W(1),Q(1),DQ(1),G(3),VMF,PVVI,Q(5)

WRITE(6,91) H,W(2),Q(2),DQ(2),G(4),VME,AV,DQ(5)

WRITE(6,903)TM,XM

903 FORMAT(1X,2E15.9)

90 FORMAT(/,F15.9,7E16.6)

91 FORMAT(F15.9,7E16.6)

RETURN

END

APPENDIX D

CHAMBER PRESSURIZATION TRANSIENT PROGRAM

```
PROGRAM PRESS(INPUT,OUTPUT,PUNCH,TAPE5=INPUT,TAPE6=OUTPUT,
1 TAPE7=PUNCH)
```

C
C
C
C
C

```
TRANSIENT PRESSURE HISTORY PROGRAM
```

```
000003 COMMON/CPLT/ IFPLOT, PLTIME, IPLTI, TMAX
```

```
000003 LOGICAL AVERGE, IDEBUG
```

```
000003 COMMON/DULOOP/ ND1,ND2,ND3
```

```
000003 COMMON /A/ TFP(2),TAU(2),TAUF(2),TAUS(2),XM(2),GAM(2),TC
1 PG(2), M(2),GEVAP(2),X1(2),XR(2) , T01
```

```
000003 COMMON/ABCDE/ X(400,2), T(400,2), R(400,2), W(400,2)
```

```
000003 COMMON/COM1/AX(5,10),COEF(5,10),ENTHPY(10),FORO(10),SPNAME(10)
```

```
000003 COMMON/COM2/ICASE,IUNIT,F(2),HFLIQ(2),MSPEC,PGTOTAL,PROD(10),
1 TFINAL,WDROP(2),WTOTAL(2),IFIRST
```

```
000003 COMMON/OUTA/ PG1(2),PGP1,REACT(2),TAVERG,DELTRE,TIME,TQP
```

```
000003 COMMON/OUTB/ NPAGE
```

C

```
000003 DIMENSION TDETON(40)
```

```
000003 DIMENSION ROL(2),CPL(2)
```

```
000003 DIMENSION PTANK(2),PCPV(2),PVV(2),CONST7(2),YREACT(10,2)
```

```
000003 DIMENSION TTABLE(10),A(12,10,2),EACTT(10),YK(20,2),PCT(20,2),
1 PTAN(20,2),TP(20,2),AAT(10)
```

```
000003 DIMENSION PV(10), TD(10),TAG(2),PVW(2),PVF(4),TDK(4)
```

```
000003 DIMENSION W1(20,2),T1(20,2)
```

```
000003 DIMENSION TA(4),CPLA(4),G(2),GCOND(2),XMNOZ(2),TQ(2)
```

```
000003 DIMENSION XMMM(2),RR2(2)
```

```
000003 DIMENSION ROP(2)
```

```
000003 DIMENSION VDROP(2),XMU(2),CPG(2),XK(2),HC(3,2), RE(2
```

```
1 ), PR(2),H(2),Z(2),QBIG(2),PHE(2),GAN(2),CVG(2),EPCOE(2)
```

```
000003 DIMENSION RON(10,2),CPN(10,2),CPGN(10,2),PVN(10,2),TRON(10,2)
```

```
1 (10,2),TCPGN(10,2),TPVN(10,2)
```

```
000003 DIMENSION TGI(2),RGI(2),WGI(2)
```

```
000003 DIMENSION RELWT(10)
```

```
000003 DIMENSION NUPPER(2), AVERGE(2), TCRIT(2), RCRIT(2), XCRIT(2)
```

```
000003 DIMENSION DELTXS(2), DELRXS(2)
```

```
000003 DIMENSION DELTX(2), DELRX(2), DELXX(2)
```

```
000003 DIMENSION PGADD(10,2), PGADDT(10,2),PAADD(2)
```

```
000003 DIMENSION WLIQ(25,2),TLIQ(25,2),NLIQ(2),WXXX(2)
```

C

```
000003 NAMELIST /DATA/
```

```
1 A, AAT, AC, ALPHA, ASTAR, CFORPR, CPGN, CPGP, CPN, CVG,
```

```
2 DELTN, DTMAX, DTMIN, EACTT, GAM,GAMP, HC, M,
```

```
3 NN, NOCP, NOCPG, NOPV, NORO, NTRAN,
```

```
4 PCT, PG, PTAN, PVN, PVV, PVW, RGI, RM, RN, RON,
```

```
5 TAU, TAUF, TAUS, TCPGN, TCPN, TFP, TGI, TMAX, TP, TPVN, TROI
```

```
6 TTABLE, TW,
```

```
7 VC, VDROP, WGI, XK, XM, XMP, XMU, XR,
```

```
8 YK, YREACT
```

```
* , ICASE, MSPEC, HFLIQ, IUNIT
```

```
* , ND1, ND2, ND3,PGP, TFINAL
```

```
* , IFPLOT, PLTIME
```

```
* , TDETON
```

```
* , TCRIT, RCRIT, XCRIT
```

```
* , PGADD, NPG, PGADDT
```

```
* , CONCR, TCR, XKBAR, HEATX
```

```

      * , IDEBUG
      * , WLIQ , TLIQ,NLIQ

C
000003 1 CONTINUE
C
000003 CALL SECOND(EXTIME)
000005 CALL PSECOND(PSEC)
000007 WRITE(6,4444) EXTIME, PSEC
000017 4444 FORMAT(1H0,30X, 9HCP TIME =,F8.3,5X, 9HPP TIME =,F8.3)
C
000017 IDETON = 1
000020 DO 1886 I = 1,40
000022 1886 TDETON(I) = 1.0E10
C
C ZERO ARRAYS
C
000026 IDEBUG = .FALSE.
000027 DO 1888 I = 1,5
000030 DO 1888 J = 1,10
000031 COEF(I,J) = 0.0
000034 1888 CONTINUE
000041 DO 2 L=1,2
000042 NUPPER(L) = 0
000043 DELTAS(L) = 1.E30
000045 DELRXS(L) = 1.E30
000046 DO 2 I = 1,400
000050 X(I,L)=0.
000053 T(I,L)=0.
000056 2 R(I,L)=0.
000065 DO 6 I=1,10
000066 PGADD(I,1) = 0.0
000067 PGADD(I,2) = 0.0
000070 PGADD(I,1) = 0.0
000071 PGADD(I,2) = 0.0
000072 PROD(I) = 0.0
000073 6 CONTINUE
000075 NPG = 0
000076 ND1 = 1
000077 ND2 = 100000
000100 ND3 = 2
000101 PGP=0.
000102 TFINAL=1.
000104 NLIQ(1) = 1
000105 NLIQ(2) = 1
C
000106 IFPLOT = 0
000107 PLTIME= 30.0
000110 IPLT1 = -1
000111 READ(5,DATA)
000114 WRITE(6,DATA)
C
C READ SPECIES INFO IN FORM OF ODE INPUT
C
000117 DO 150 I = 1,MSPEC
000121 READ(5,190) (AX(J,I),COEF(J,I),J=1,5), ENTHPY(I),FORO(I),SPNAME(
000145 WRITE(6,191) (AX(J,I),COEF(J,I),J=1,5), ENTHPY(I),FORO(I),SPNAME
000172 190 FORMAT(5(A2,F7.5),8X,F9.0,9X,A1,2X,A6)
000172 191 FORMAT(1H0,5(A2,F7.5),8X,F9.0,9X,A1,2X,A6)

```

```

000172      150  CONTINUE
000175          DO 24 N=1,2
000176          DO 24 I=1,NOPV
000177      24  PVN(I,N)=ALOG10(PVN(I,N))
000212          NSAVE1=1
000213          NSAVE2=2
000214          NSAVE3=3
000215          NSAVE4=4
000216          IWSAVE = 1

C
C          COMPUTE INITIAL CONDITIONS
C

000217      RC = 1545.0
000220      NSTOP=520
000221      NPAGE=1
000222      DO 10 I = 1,2
000224      T(1,I) = TGI(I)
000227      TG(I) = TGI(I)
000231      R(1,I) = RGI(I)
000234      W(1,I) = WGI(I)
000237      TAG(I) = 0.0
000240      REACT(I) = 0.0
000241      GCOND(I) = 0.0
000242      WTOTAL(I) = 0.0
000243      WDROP(I) = 0.0
000244      XMNOZ(I) = 0.0
000245      RR2(I) = R(1,I)**3
000250      10  CONTINUE
000252      IF(XM(1) .GT. 0.) XMMM(1)=SQRT(XM(1))
000256      IF(XM(2) .GT. 0.) XMMM(2)=SQRT(XM(2))
000262      GEVAP1=0.
000263      GEVAP2=0.
000264      DT1000=1000.*DELTN
000266      RPN=0.
000267      XMNOZP=0.
000270      TRUE=0.
000271      INDICA = 0
000272      GCONDP=0.
000273      TGP=TG(1)
000274      TQP=TGP
000275      PGTOTAL=0.
000276      DENOMP=0.
000277      PGTOTL=0.
000300      IFIRST=0
000301          CONST1= 4.*ALPHA*          3.1415/SQRT(6.2831853*RC/32.2)
000311          CONST2= 3.*ALPHA/          SQRT(6.2831853*RC/32.2)
000320          CONST3= CONST2*AC/3.
000322          CONST4 = ASTAR*SQRT(32.2/1545.)
000326          CONST5=SQRT((32.2*XMP/RC)*(2./(GAMP+1.))**((GAMP+1.)/(GAMP-1.
1          ASTAR

C
C          TIME1=DELTN
000345      TIME=DELTN*1000.
000346
000350      N22=NOW-1
000352      NSTOP = NSTOP+1

C
C          SELECT THE CORRECT PROBLEM
C

```



```

000353      NPP = 0
000354      NPF = 0
000355      IF(M(1).EQ.0) NPF = 2
000357      IF(M(2).EQ.0) NPF = 1
000361      IF(NPF .EQ. 0) NPF=3
000363      IF(M(1).EQ.M(2)) NPF =4
000366      IF((M(1).LE.M(2)).AND.(M(1).GE.1))      N=1
000400      IF((M(2).LE.M(1)).AND.(M(2).GE.1))      N=2
000412      IF(NPF.LT.3) N=NPF

```

C
C
C

THE TIME LOOP

```

000415      L=0
000416      25 L=L+1
000420      GEVAP2=GEVAP1
000421      QBIG(1)=0.
000422      QBIG(2)=0.
000423      TAG(N)=0.
000424      GEVAP(1) =0.
000425      GEVAP(2) =0.
000426      X1(1) =0.
000427      X1(2) =0.
000430      LX=L
000431      IF(NPF.NE.4) GO TO 205
000433      50 N=1
000434      TAG(N)=0.
000436      LX=L-M(1)+1
000440      IF((LX.GE.1).AND.(M(1).GT.0)) GO TO 205
000447      100 N=2
000450      TAG(N)=0.
000452      LX=L-M(2)+1
000454      IF((LX.GE.1).AND.(M(2).GT.0)) GO TO 205
000465      GO TO 800
000466      205 BB=XMMM(N)
000470      AVERGE(N) = .FALSE.
000471      NUP = LX - NUPPER(N)
000473      IF(NUP.GT.399) GO TO 999
000476      DO 700 NNN = 1,NUP
000477      CC = W(NNN,N)
000503      J = NUP - NNN + 1
000505      TT=T(J,N)
000510      RR=R(J,N)
000513      XX=X(J,N)
000516      CALL LINI(TRON(1,N),RON(1,N),NORO,TT,ROL(N),NSAVE1)
000525      CALL LINI(TCPN(1,N),CPN(1,N),NOCP,TT,CPL(N),NSAVE2)
000534      CALL LINI(TCPGN(1,N),CPGN(1,N), NOCPG,TT,CPG(N),NSAVE3)
000543      CALL LINI(TPVN(1,N),PVN(1,N),NOPV,TT,PP,NSAVE4)
000552      PP=10.**PP
000556      310 CONTINUE
000556      IF(XX .GE. 1.) GO TO 312
000561      G(N) = ((PP-PG(N))*RR**2/SQRT(TT))*CONST1*BB*DELTN
000572      IF(G(N).LT.0.) G(N)=0.
000574      GO TO 316
000575      312 G(N)=0.
000577      316 TOG=(G(N)*CC*XR(N)/(ROL(N)*RR2(N)))*.2387
000605      GEVAP(N) = GEVAP(N) + TOG
000607      TAG(N)=TAG(N)+TOG*TT
000612      IF(IDEBUG) WRITE(6,6400) NNN,LX,J,N, TT,RR,XX,PP,

```

```

1 G(N),TOG,GEVAP(N),TAG(N),CC
000651 6400 FORMAT(1H0,* NNN,LX,J,N*,4I10/ * TT,RR,XX,PP*,4E20.8/
1 * G(N),TOG,GEVAP(N),TAG(N) * , 4E16.8,* CC *,E15.7)
000651 IF(XX .GE. 1.) X(J+1,N)=1.
000660 IF(PP .LE. PG(N)) GO TO 315
000663 IF(XX .GE. 1.) GO TO 315
000665 XTEMPX= (1.-BB*(PP-PG(N))*DEL TN*CONST2/(ROL(N)*SQRT(TT) *RR)
000701 IF(XTEMPX.LE.0.0) GO TO 315
000702 R(J+1,N) =RR* XTEMPX**0.3333
000711 GO TO 320
000711 315 R(J+1,N)=RR
000715 320 RE(N)=2.*RR*VDROP(N)*XM(N)*PG(N)/(XMU(N)*RC*TG(N))
000725 PR(N)= CPG(N)*XMU(N)/XK(N)
000731 PRO = PR(N)**.33333
000734 REO = RE(N)**.5
000740 H(N) = XK(N)*(2.+.6*PRO*REO)/(2.*RR)
000750 Z(N) = G(N)*CPG(N)/(12.566*H(N)*DEL TN*RR**2)
000756 IF(Z(N) .GT. 30.) Z(N)=30.
000762 IF(Z(N) .LT. 1.E-10) GO TO 325
000765 Z(N) = Z(N)/(2.71828**Z(N)-1.)
000772 GO TO 326
000773 325 Z(N)=1.
000775 326 PHE(N)=3.*H(N)*(TG(N)-TT)*RR**2 *Z(N)*DEL TN/(ROL(N)
1CPL(N)*RR**3)
001010 QBIG(N)=QBIG(N)+3.*H(N)*RR**2 *Z(N)*DEL TN*(TG(N)-TT)*
1XR(N)*CC /((RR2(N)*ROL(N))
001025 IF(XX .GE. 1.) GO TO 360
001030 IF(PP .GT. PG(N)) GO TO 340
001034 T(J+1,N)=TT
001037 IF(T(J+1,N) .LE. TFP(N)) GO TO 350
001044 GO TO 370
001044 340 T(J+1,N)= TT -CONST2*DEL TN*TAU(N)*(PP-PG(N))/(ROL(N)
1*CPL(N)*RR *SQRT(TT) ) *BB+PHE(N)
001066 IF(T(J+1,N) .LT. TFP(N)) T(J+1,N)=TFP(N)
001077 IF(T(J+1,N) .GT. TFP(N)) GO TO 370
001105 350 X(J+1,N)=XX + (G(N)*TAUS(N)/(ROL(N)* RR**3*TAUF(
1*.2387-CPL(N)*PHE(N)/TAU(N)
GO TO 370
001122 360 T(J+1,N)=TFP(N)
001122 370
001126 700 CONTINUE
001126 700 CONTINUE
C
C COMPUTE DIFFERENCE TERMS BETWEEN DROPS WITH LONGEST RESIDENCE
C
001131 DELTX(N)= ABS(T(NUP+1,N)-T(NUP,N)) / (T(NUP,N)+1.0E-35)
001142 DELRX(N)= ABS(R(NUP+1,N)-R(NUP,N)) / (R(NUP,N)+1.0E-35)
001152 DELXX(N)= ABS(X(NUP+1,N)-X(NUP,N)) / (X(NUP,N)+1.0E-35)
001162 IF(IDEBUG) WRITE(6,6405)N,NUPPER(N),DELTX(N),DELRX(N)
001177 6405 FORMAT(1H , *N,NUPPER(N),DELTX(N),DELRX(N) *,2I5,2E20.8)
001177 IF(L.LE.2) GO TO 7000
001202 IF(ABS(DELTXS-DELTX) .GT.1.0E-12) GO TO 6990
001207 IF(ABS(DELRXS-DELRX) .GT.1.0E-12) GO TO 6990
C
C AUTOMATIC AVERAGING
C
001214 GO TO 6995
001214 6990 CONTINUE
001214 IF(DELTX(N) .GT.TCRIT(N)) GO TO 7000

```

```

001220     IF (DELRX(N).GT.RCRIT(N)) GO TO 7000
001223     IF (DELXX(N).GT.XCRIT(N)) GO TO 7000
001226 6995 CONTINUE
001226     AVERGE(N) = .TRUE.
001230     T(NUP,N) = (T(NUP+1,N) + T(NUP,N)) / 2.0
001236     R(NUP,N) = (R(NUP+1,N) + R(NUP,N)) / 2.0
001243     X(NUP,N) = (X(NUP+1,N) + X(NUP,N)) / 2.0
001247 7000 CONTINUE
001247     DELTXS(N) = DELTX(N)
001251     DELRXS(N) = DELRX(N)
001253     PPG=PG(N)
001254     IF (NPF .EQ. 4) PPG=PGTOTL
001260     DO 2500 K1=1,NTRAN
001262     IF (PPG .GE. PCT(K1,N) .AND. PPG .LE. PCT(K1+1,N)) GO TO 2507
001276     K1=K1
001277 2500 CONTINUE
001301 2507 CONST7(N)=(YK(K1+1,N)-YK(K1,N))*(PCT(K1+1,N)-PPG)/(PCT(K1,N)
1-PCT(K1+1,N))+YK(K1+1,N)
001321     DO 2600 K=1,NTRAN
001322     IF (TIME1.GE. TP(K,N) .AND. TIME1.LE. TP(K+1,N)) GO TO 2607
001336     K=K
001337 2600 CONTINUE
001341 2607 PTANK(N)=(PTAN(K+1,N)-PTAN(K,N))*(TP(K+1,N)-TIME1)/(TP(K,N)
1-TP(K+1,N))+PTAN(K+1,N)
001361     PCPV(N)= PG(N)
001362     IF (PG(N) .LE. PVV(N)) PCPV(N)=PVV(N)
001367     IF (NPF.EQ.1) GO TO 800
001371     IF (NPF.EQ.2) GO TO 800
001373     IF (NPF.EQ.3) GO TO 710
001374     IF ((NPF.EQ.4).AND.(N.EQ.2)) GO TO 800
001402     IF ((NPF.EQ.4).AND.(N.EQ.1)) GO TO 100
001411 710     IF (N.EQ.1) MPF=2
001414     IF (N.EQ.2) MPF=1
001417     IF (M(MPF).EQ.L) NPF=4
001423     IF (NPF.NE.4) GO TO 800
001425     IF (MPF.EQ.2) GO TO 100
001427     IF (MPF.EQ.1) GO TO 50
001430 800     CONTINUE

C
001430     IF (NPF.EQ.4) N=1
001433 810     GCOND(N)=((PG(N)-PVW(N))*CONST3*DELTN/SQRT(TG(N)))*BB
001444     IF (GCOND(N).LT.0.) GCOND(N)=0.
001447     LX = L - M(N) + 1 - NUPPER(N)
001453     WTOTAL(N)=WTOTAL(N)+W(LX,N)-XMNOZ(N)-REACT(N)
001461     TO(N)=WTOTAL(N)
001463     WDROP(N)=W(LX,N) -GCOND(N)-GEVAP(N)+WDROP(N)
001471     F(N)=WDROP(N)/WTOTAL(N)
001473     XMNOZ(N) = (PG(N)/SQRT(TG(N)))*CONST4*BB*SQRT(GAM(N)*(2./(GAM
11.))*((GAM(N)+1.)/(GAM(N)-1.)))
001521     XMNOZ(N)=XMNOZ(N)*DELTN
C
C     IF THE COMPUTED VALUE OF MASS OUT NOZZLE IS GREATER THAN
C     THE MASS OF GASS PRESENT, ADJUST XMNOZ
001522     QUALX = PG(N) * VC / (RC * TG(N))
001526     IF (IDEBUG)WRITE(6,9513) QUALX,XMNOZ(N),N
001541 9513 FORMAT(1H ,* QUALX,XMNOZ(N),N ,*2E16.5,I5)
001541     IF (XMNOZ.GE.QUALX) XMNOZ = QUALX
001545     DENOM=GEVAP(N)+VC*XM(N)*PG(N)/(RC*TG(N))-GCOND(N)-XMNOZ(N)
001557     X1(N)=DENOM

```

```

001561      C1=0.
001561      C2=0.
001562      IF(PG(N) .LT. 144.) GO TO 4
001565      IF(TW.GT.TG(N)) GO TO 3
001570      C2=HC(2,N)*AC*(TG(N)-TW)*DEL TN/CPG(N)
001575      C1=0.
001576      GO TO 4
001576      3 C1=HC(1,N)*AC*(TW-TG(N))*DEL TN/CPG(N)
001605      C2=0.
001606      4 TQ(N)=(TAG(N)+VC*XM(N)*PG(N)/RC-(GCOND(N)+XMNOZ(N))*TG(N)+C1-(
IDENOM

C
001623      PG(N)=GEVAP(N)*RC*TQ(N)/(VC*XM(N))-RC*TQ(N)*GCOND(N)/(VC*XM(N)
1-RC*TQ(N)*XMNOZ(N)/(VC*XM(N))+PG(N)*TQ(N)/TG(N)
001641      IF(NPG.EQ.0) GO TO 7850
001642      CALL LINI (PGADD(1,N),PGADD(1,N),NPG,TIME1,PADD(N),ISAVE)
001651      PG(N) = PG(N) + PADD(N)
001654      7850 CONTINUE
001654      PG1(N)=PG(N)/144.
C
001657      COMPUTE LIQUID WEIGH T FLOW FROM INPUT TABLES
001666      CALL LINI(TLIQ(1,N),wLIQ(1,N),NLIQ(N),TIME1,wXXX(N),IWSAVE)
001703      4487 IF(IDEBUG)WRITE(6,4487)N,IWSAVE,TIME1,wXXX(N)
001703      FORMAT(1H0,* N,IWSAVE,TIME1,wXXX(N) *,2I5,2E20.8)
001707      W(LX+1,N) = wXXX(N)
001707      IF(.NOT.AVERGE(N)) GO TO 6710
C
C
C
AVERAGE W FOR GROUPS WITH LONGEST RESIDENCE TIME I.E. 1 AND 2
C
001711      NUPPER(N) = NUPPER(N) + 1
001713      W(1,N) = W(1,N) + W(2,N)
001717      IF(LX.LT.2) GO TO 6701
001721      DO 6700 J = 2,LX
001723      W(J,N) = W(J+1,N)
001732      6700 CONTINUE
001735      6701 CONTINUE
001735      6710 CONTINUE
C
001735      IF(NPF.NE.4) GO TO 820
001737      IF((NPF.EQ.4) .AND. (N.EQ.2)) GO TO 1100
001746      N=2
001747      GO TO 810
001747      815 PGTOTL=PG1(1)+PG1(2)
001751      GO TO 825
001752      820 PGTOTL=PG(N)
001754      825 IF(NPAGE .EQ. 1) WRITE(6,2000)
001762      IF(NPF .EQ. 4) GO TO 900
001764      IF(N .EQ. 1) GO TO 920
001766      WRITE(6,2030) TIME,PG1(2),GEVAP(2),GCOND(2),TG(2),WTOTAL(2),F(
002010      NPAGE=NPAGE+1
002012      IF(NPAGE.GE.60) NPAGE=1
002015      GO TO 990
002016      920 WRITE(6,2030) TIME,PG1(1),GEVAP(1),GCOND(1),TG(1),WTOTAL(1),F(
002040      NPAGE=NPAGE+1
002042      IF(NPAGE.GE.60) NPAGE=1
002045      GO TO 990
002046      900 WRITE(6,2030) TIME,PG1(1),PG1(2),GEVAP(1),GEVAP(2),GCOND(1),G
1(2),TG(1),TG(2)
002074      NPAGE=NPAGE+1

```

```

002076      IF(NPAGE.GE.60) NPAGE=1
002101      990 CONTINUE
002101      2000 FORMAT(1H1,4X,4HTIME,9X,2HMPG,12X,5HG EvAP,9X,5HGCOND,9X,2HTG,12X
           2WTOTAL,8X,2HF )
           1P(2),5X,8HGCOND(1),5X,8HGCOND(2),5X,5HTG(1),8X,5HTG(2))
002101      2010 FORMAT(1H ,E13.4,13X,E13.4,13X,E13.4,13X,E13.4,13X,E13.4)
002101      2020 FORMAT(1H ,E13.4,E13.4,13X,E13.4,13X,E13.4,13X,E13.4,E13.4)
002101      2030 FORMAT(1H ,9E13.4)
002101      3000 CONTINUE
002101      TG(N)=TQ(N)
002103      LLLLLL=L+1
002105      IF((NPF .EQ. 3) .AND. (M(MPF) .EQ. LLLLLL)) NPF=4
002116      GO TO 1150
002117      1100 CONTINUE
           C
           C      COMPUTE TFINAL ON FIRST TIME STEP
           C
002117      IF(L.NE.1) GO TO 425
           C
002121      TOP1= PG(1)*XM(1)*CPG(1)
002124      TOP2= PG(2)*XM(2)*CPG(2)
002126      BOT1= TOP1 * TQ(2)
002130      BOT2= TOP2 * TQ(1)
           C
002132      TFINAL = TQ(1)*TQ(2) * ( (TOP1+TOP2) / (BOT1+BOT2) )
002136      WRITE(6,424) TFINAL
002144      424 FORMAT(1H0,* COMPUTED TFINAL ON FIRST STEP = *,E20.8)
002144      425 CONTINUE
           C
           C
002144      TAVERG=(PG(1)*XM(1)*CPG(1)+PG(2)*XM(2)*CPG(2)+PGP*XMP*CPGP)/(PG
           1*XM(1)*CPG(1)/TQ(1)+PG(2)*XM(2)*CPG(2)/TQ(2)+PGP*XMP*CPGP/TFINA
           2-(QBIG(1)+QBIG(2))/(X1(1)*CPG(1)+X1(2)*CPG(2)+DENOMP*CPGP)
           C
           C
           C
002202      CON=PG(1)*VC/(RC*TQ(1))
002206      CFN=PG(2)*VC/(RC*TQ(2))
002210      IF(L.LT.3) GO TO 9270
           C
           C      UNDER CERTAIN TEMP AND OX CONC CONDITIONS HAVE DIFFUSION AND A
           C      SURFACE REACTION
           C
           C      COMPUTE TOTAL VAPOR MASS TO DETERMINE MASS FRACTION OF OX
002213      VAPMAS = CON + CFN
002215      DO 8270 I = 3,8
002216      8270 VAPMAS = VAPMAS + PROD(I)
002222      OXMF = CON / VAPMAS
002224      IF(OXMF.LT.CONCR) GO TO 9270
           C
002226      FOURPI = 4.0*3.14159
           C
002230      COMPUTE DENSITY OF OXIDIZER VAPOR
002233      ROGAS = PG(1) / (RC * TAVERG)
           C
           C      MUST CONSIDER DIFFUSION ONLY FOR FUEL DROPLETS BELOW T CRITICAL
           C
002234      NUPX = L - M(2) + 1 - NUPPER(2)

```

```

002237      DO 9255 MXZ = 1,NUPX
002241      MXY = NUPX - MXZ + 1
002243      IF(T(MXY,2).GE.TCR) GO TO 9255
C
C      MUST CONSIDER DIFFUSION AND SURFACE REACTION
C      CALCULATE DIFFUSION COEF (UNITS FT2/SEC) (FROM T-DEGK, P-ATM
C
002246      TUSE = T(MXY,2) / 1.8
002250      PUSE = PGTOTL / 14.696
C
002252      DIFX = 2.5E-8 * TUSE**1.5 / PUSE
C
C      CALCULATE VAPOR DIFFUSED, OVER ALL DROPLETS
C
002260      CONST = ROGAS * DIFX * OXMF * DELTN
002263      TEMPX = FOURPI * R(MXY,2) * W(MXZ,2)
C
002266      WRITE(6,9246) MXY,MXZ,R(MXY,2),W(MXZ,2),TEMPX
002304      9246 FORMAT(1H0, * MXY,MXZ,R(MXY,2),W(MXZ,2),TEMPX *,2I5,3E18.6)
002304      WOXD = TEMPX * CONST
002306      WOXDIF = WOXDIF + WOXD
C
C      ADJUST HEAT BALANCE FOR THE DROPLET TO REFLECT SURFACE REACTI
C
002310      DTX = HEATX * WOXD / CPL
002312      T(MXY,2) = T(MXY,2) + DTX
C
C      MAY ALSO HAVE TO ADJUST RADIUS
C
C      ADJUST MASS
C
002314      W(MXZ,1) = W(MXZ,1) - WOXD
002317      AMTFL = WOXD * (32./92.) * 2.0
002322      W(MXZ,2) = W(MXZ,2) - AMTFL
002324      9255 CONTINUE
C
C      ADJUST TOTAL MASS
C
002327      WTOTAL(1) = WTOTAL(1) - WOXDIF
002331      WTOTAL(2) = WTOTAL(2) - 2.0 * (32./92.) * WOXDIF
C
C      ADJUST LIQUID DROPLET MASS TO REFLECT SURFACE REACTION
C
002335      WDROP(2) = WDROP(2) - 2.0 * (32./92.) * WOXDIF
C
C      DISTRIBUTE PRODUCTS (N2O,NH3,N2H5NO3)
C
002342      PROD(4) = PROD(4) + WOXDIF * (44./92.)
002346      PROD(6) = PROD(6) + WOXDIF * (17./92.)
002351      PROD(9) = PROD(9) + WOXDIF * (95./92.)
002354      9270 CONTINUE
002354      DO 1105 K=1,NN
002356      IF(TAVERG .GE. TTABLE(K) .AND. TAVERG .LE. TTABLE(K+1)) GO TO
002367      K=K
002370      1105 CONTINUE
002372      1107 AA=AAT(K)
002374      EACT=EACTT(K)
002376      K3=1
002377      IF(CON/CFN .GT. CFORPR) K3=2

```

```

002403 HREACT=YREACT(K,K3)
002407 REACT(1)=VC*AA*XM(1)*(CON/VC)**RN*(CFN/VC)**RM*2.71828**(-EACT/
1(RC*TAVERG))*DELTN
002433 RPN=0.
002434 C1=0.
002435 C2=0.
002436 IF(React(1) .GT. CON*XM(1)) REACT(1)=CON*XM(1)
002442 REACT(2)=A(2,K,K3)*REACT(1)/A(1,K,K3)
002454 IF(React(2) .LT. CFN*XM(2)) GO TO 1110
002457 REACT(2)=CFN*XM(2)
002460 REACT(1)=A(1,K,K3)*REACT(2)/A(2,K,K3)
002465 1110 DO 1120 I=1,10
002467 DPRN=REACT(1)*A(I+2,K,K3)/A(1,K,K3)
002500 IF(I .GT. 8) GO TO 1120
002504 RPN=RPN+DPRN
002506 1120 PROD(I)=PROD(I)+DPRN
002513 DENOMR=(X1(1)-REACT(1))*CPG(1)+(X1(2)-REACT(2))*CPG(2)+DENOMP*C
002523 DELTRE=REACT(1)*HREACT/DENOMR
002525 TFINAL=TAVERG+DELTRE
002527 DO 1130 NX=1,2
002531 PG(NX)=PG(NX)*TFINAL/TQ(NX)
002534 PG(NX)=PG(NX)-REACT(NX)*RC*TFINAL/(XM(NX)*VC)
002543 IF(PG(NX) .LT. 0.) PG(NX)=0.
002546 PG1(NX)=PG(NX)/144.
002551 1130 CONTINUE
002553 PGP=(TFINAL*(RPN*RC/(VC*XMP)-RC*XMNOZP/(VC*XMP)+PGP/TGP)
002562 XMNOZP=(PGP*ASTAR*DELTN/SQRT(TFINAL))*CONST5*DELTN
002571 DENOMP = RPN+VC*XMP*PGP/(RC*TGP)-XMNOZP
002600 IF(PGP .LT. 144.) GO TO 1140
002602 IF(TW.GT.TGP) GO TO 1135
002605 C1=0.
002605 C2=HC(3,2)*AC*(TGP-TW)*DELTN/CPGP
002612 GO TO 1140
002612 1135 C2=0.
002613 C1=HC(3,1)*AC*(TW-TGP)*DELTN/CPGP
002621 1140 TGP = (RPN*TGP+VC*XMP*PGP/RC -XMNOZP*TGP-C2+C1)/DENOMP
002634 TG(1)=TFINAL
002635 TG(2)=TFINAL
002636 TGP =TFINAL
002637 PGP1=PGP/144.
002641 PGTOTAL=PGP1+PG1(1)+PG1(2)
002644 PGTOTL=PG(1)+PG(2)+PGP
002646 IF(L.GE.ND1.AND.L.LE.ND2.AND.MOD(L-ND1,ND3).EQ.0) CALL OUT1
C
002666 IF(IFPLOT.NE.0) CALL PLTSUB(TIME,TFINAL)
C
C
C
C
002671 IF(TIME.LT.TDETON(IDETON)) GO TO 4341
002674 CALL OUTX
002675 IF(IDETON.LT.40) IDETON = IDETON + 1
002701 4341 CONTINUE
C
002701 1150 CONTINUE
002701 TIME=TIME+DT1000
002703 TIME1=TIME1+DELTN
002705 1000 CONTINUE

```

```
002705      DELTN=(TIME+.1)/1.E+5
002710      IF(IDEBUG) WRITE(6,3794) DELTN
002717 3794  FORMAT(1H0,*NEW TIME STEP IS*,E20.8)
002717      IF(PGTOTAL .GE.100.) GO TO 1
002722      IF(TIME1 .GE. TMAX) GO TO 1
002724      IF( L .GE. NSTOP) GO TO 1
002727      DT1000=DELTN*1000.
002731      GO TO 25
002731 999  CONTINUE
002731      WRITE(6,9999)
002735 9999  FORMAT(1H0, * VARIABLE DIMENSIONS EXCEEDED *)
002735      GO TO 1
002736      END
*DECK,DSCPLT
```



```
SUBROUTINE USCPLT(X,Y,XLABEL,YLABEL,PLABEL,N,KX,KY,KP,IFIRST  
I,SCALEP,XUNITS,YUNITS,SYMHIT,ILINE,ISYMBL)
```

```
C  
000023 DIMENSION X(1),Y(1),PLABEL(1)  
000023 DIMENSION XLABEL(1),YLABEL(1)  
C  
000023 NN = N  
000023 IF(IFIRST.EQ.1) CALL PLOTS ( 9HDSC PLOTS,9)  
C  
000034 CALL MAXMIN(X,Y,NN,XMIN,YMIN,XMAX,YMAX)  
C  
000042 CALL SCAL (XMAX,XMIN,XUNITS,XSCALE,XADJM,XEFF)  
000047 CALL SCAL (YMAX,YMIN,YUNITS,YSCALE,YADJM,XEFF)  
C  
000054 IF(YMIN.NE.YMAX) GO TO 5  
000062 YADJM = YMIN * 0.5  
000063 YSCALE = 2.0 * YMAX / YUNITS  
000066 CONTINUE  
5  
C  
000066 Y(NN+1) = YADJM  
000070 X(NN+1) = XADJM  
C  
000072 Y(NN+2) = YSCALE  
000073 X(NN+2) = XSCALE  
C  
000075 ICARX = 10 * KX  
000077 ICARY = 10 * KY  
C  
000102 CALL AXIS(0.0,0.0,XLABEL,-ICARX,XUNITS,0.0,XADJM,XSCALE)  
000113 CALL AXIS (0.0,0.0,YLABEL,+ICARY,YUNITS,90.,YADJM,YSCALE)  
C  
000130 CALL LINE(X,Y,NN,1,ILINE,ISYMBL)  
C  
000137 ILAB = 10*KP  
C  
000142 CALL SYMBOL(0.0,YUNITS,SYMHIT,PLABEL(1),0.0,ILAB)  
C  
000153 XNEXT = XUNITS + XUNITS*0.5  
C  
000156 CALL PLOT(XNEXT,0.0,-3)  
C  
000161 RETURN  
000162 END  
*DECK,LINI
```

SUBROUTINE LINI(X,Y,N,ARG,YARG,NSAVE)

C
C
C

LINEAR INTERPOLATION ROUTINE

000011 DIMENSION X(1), Y(1)
000011 NN=N
000011 XV=ARG
000012 IF (XV.GE.X(NN))GO TO 40
000016 IF(XV.LE.X(1))GO TO 50

C

000020 J= NSAVE
000021 IF(J .LT. 1 .OR. J .GT. NN) J=1
000033 K= SIGN(1.0,(XV-X(J)))
000041 5 J=J+K
000043 IF((XV-X(J)) * FLOAT(K)) 10,30,5
000047 10 IF(K.EQ.-1)J=J+1
000053 I=J-1

C
C
C

INTERPOLATION CALC

000055 H=X(J)-X(I)
000060 DX=XV-X(I)
000063 DY=Y(J)-Y(I)
000066 YARG= Y(I) + DX*DY/H
000072 NSAVE=I
000073 RETURN
000073 30 YARG=Y(J)
000075 NSAVE=J
000076 RETURN
000076 40 YARG=Y(NN)
000100 RETURN
000101 50 YARG=Y(1)
000102 RETURN
000103 END

*DECK,MAXMIN

SUBROUTINE MAXMIN (X,Y,N,XMIN,YMIN,XMAX,YMAX)

C

```
000012      DIMENSION X(1),Y(1)
000012      XMIN = X(1)
000013      YMIN = Y(1)
000014      YMAX = Y(1)
000015      XMAX = X(1)
000016      DO 10 I = 2,N
000020      XMIN = AMINI(XMIN,X(I))
000024      YMIN = AMINI(YMIN,Y(I))
000030      XMAX = AMAXI(XMAX,X(I))
000034      YMAX = AMAXI(YMAX,Y(I))
000040  10  CONTINUE
000042      RETURN
000042      END
```

*DECK,OUTX

SUBROUTINE OUTX

```

C
000002 COMMON/COM1/A(5,10),COEF(5,10),ENTHPY(10),FORO(10),SPNAME(10)
000002 COMMON/COM2/ICASE,IUNIT,F(2),HFLIQ(2),MSPEC,PGTOTAL,PROD(10),
I      TFINAL,WDROP(2),WTOTAL(2),IFIRST
000002 DIMENSION RELWT(10),FACTOR(2)
000002 DIMENSION SUMX(2),XCOEF(5,10),AX(5,10)
000002 LOGICAL DETN,PSIA
C
000002 DATA REACTX,REACTY / 6HREACTA,3HNNTS/ , FUELX/1HF/
000002 DATA XNAME,XLISTS/ 4HNAME,5HLISTS/, XEND/4HSEND/
000002 DATA XINPT2 /6H$INPT2/ , XPIS,XTIS/2HP=,2HT=/, COMMA /1H,/
000002 DATA XFPCT,XOF,XKASE/5HFPCT=,3HOF=,5HKASE=/, XTRUE/6H.TRUE./
000002 DATA TFPSIA,TFDETN /6HPSIA= ,6HDETN= /
000002 DATA BLANK /2H /
C
C
000002 DO 300 I = 1,5
000004 DO 300 J = 1,10
000005 AX(I,J) = BLANK
000011 XCOEF(I,J) = 0.0
000014 300 CONTINUE
000017 DO 310 J = 1,10
000021 DO 310 I = 1,5
000022 IF(COEF(I,J).LE.0.0) GO TO 310
000026 AX(I,J) = A(I,J)
000033 XCOEF(I,J) = COEF(I,J)
000036 310 CONTINUE
C
C
C      OXIDIZER / FUEL WT RATIO
C
000042 OF = WTOTAL(1) / WTOTAL(2)
C
C      COMPUTE COEF MULTIPLICATIVE FACTORS
C
000044 FACTOR(1) = F(1) / (1.0-F(1))
000047 FACTOR(2) = F(2) / (1.0-F(2))
C
C      COMPUTE OXID AND FUEL COEFFICIENTS FOR DETONATION CALC
C
000051 DO 410 N = 1,2
000052 DO 400 I = 1,5
000053 IF(COEF(I,N).EQ.0.0) GO TO 400
000056 AX(I,N) = A(I,N)
000063 XCOEF(I,N) = COEF(I,N) * FACTOR(N)
000070 400 CONTINUE
C
C      COMPUTE ENTHALPY
C
000072 ENTHPY(N) = ENTHPY(N) + HFLIQ(N)*FACTOR(N)
C
000077 PROD(N) = WTOTAL(N)
C
000102 410 CONTINUE
C
C      COMPUTE TOTAL WEIGHTS OF OX AND FUEL
C

```

```

000104      SUMX(1) = 0.0
000105      SUMX(2) = 0.0
000106      DO 14 I = 1,10
000107      N = 1
000110      IF(FORO(1).EQ.FUELX) N = 2
000114      SUMX(N) = SUMX(N) + PROD(I)
000120      14 CONTINUE
C
C      COMPUTE RELATIVE WEIGHTS
C
000121      DO 420 I = 1,10
000123      N = 1
000124      IF(FORO(1).EQ.FUELX) N = 2
000130      RELWT(I) = PROD(I) / SUMX(N)
000135      420 CONTINUE
C
000137      DO 200 I = 1,10
000140      IF(PROD(I).LE.0.0) GO TO 200
000142      IF(RELWT(I).GE.1.0E-5) GO TO 200
000145      WRITE(6,176)
000151      176 FORMAT(1H0,*NO DETONATION CARDS PUNCHED*)
000151      RETURN
000152      200 CONTINUE
C      WRITE REACTANTS CARD
C
000154      WRITE(IUNIT,900) REACTX,REACTY
000164      900 FORMAT(A6,A3,71X)
C
C      WRITE REACTANT CARDS
C
000164      DO 430 I = 1,10
000166      IF(RELWT(I).LE.0.0) GO TO 430
000170      WRITE(IUNIT,191) (AX(J,I),XCOEF(J,I),J=1,5),RELWT(I),ENTHPY(I)
                                     1                                     ,FORO(I)
000222      191 FORMAT(5(A2,F7.5),F7.5,1X,F9.0,9X,A1)
000222      430 CONTINUE
000224      WRITE(IUNIT,192)
000230      192 FORMAT(80X)
C
C      WRITE NAMELISTS CARD
C
000230      WRITE(IUNIT,193) XNAME,XLISTS
000240      193 FORMAT(A4,A5)
C
000240      TI = TFINAL / 1.8
000242      PI = PGTOTAL
C
C      CONSTRUCT NAMELIST $INPT2
C
000244      WRITE(IUNIT,194) XINPT2
000251      194 FORMAT(1X,A6)
000251      WRITE(IUNIT,195) XPIS,PI,COMMA, XTIS,TI,COMMA
000271      195 FORMAT(1X,A2,E20.8,A1,5X,A2,E20.8,A1)
000271      WRITE(IUNIT,196) TFPSIA,XTRUE,COMMA,TFDET,XTRUE,COMMA
000311      196 FORMAT(1X,A6,A6,A1,5X,A6,A6,A1)
000311      WRITE(IUNIT,197) XOF,OF,COMMA,XKASE,ICASE,COMMA
000331      197 FORMAT(1X,A3,E16.7,A1,3X,A5,I7,A1)

```

```
000331      WRITE(IUNIT,198) XEND
000337      198  FORMAT(IX,A4)
      C
000337      ICASE = ICASE + 1
      C
000341      RETURN
000341      END
      #DECK,OUT1
```

SUBROUTINE OUT1

```

C
000002 COMMON /A/ TFP(2),TAU(2),TAUF(2),TAUS(2),XM(2),GAM(2),TG(2),
1 PG(2),M(2),GEVAP(2),X1(2),XR(2),T0(2)
000002 COMMON/COM1/ DUMXYZ(120),SPNAME(10)
000002 COMMON/COM2/ ICASE,IUNIT,F(2),HFLIQ(2),MSPEC,PGTOTAL,PROD(10),
1 TFINAL,WDROP(2),WTOTAL(2),IFIRST
000002 COMMON/DOLOOP/ ND1,ND2,ND3
000002 COMMON/OUTA/ PG1(2),PGP1,REACT(2),TAVERG,DELTRE,TIME,TQP
000002 COMMON/OUTB/ NPAGE
000002 899 FORMAT(1H1)
000002 IF(NPAGE.LE.4) GO TO 10
000005 WRITE(6,899)
000010 NPAGE = 0
000011 10 NPAGE= NPAGE + 1
C
000013 DO 20 N = 1,2
000014 PROD(N) = WTOTAL(N)
000017 20 CONTINUE
C
000020 900 FORMAT(1H0,35X,16HTIME(MILLISEC) =,E11.4//
1 1X,41HPRESSURES(PSIA) TEMPERATURES(DEGR)
2 42HREACTION PARAMETERS WEIGHTS AND FACTORS)
000020 901 FORMAT(1H ,7HOXID =,E11.4,2X,7HTFINAL=,E11.4,3X,9HREACT(O)=,E1
1,3X,10HWTOTAL(O)=,E11.4)
000020 902 FORMAT(1H ,7HFUEL =,E11.4,2X,7HTAVERG=,E11.4,3X,9HREACT(F)=,E1
1,3X,10HWTOTAL(F)=,E11.4)
000020 903 FORMAT(1H ,7HTOTAL =,E11.4,2X,7HTQP =,E11.4,3X,9HDELTRE =,E1
1,3X,10HF(O) =,E11.4)
000020 904 FORMAT(1H ,7HPGP =,E11.4, 46X,10HF(F) =,E11.4)
000020 905 FORMAT(1H0,22HPRODUCT CONCENTRATIONS//)
000020 906 FORMAT(1H ,4(1H ,A6,1H=,E11.4,3X))
000020 WRITE(6,900) TIME
000026 WRITE(6,901) PG1(1), TFINAL, REACT(1), T0(1)
000042 WRITE(6,902) PG1(2), TAVERG, REACT(2), T0(2)
000056 WRITE(6,903) PGTOTAL,TQP, DELTRE, F(1)
000072 WRITE(6,904) PGP1,F(2)
000102 WRITE(6,905)
000106 WRITE(6,906) (SPNAME(I),PROD(I),I=1,MSPEC)
000124 RETURN
000125 END
*DECK,PLTPAK

```

```

SUBROUTINE PLTPAK(X,Y,PLABEL,XLABEL,YLABEL,NPTS,IDEBUG)
000012 DIMENSION X(1),Y(1),PLABEL(6),XLABEL(2),YLABEL(2)
000012 DATA IFIRST/0/
000012 XUNITS= 10.0
000013 YUNITS= 10.0
000013 SCALEP= 1.0
000015 ILINE = 1
000016 ISYMBL= 3
000017 SYMHIT= 0.2
000020 IPLNUM= 6
000021 IXLNUM= 2
000022 IYLNUM= 2
000024 1 IFIRST = IFIRST + 1
000026 IF(NPTS.LE.0) GO TO 210
000027 IF(IDEBUG.EQ.0) GO TO 10
000031 WRITE(6,110) (PLABEL(I),I=1,6), (XLABEL(I),I=1,2), (YLABEL(I),I=1
000067 110 FORMAT(1H1,9X,*PLOT LABEL *,3X,6A10//10X,*X AXIS LABEL*,3X,2A
1 //10X,*Y AXIS LABEL*,3X,2A10)
000067 WRITE(6,111) NPTS, (I,X(I),Y(I),I=1,NPTS)
000125 111 FORMAT(1H0,9X,*NUMBER OF POINTS =*,110//10X,1H1,14X,1HX,14X,1H
1 (8X,15,2E16.8))
000125 10 CONTINUE
000125 CALL DSCPLT (X,Y,XLABEL,YLABEL,PLABEL,NPTS,IXLNUM,IYLNUM,IPLNU
1 IFIRST,SCALEP,XUNITS,YUNITS,SYMHIT,ILINE,ISYMBL)
000147 RETURN
000150 210 WRITE(6,211) NPTS
000162 211 FORMAT(1H0,*NPTS =*,110,3X,*MUST BE .GE. 1*)
000162 RETURN
000163 END
*DECK,PLTSUB

```



```

SUBROUTINE PLTSUB (TIME,TFINAL)
C
000005 COMMON/CPLT/ IFPLOT,PLTIME,IPLT1,TMAX
C
000005 DIMENSION X(100),Y(100),PLABEL(6),XLABEL(6),YLABEL(6)
C
000005 DATA (PLABEL(I),I=1,6)/10HTRANSIENT ,10HSTART PROG, 3HRAM,1H ,
1 1H ,1H /
000005 DATA (XLABEL(I),I=1,2)/10HTIME(MILLI,10HSEC) /
000005 DATA (YLABEL(I),I=1,2)/10HTFINAL (DE,10HG-R) /
000005 CALL SECOND(CPSEC)
000006 TEST = TIME / 1.0E3
C
000011 IF(CPSEC.GT.(PLTIME-5.0)) IPLT1 = +1
000016 IF(ABS(TEST-TMAX).LE.1.0E-8) IPLT1 = +1
C
000024 CALL TABGEN(IPLT1,100,X,Y,NUM,TIME,TFINAL,IX)
000034 IF(IPLT1.NE.+1) GO TO 998
C
C
C
000037 NUM = MIN0 (100,NUM)
000043 IDEBUG = 1
000044 CALL PLTPAK(X,Y,PLABEL,XLABEL,YLABEL,NUM,IDEBUG)
000052 IFPLOT = 0
000053 998 IPLT1 = 0
000054 RETURN
000055 END
*DECK,SCAL

```

```

SUBROUTINE SCAL (XMAX,XMIN,XI,DX,X0,XE)
C
C FORTRAN IV PLOT SCALE OPTIMIZATION ROUTINE.
C
000011 DIMENSION S(3)
000011 DATA S/1.,2.,5./
C
C
000011 DX=0.0
000011 X0=0.0
000012 XE=0.0
000012 W=(XMAX-XMIN)/XI
000014 IF(W)21,21,6
000016 6 DO 20 I=1,3
000020 A=1.0+ALOG10(W/S(I))
000026 B=AIN(T(A)
000027 IF((A.EQ.B).OR.(A.LT.0.0))B=B-1.0
000041 C=S(I)*10.0**B
000046 D=AIN(T(XMIN/C)
000054 IF(C*D.GT.XMIN)D=D-1.0
000062 D=C*D
000063 IF(XI*C-XMAX+D)20,15,15
000066 15 E=W/C
000070 IF(XE-E)17,20,20
000072 17 DX=C
000073 X0=D
000074 XE=E
000075 20 CONTINUE
000077 21 RETURN
000100 END
*DECK,TABGEN

```

```

SUBROUTINE TABGEN (IFLAG,LTABLE,XTAB,YTAB,LUSED,X,Y,IERROR)
C
000013 DIMENSION XTAB(1), YTAB(1)
C
C IFLAG DENOTES THE TYPE OF ENTRY TO THIS SUBROUTINE. (3 TYPES)
C IFLAG = -1 FIRST ENTRY FOR A PARTICULAR TABLE
C IFLAG = 0 NORMAL ENTRY (NEITHER FIRST NOR LAST ENTRY)
C IFLAG = +1 LAST ENTRY TO THE SUBROUTINE FOR THIS TABLE
C
C THE ABOVE OPTIONS ALLOW THE ASSURANCE THAT THE FIRST AND LAST
C EVENTS WILL ALWAYS BE TABULATED IN THE FINAL TABLE.
C
C IF THIS IS THE FIRST ENTRY TO THIS SUBROUTINE, MUST INITIALIZE
C FLAGS AND VARIABLES.
C
000013 IF(IFLAG.NE.-1) GO TO 10
C
000015 N = 0
000015 LUSED = 0
000016 IENTER = 0
000017 IXMOD = 1
000020 IEVENT = 0
000021 IEVM1 = 0
000021 IEVLST = 0
C
C FORCE THE TABLE DIMENSION TO BE USED TO AN EVEN NUMBER.
C
000022 LTAB = (LTABLE/2) * 2
C
000024 10 CONTINUE
000024 IENTER = IENTER + 1
000026 IEVENT = IEVENT + 1
C
C CHECK FOR TABLE OVERFLOW PRIOR TO PROCESSING ENTRY
C
000027 LOVFL = LUSED + 1
000027 IF(LOVFL.LE.LTAB) GO TO 30
C
C OVERFLOW COULD BE CAUSED BY THIS ENTRY, REPACK TABLE.
C
000032 WRITE(6,100) LUSED,N,LTAB
000044 100 FORMAT(1H0,*AM REPACKING TABLE,LUSED,N,LTAB*,3I10)
000044 INEW = 0
000045 DO 20 I = 1,LTAB, 2
000052 INEW = INEW + 1
000054 XTAB(INEW) = XTAB(I)
000057 YTAB(INEW) = YTAB(I)
000061 20 CONTINUE
C
C RESET THE CURRENT NUMBER OF TABLE ENTRIES (LUSED)
C
000063 LUSED = INEW
000063 IENTER = IEVENT - IEVM1
000065 IEVLST = IEVM1
000066 N = N + 1
000070 IXMOD = 2**N
C

```

```

000073      30  CONTINUE
C
C  DETERMINE IF CURRENT CALL IS TO RESULT IN AN ENTRY IN THE TABL
C
000073      IF (IFLAG.EQ.1) GO TO 35
000075      IF (MOD(IENTER,IXMOD).NE.0) GO TO 40
000101      35  CONTINUE
000101      LUSED = LUSED + 1
000102      XTAB(LUSED) = X
000104      YTAB(LUSED) = Y
000106      IEVM1 = IEVLST
000107      IEVLST = IEVENT
000111      40  CONTINUE
000111      999 RETURN
000112      END

```

<p>NASA Headquarters Washington, D.C. 20546 Attn: Patent Office</p>	<p>*</p>	<p>Director, Technology Utilization Div. Office of Technology Utilization NASA Headquarters Washington, D.C. 20546</p>	
<p>NASA Lewis Research Center 21000 Brookpark Road Cleveland, Ohio 44135 Attn: Office of Technical Information Contracting Officer Patent Office Dr. R. J. Priem</p>		<p>NASA Scientific & Technical Information Facility P. O. Box 33 College Park, Maryland 20740</p>	<p>25</p>
<p>NASA Manned Spacecraft Center Houston, Texas 77001 Attn: Office of Technical Information Contracting Officer Patent Office</p>		<p>Director, Launch Vehicles & Propulsion, SV Office of Space Science & Applications NASA Headquarters Washington, D.C. 20546</p>	
<p>NASA Marshall Space Flight Center Huntsville, Alabama 35812 Attn: Office of Technical Information, MS-IP Technical Library Purchasing Office, PR-FC Patent Office, M-PAT Keith Chandler, R-P&VE-PA Technology Utilization Office, MS-T</p>	<p>2</p>	<p>Director, Advanced Manned Missions, MT Office of Manned Space Flight NASA Headquarters Washington, D.C. 20546</p>	
<p>NASA Pasadena Office 4800 Oak Grove Drive Pasadena, California 91103 Attn: Patents and Contracts Management</p>		<p>Missi on Analysis Division NASA Ames Research Center Moffett Field, California 24035</p> <p><u>NASA Field Centers</u></p> <p>Ames Research Center Moffett Field, California 94035 Attn: Hans M. Mark</p>	<p>2</p>
<p>Jet Propulsion Laboratory 4800 Oak Grove Drive Pasadena, California 91103 Attn: Richard M. Clayton</p>	<p>2</p>	<p>Goddard Space Flight Center Greenbelt, Maryland 20771 Attn: Merland L. Moseson, Code 620</p>	
<p>Chief, Liquid Propulsion Technology RPL Office of Advanced Research and Technology NASA Headquarters Washington, D.C. 20546</p>		<p>Jet Propulsion Laboratory California Institute of Technology 4800 Oak Grove Drive Pasadena, California 91103 Attn: Henry Burlage, Jr. Propulsion Div. 38</p>	<p>2</p>
		<p>Langley Research Center Langley Station Hampton, Virginia 23365 Attn: Ed Cortwright, Director</p>	<p>2</p>

*One copy unless otherwise designated.
Copies sent direct to first section (NASA).
All others sent to librarian with copy of letter to addressee.

Lewis Research Center 2
21000 Brookpark Road
Cleveland, Ohio 44135
Attn: Dr. Abe Silverstein, Director

Marshall Space Flight Center 2
Huntsville, Alabama 35812
Attn: Hans G. Paul, R-P&VED

Manned Spacecraft Center 2
Houston, Texas 77001
Attn: J. G. Thibodaux, Jr.
Chief, Prop. & Power Div.

John F. Kennedy Space Center, NASA
Cocoa Beach, Florida 32931
Attn: Dr. Kurt H. Debus 2

Government Installations

Aeronautical Systems Division
Air Force Systems Command
Wright-Patterson Air Force Base
Dayton, Ohio 45433
Attn: D. L. Schmidt, ASRCNC-2

Air Force Missile Development Center
Holloman Air Force Base
New Mexico 88330
Attn: Maj. R. F. Bracken

Air Force Missile Test Center
Patrick Air Force Base, Florida
Attn: L. J. Ullian

Space and Missile Systems
Organization
Air Force Unit Post Office
Los Angeles, California 90045
Attn: Col. Clark,
Technical Data Center

Arnold Engineering Development Center
Arnold Air Force Station
Tullahoma, Tennessee 37388
Attn: Dr. H. K. Doetsch

Bureau of Naval Weapons
Department of the Navy
Washington, D.C. 20546
Attn: J. Kay, RTMS-41

Defense Documentation Center Hdqtrs.
Cameron Station, Building 5
5010 Duke Street
Alexandria, Virginia 22314
Attn: Tisia

Headquarters, U.S. Air Force
Washington, D. C. 20546
Attn: Col. C. K. Stambaugh, AFRST

Picatinny Arsenal
Dover, New Jersey 07801
Attn: I. Forsten, Chief
Liquid Propulsion Lab.

A.F. Rocket Propulsion Laboratory
Research and Technology Div.
Air Force Systems Command
Edwards, California 93523
Attn: Mr. H. Main, RPRPD

U. S. Army Missile Command
Redstone Arsenal
Alabama 35809
Attn: Mr. Walter Wharton

U.S. Naval Ordnance Test Station
China Lake, California 93557
Attn: Chief, Missile Propulsion Div.
Code 4562

U. S. Bureau of Mines
4800 Forbes Avenue
Pittsburgh, Penn. 15213
Attn: Mr. Henry Perlee

CPIA

Chemical Propulsion Information Agency
Applied Physics Laboratory
8621 Georgia Avenue
Silver Spring, Maryland 20910

Industry Contractors

Aerojet-General Corporation
P. O. Box 296
Azusa, California 91703
Attn: W. L. Rogers

Aerojet-General Corporation
P. O. Box 1947
Technical Library, Bldg. 2015
Dept. 2410
Sacramento, California 95809
Attn: R. Stiff

Space Division
Aerojet-General Corporation
9200 East Flair Dr.
El Monte, California 91734
Attn: S. Machlawski

Aerospace Corporation
2400 East El Segundo Blvd.
P. O. Box 95085
Los Angeles, Calif. 90045
Attn: John G. Wilder, MS-2293

Astrosystems International, Inc.
1275 Bloomfield Avenue
Fairfield, New Jersey 07007
Attn: A. Mendenhall

Atlantic Research Corp.
Edsall Road & Shirley Hwy.
Alexandria, Virginia 22314
Attn: Dr. Ray Friedman

Avco Systems Division
Wilmington, Massachusetts
Attn: Howard B. Winkler

Beech Aircraft Corporation
Boulder Division
Box 631
Boulder, Colorado
Attn: J. H. Rodgers

Bell Aerosystems Company
P. O. Box 1
Buffalo, New York 14240
Attn: W. M. Smith

Bellcomm
955 L-Enfant Plaza, S.W.
Washington, D. C.
Attn: H. S. London

Bendix Systems Division
Bendix Corporation
3300 Plymouth Road
Ann Arbor, Michigan 48105
Attn: John M. Brueger

Boeing Company
P. O. Box 3707
Seattle, Washington 98124
Attn: J. D. Alexander

Boeing Company
1625 K Street, N.W.
Washington, D. C. 20006
Attn: Library

Boeing Company
P. O. Box 1680
Huntsville, Alabama 35801
Attn: Ted Snow

Missile Division
Chrysler Corporation
P. O. Box 2628
Detroit, Michigan 48231
Attn: Mr. John Gates

Wright Aeronautical Division
Curtiss-Wright Corporation
Wood-Ridge, New Jersey 07075
Attn: G. Kelley

Research Center
Fairchild Hiller Corporation
Farmingdale, L.I., New York
Attn: Library

General Dynamics, Convair Div.
Library & Information Services (128-00)
P. O. Box 1128
San Diego, California
Attn: Frank Dore

Missile & Space Systems Center
General Electric Company
Valley Forge Space Technology Ctr.
P.O. Box 8555
Philadelphia, Pa.
Attn: F. Mezger
F. E. Schultz

Grumman Aircraft Engineering Corp.
Bethpage, Long Island
New York 11714
Attn: Joseph Gavin

Honeywell, Inc.
Aerospace Division
2600 Ridgway Road
Minneapolis, Minn.
Attn: Mr. Gordon Harms

Hughes Aircraft Co.
Aerospace Group
Centinela and Teale Streets
Culver City, Calif. 90230
Attn: E. H. Meier, V.P. & Div. Mgr.
Research & Dev. Div.

Walter Kidde and Company, Inc.
Aerospace Operations
567 Main Street
Belleville, New Jersey
Attn: R. J. Hanville
Dir. of Research Engr.

Ling-Temco-Vought Corporation
P. O. Box 5907
Dallas, Texas 75222
Attn: Warren G. Trent

Arthur D. Little, Inc.
20 Acorn Park
Cambridge, Mass. 02140
Attn: Library

Lockheed Missiles and Space Co.
Technical Information Center
P. O. Box 504
Sunnyvale, Calif. 94088
Attn: J. Guill

Lockheed Propulsion Company
P. O. Box 111
Redlands, Calif. 92374
Attn: H. L. Thackwell

The Marquardt Corporation
16555 Saticoy Street
Van Nuys, Calif. 91409
Attn: Howard McFarland

Baltimore Division
Martin Marietta Corporation
Baltimore, Maryland 21203
Attn: Mr. John Calathes (3214)

Denver Division
Martin Marietta Corporation
P. O. Box 179
Denver, Colorado 80201
Attn: Dr. Morganthaler
A. J. Kullas

Orlando Division
Martin Marietta Corp.
Box 5837
Orlando, Florida
Attn: J. Ferm

Astropower Laboratory
McDonnell Douglas Corporation
2121 Paularino
Newport Beach, Calif. 92663
Attn: Dr. George Moe -
Director, Research

McDonnell Douglas Corporation
P.O. Box 516
Municipal Airport
St. Louis, Missouri 63166
Attn: R. A. Herzmark

McDonnell Douglas Astronautics Company
Western Division
5301 Bolsa Avenue
Huntington Beach, California 92646
Attn: Mr. R. W. Hallet, Chief Engr.
Adv. Space Tech.

Space & Information Systems Division
North American Rockwell
12214 Lakewood Boulevard
Downey, California 90241

Rocketdyne (Library 586-306)
6633 Canoga Avenue
Canoga Park, Calif. 91304
Attn: Dr. R. J. Thompson
S. F. Iacobellis

Northrop Space Laboratories
3401 West Broadway
Hawthorne, Calif. 90250
Attn: Dr. William Howard

Aeronutronic Division
Philco Corporation
Ford Road
Newport Beach, Calif. 92663
Attn: D. A. Garrison

Astro-Electronics Division
Radio Corporation of America
Princeton, New Jersey 08540
Attn: Y. Brill

Rocket Research Corporation
520 South Portland Street
Seattle, Washington 98108
Attn: Foy McCulloch, Jr.

Sunstrand Aviation
2421 - 11th Street
Rockford, Illinois 61101
Attn: R. W. Reynolds

Stanford Research Institute
333 Ravenswood Avenue
Menlo Park, California 94025
Attn: Dr. Gerald Marksman

TRW Systems Group
TRW Incorporated
One Space Park
Redondo Beach, Calif. 90278
Attn: G. W. Elverum

Tapco Division
TRW, Incorporated
23555 Euclid Avenue
Cleveland, Ohio 44117
Attn: P. T. Angell

Reaction Motors Division
Thiokol Chemical Corporation
Denville, New Jersey 07832
Attn: Dwight S. Smith

Research Laboratories
United Aircraft Corp.
400 Main Street
East Hartford, Conn. 06108
Attn: Erle Martin

Hamilton Standard Division
United Aircraft Corp.
Windsor Locks, Conn. 06096
Attn: Mr. R. Hatch

United Technology Center
587 Methid a Avenue
P. O. Box 358
Sunnyvale, California 94088
Attn: Dr. David Altman

Florida Research and Development
Pratt and Whitney Aircraft
United Aircraft Corporation
P. O. Box 2691
West Palm Beach, Florida 33402
Attn: R. J. Coar

Vickers, Inc.
Box 302
Troy, Michigan

Dynamic Science
2400 Michelson Drive
Irvine, Calif. 92664
Attn: Dr. B. P. Breen

Multi-Tech, Inc.
Glenoaks Boulevard
San Fernando, Calif. 91340
Attn: Mr. F. B. Cramer

Mathematical Applications Group, Inc.
180 S. Broadway
White Plains, New York 10605
Attn: Dr. S. Z. Burnstein

Universities

Ohio State University
Dept. of Aeronautical Eng.
Columbus, Ohio 43210
Attn: R. Edse

Pennsylvania State University
Mech. Engineering Dept.
207 Mechanical Engineering Blvd.
University Park, Pa. 16802
Attn: G. M. Faeth

University of Southern California
Dept. of Mech. Engineering
University Park
Los Angeles, Calif. 90007
Attn: Dr. M. Gerstein

Princeton University
Forrestal Campus
Guggenheim Laboratories
Princeton, New Jersey 08540
Attn: D. Harrje

University of Wisconsin
Mechanical Engineering Dept.
1513 University Ave.
Madison, Wisconsin 53705
Attn: P. S. Myers

University of Michigan
Aerospace Engineering
Ann Arbor, Michigan 48104
Attn: J. A. Nicholls

University of California
Dept. of Chem. Engineering
6161 Etcheverry Hall
Berkeley, Calif. 94720
Attn: A. K. Oppenhiem
R. Sawyer

Purdue University
School of Mechanical Engineering
Lafayette, Indiana 47907
Attn: J. R. Osborn

Sacramento State College
Engineering Division
60000 J. Street
Sacramento, Calif. 95819
Attn: E. H. Reardon

Massachusetts Institute of Tech.
Dept. of Mechanical Engineering
Cambridge, Mass. 02139
Attn: T. Y. Toong

Illinois Institute of Technology
Room 200 M.H.
3300 S. Federal Street
Chicago, Illinois 60616
Attn: T. P. Torda

Polytechnic Institute of Brooklyn
Graduate Center
Route 110
Farmingdale, New York
Attn: V. D. Agosta

Georgia Institute of Technology
Atlanta, Georgia 30332
Attn: B. T. Zinn

University of Denver
Research Institute
Denver, Colorado
Attn: W. H. McLain

New York University
Dept. of Chem. Eng.
University Heights
New York 53, New York
Attn: Leonard Dauerman